# THERMAL DEFORMATION ANALYSIS

# OF

# HIGH DENSITY PHASE CHANGE

# OPTICAL DISKS

Yang Hongxin

M.Eng., Huazhong University of Science & Technology, P.R.China

B.Eng., Huazhong University of Science & Technology, P.R.China

A THESIS SUBMITTED

FOR THE DEGREE OF MASTER OF ENGINEERING

NATIONAL UNIVERSITY OF SINGAPORE

2005

# Abstract

The laser-beam spot size and the track pitches of the high-density phase change optical disks are smaller and smaller. Any slight deformation in the phase change optical disks will affect the data storage efficiency. The thermal deformation becomes an important issue. A thermo-mechanical analysis simulator has been designed for phase change optical disks based on finite element method (FEM). The thermal deformation in Blu-ray Disc and advanced optical disk(AOD) have been investigated using this simulator. The relationships between the thermal deformation and disk structure parameters and optical parameters have been investigated. It was found that the peak temperature and peak deformation lies in different layers. Several methods have been proposed to decrease the deformation. It can be referred to optimize the phase change optical disk structure.

# Acknowledgement

First and foremost, I wish to thank my supervisor, Professor Chong Tow Chong and Dr. Shi Luping for giving me this opportunity to continue my study in Singapore and work on such an interesting and challenging project. Without their support and guidance, I cannot complete this project so smoothly.

I would like to express my sincere gratitude to Dr. Li Jianming and Mr. Lim Kian Guan for instruction help during my research and programming.

Special thanks must give Dr. Miao Xiangshui, Dr. Zhao Rong, Dr. Hu Xiang, and Mr. Tan Pik Kee for their help during my research.

Finally I wish to thank my friends in DSI, including Wei Xiaoqian, Wang Qinfang, Yan Da, Yin Si, He Wanshun, Chen Yang, Long Haohui et al. Their kind help in my studies and living make the two years for master's degree as a happy journey in my life.

# List of Figures

IV

# List of Tables

# Contents

VIII

# Chapter 1  Phase change optical disks

The idea of recording information using the energy of concentrated light is not a new one. A child focusing the rays of the sunlight through a magnifying glass to burn a black point in a block of wood has learned the basic conception. Substituting a laser to precisely align the beams of sunlight through a lens, pointing it at phase change layer of an optical disk, burning some microscopic marks in the layer, and you have the essence of optical recording. In this chapter, the development history of optical disk, phase change recording and project objectives will be discussed.

## 1.1  Development history of optical disks

After the emerging of audio compact disk(CD) in 1983 [1], much progress have been made in optical storage medium such as CD-ROM, CD-I, CD-R, DVD-Video, DVD-ROM, DVD-RAM and so on [2]. From Figure 1-1, the development history of optical disks can be seen clearly. Compared to other information storage memories, optical disks have the advantages of large capacity, removability, low cost, and non-contact data retrieval using non-contact optical pick-up system. They are widely used as carriers of software, audio, video, electronic books, large databases and all other kinds of information that can be stored in computer [3].
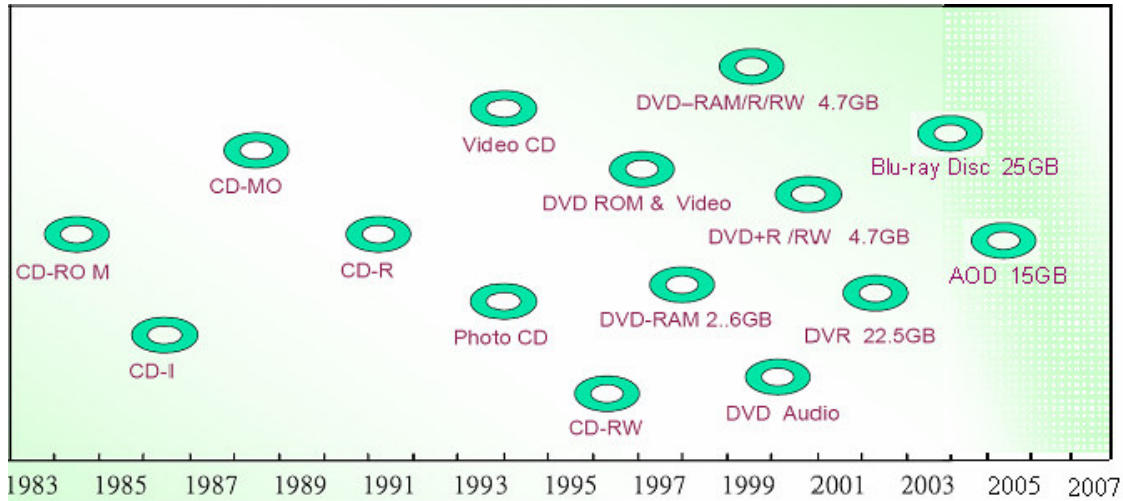
Figure 1-1 Development history of optical disks

These optical disks can be classified into three categories: Read-Only, Recordable and Rewritable. The first category includes CD-ROM, VCD, DVD-Video, DVD-ROM and DVD-Audio. CD-R and DVD-R belong to the second category. The rewritable optical disks include CD-RW, DVD-RAM, DVD-RW, DVD+RW, DVR Blu-ray Disc and Advanced Optical disk (AOD).

During two decades, many formats of read only and recordable optical disks have been developed, such as CD-ROM, write once read many(WORM) CD-recordable and digital versatile disk recordable(DVD-R). These disks are very popular as carriers of software, movies and many kinds of information. The disadvantages of them are the data recorded can't be updated once written.

Rewritable optical disks overcame these problems. In 1968, Ovshinsky discovered a new memory phenomenon in chalcogenide film materials [5]. People called this kind of order-disorder phase change memory effect as "Ovonic Memory". In developing this storage

medium, the main issues focused on the stability of reversible cycle characteristics, overwrite function and so on[6]. Few years later, phase change optical disks were proposed as a viable form of rewritable high-density optical data storage. However, the rewritable optical disks were contending between the phase-change rewritable optical disks and magneto-optical(MO) disks [6]. The characteristics of CD, phase-change optical disk and MO disk are listed in Table 1-1 for comparison. In table 1-1, the three columns are CD phase-change optical disk and MO disk respectively.

The marks are respectively emboss-pit, amorphous mark and magnetization domain for three technologies. The signal detection methods are through detection of reflectivity change, reflectivity change and kerr rotation change. The read/write head are optical head, optical head and two heads(optical head and magnetic head) respectively.

Although MO recording is one of the most matured technologies, phase-change optical storage has its own advantages[6]. The first is the optical head has fewer components, which can simplify the structure of the optical head. The second is that only one optical head is needed so that future development of a compact integrated optical head will be more feasible. The third is that the magnitude of the phase-change signal is several orders greater than that of the MO media.

Then, the signal readout process of phase-change optical disk technology is the same as CD-ROM disk. Similarly, the phase-change optical disk drives are the same as those of CD-ROMs. That means new generation phase-change optical disk drives, such as the DVD-RAM drive, are compatible with CD-ROMs, CD-Rs and CD-RWs, as the signal

readout process of them are all based on the reflectivity differences. For those reasons, phase change rewritable optical disks are becoming more popular than MO disks. So in this research, phase-change optical disks are mainly focused.

Table 1-1 Technology comparison of CD-ROM, phase change and MO disk

|  | CD-ROM | Phase-Change Optical disk | Magneto-optical disk |
|---|---|---|---|
| Read/write head | Optical head | Optical head | Optical head and magnetic head |
| Recording method | Emboss-Pit | Amorphous/ Crystalline states | Magnetization Reversal |
| Reading method | Diffraction | Optical constant change | Polarization Change |
| Signal detection | Reflectivity | Reflectivity | Kerr Rotation |
| Normalized readout signal Amplitude to CD-ROM | 1 | 1/4 | 1/80 |

## 1.2 Phase change recording

For phase change optical disks, writing and erasing are based on phase-change media that change form crystalline phase to amorphous phase, and vice versa. The recorded information can be obtained by detecting the reflectivity difference between the crystalline phase and amorphous phase. The phase-change leads to a change in optical reflectivity typically greater than 15% [7]. The following sections will give the details of the principle and materials of phase change recording.

### 1.2.1    Principle of phase change recording

In phase change optical disks, both writing and erasing are realized by the

crystallographic structure changes of thin films when the films are heated by laser light irradiations. Retrieval of the recorded information is performed by detecting the reflectivity changes caused by the differences of optical constants between the two states, amorphous and crystalline(Figure 1-2). There are two types of phase change materials: one is irreversible from crystalline to amorphous and the other is reversible. The materials put in practice are reversible amorphous-crystalline types. In

Table 1-2 materials reported to be the candidates are shown.
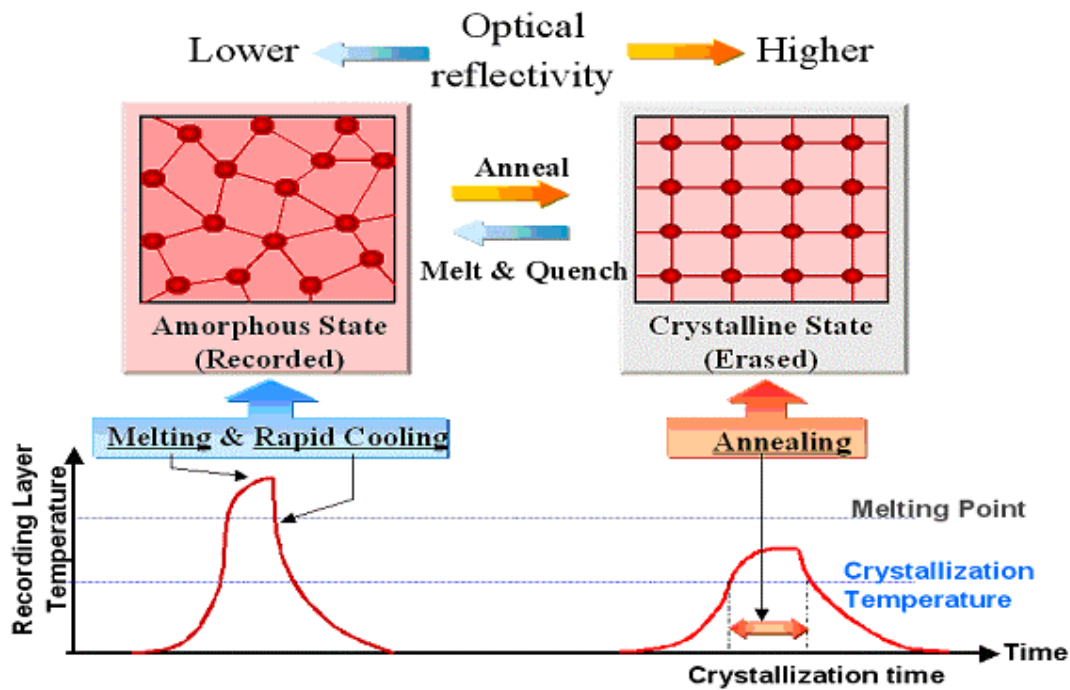


Figure 1-2 Principle of Phase Change Recording

Table 1-2 Phase change materials

| Type of Phase Change | Materials |
|---|---|
| Amorphous $\Longrightarrow$ Crystalline (Irreversible) | Te-TeO$_2$, Te-TeO$_2$-Pd Bi$_2$Te$_3$ |
| Amorphous $\Longleftrightarrow$ Crystalline (Reversible) | Ge-Te, Sb-Te Ge-Te-Sb-S Te-TeO2-Ge-Sn, Te-Ge-Sn-Au Ge-Te-Sn Sn-Se-Te Sb-Se-Te, Sb-Se Ga-Se-Te, Ga-Se-Te-Ge In-Se, In-Se-Tl-Co Ge-Sb-Te In-Se-Te, Ag-In-Sb-Te In-Sb-Te |

The amorphous state takes place by heating the material film with sufficient laser irradiation power to melt the material over its melting point and by rapid quenching to the room temperature. The crystalline state is realized by annealing the film at the temperature between the crystallizing temperature and the melting point. Although the absolute quenching rates required for amorphization are different for materials, generally the rates are in the range of $10^{7-9}$deg/sec[8].

To realize the phase change optical disks, it is required to accomplish such phase changes only by the irradiations of the laser light converged to a 1μm order in the diameter. As shown in Figure 1-3, when a laser beam having 1 μm diameter traces on the recording thin film at the linear velocity of 10m/s, irradiation time of a point on the film is only

100ns. So, all changes are required to be accomplished in this time duration. On the other hand, assuming the laser power is 10mW, the power density of the converged light spot is up to the order of 10kW/mm$^2$. It is possible to shorten the time for amorphizing because the amorphization is made by melting and quenching. But the crystallization requires a time duration determined by the physical characteristics of the material. In other word, each material has its own crystallization speed. Consequently, material for phase change optical disks are required to have not only the high thermal stability of the amorphous state but also high crystallization speed to be crystallized within the order of 100ns duration or shorter[6][9].
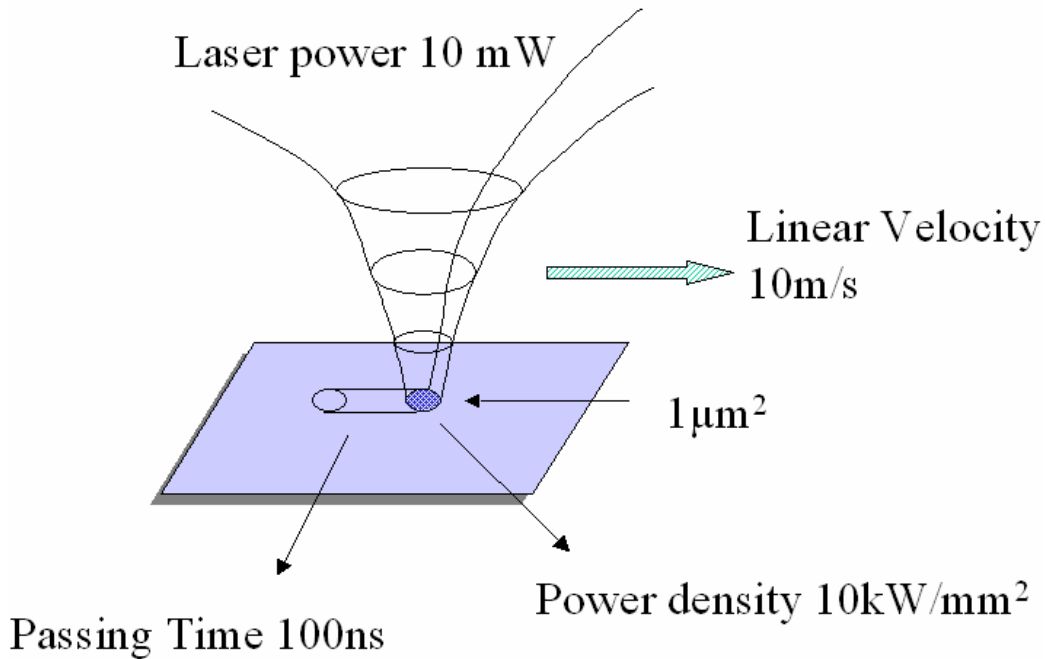


Figure 1-3 Principle of phase change optical recording

The direct overwriting is a common performance in magnetic recordings. It is however an issue for optical recording, because current optical recording use the heat mode

technology. In case of magneto-optical disks, the magnetic field modulation method is used to solve this problem.

If a thin film material has sufficiently high crystallization speed and can be crystallized within the short passing time of the laser beam, the direct overwriting is accomplished by laser power modulation between a peak recording power level and bias erasing level as shown in Figure 1-4 [10]. Whether the phase before overwriting was amorphous or crystalline, films irradiated with the peak recording power become amorphous, and those irradiated with bias erasing power are crystallized.
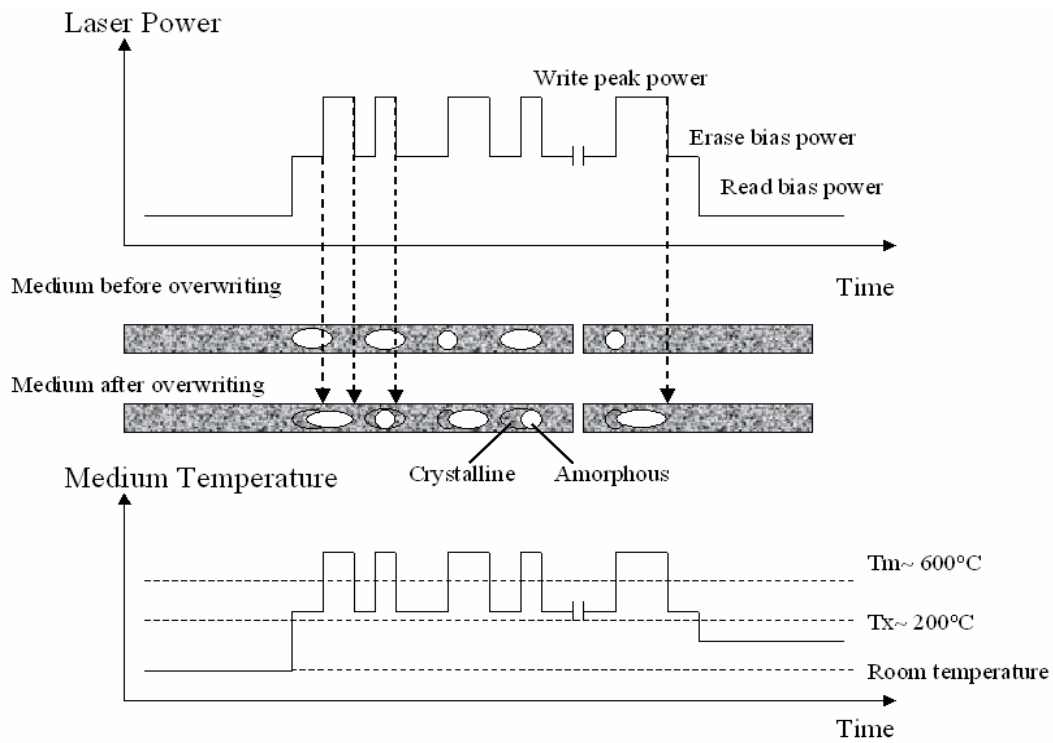
Figure 1-4 Overwriting method

## 1.2.2    Phase change materials

Ge-Sb-Te system materials have both the stability of the amorphous states and high crystallization speeds. Ge-Sb-Te, especially GeTe-Sb$_2$Te$_3$ pseudo-binary system and its neighboring compositions, have high crystallization speeds able to be crystallized within 100ns laser irradiation [8][11][13]. From Figure 1-5, the crystallization time required for the various compositions within the GeSbTe system can be observed.
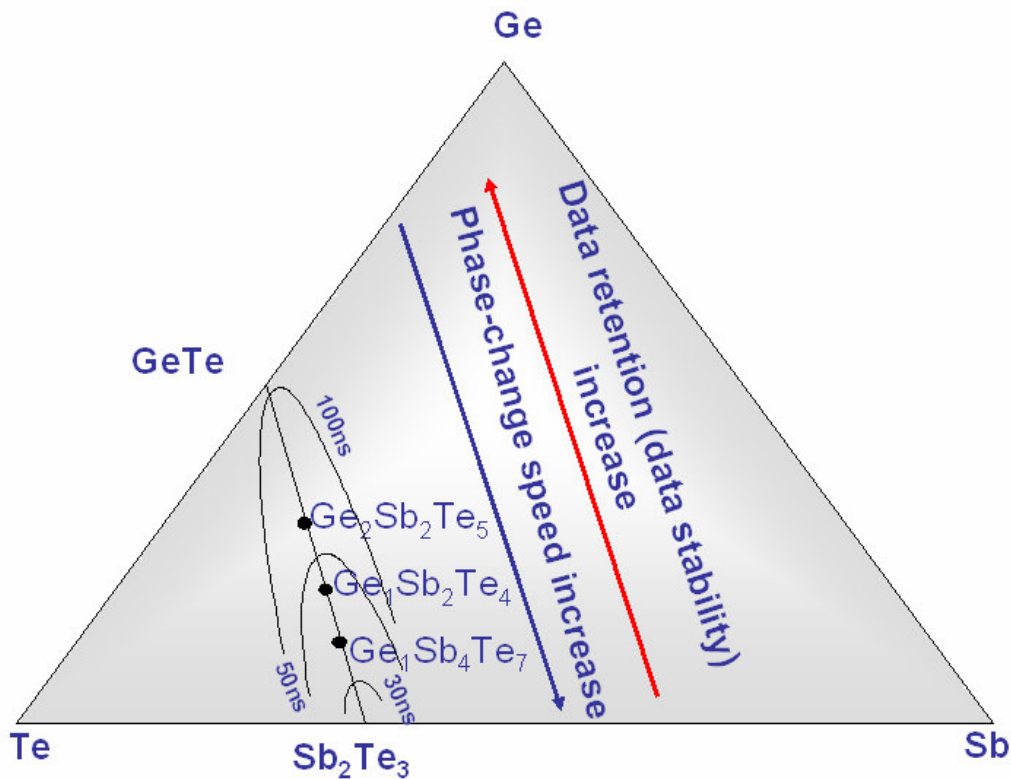


Figure 1-5 Phase transition time

These compositions show small degradation when repeating of amorphizing and crystallizing and good overwriting characteristics. It is explained by the existence of the stoichiometric compounds such as Ge$_2$Sb$_2$Te$_5$ or GeSb$_2$Te$_4$ on the GeTe-Sb$_2$Te$_3$ pseudo-binary composition line, and then these materials are supposed to be hard to segregate on

repeatedly melting. It is also reported that the compositions added excess Sb to GeTe-$Sb_2Te_3$ pseudo-binary compositions show good cyclability, because amorphizing ability and crystallizing one.

$Ge_2Sb_2Te_5$ has been selected for use throughout the project, as it is one of the more commonly used phase change recording media and been found to exhibit useful characteristics as described above.

### 1.2.3    Method to increase the recording capacity of phase change optical disks

As the high quality television and movies emerging, the higher capacity and data transfer rate disks are needed. From Figure 1-6, the trend can be seen clearly. In order to increase the recording capacity of optical disks(Figure 1-7), four basic methods can be used: reducing the spot size, improving data format(coding), exploring volumetric storage and disc fabrication [6][7]. To reduce the spot size, the methods include shorting laser wavelength($\lambda$=405nm), increasing numerical aperture(NA=0.85) of objective lens and exploring near-field and super resolution method. Modulation, multi-level coding and error correction coding are methods to increase the coding efficiency. The volumetric storage includes multi-layer recording, photo-induced recording and holographic recording. High-tech mastering and land-groove structure with deep groove[12][14] are two methods for disk fabrication to increase the disk capacity. Based on these technologies, the Blu-ray Disc(Blu-ray) and advanced optical disks(AOD) are designed for next generation phase change optical disks. The characteristics of those optical disks

can be seen from Table 1-3.
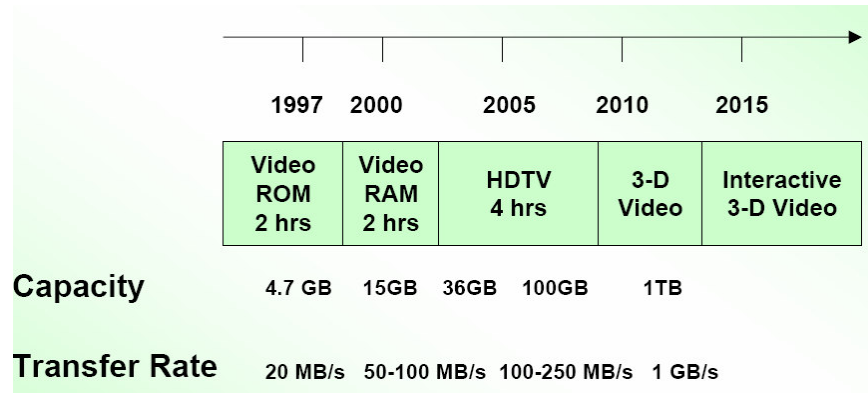


Figure 1-6 Trend for multi-media applications
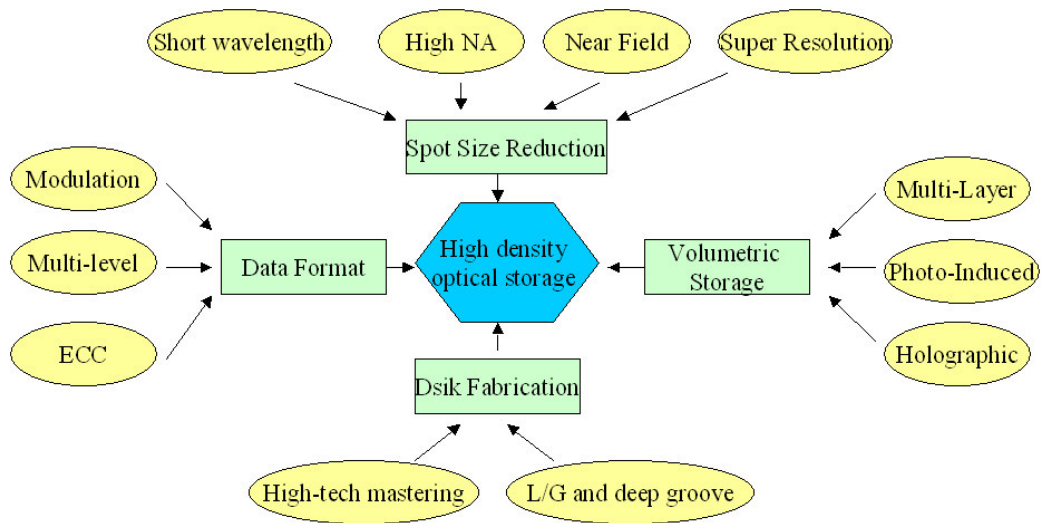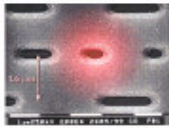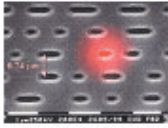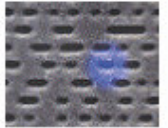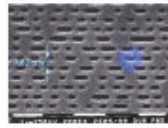


Figure 1-7 Methods to increase the recording capacity

Table 1-3 Development history of Phase change optical disks

| | CD-RW | DVD-RAM | AOD | Blu-Ray Disk |
|---|---|---|---|---|
| | | | | |
| Driving force | Digital Audio | Digital Video | High Definition TV (HD TV) | High Definition TV (HDTV) |
| Wavelength (nm) | 780 | 650 | 405 | 405 |
| NA | 0.45 | 0.6 ~ 0.65 | 0.65 | 0.85 |
| Capacity | 0.65 ~ 0.70GB | 4.7 ~ 8.5GB | 15 ~ 20GB | 23 ~ 27GB |
| Data transfer rate | 1.2Mbps | 11Mbps | Depend on coding | 36Mbps |
| Writing speed at 1x | 1.20 ~ 1.40m/s | 3.49m/s | 4.55 ~ 5.28m/s | 4.55 ~ 5.28m/s |

## 1.3 Structures of phase change optical disks

Reduction of the spot size has serious consequences for the tolerances of the recording system [7]. The decreased tilt margins due to a higher NA is effectively compensated by applying thinner substrates or cover layer, which is obvious in going from CD(1.2mm thick substrate, NA=0.45) to DVD, AOD(0.6mm substrate, NA=0.65) and then Blu-ray Disc(0.1mm cover layer, NA=0.85). Then the detail of the structures of phase change optical disks will be discussed later.

### 1.3.1 Structure of conventional DVD

Figure 1-8 shows the structure of the conventional phase change DVD. Quadri-layered thin films are formed on the polycarbonate substrate. The phase change layer is sandwiched by dielectric protective layers made of ZnS-SiO2 [15], and a reflective layer made of Al alloy is attached to the dielectric layer. The dielectric layer and the reflective metallic layer have three different functions. The first function is the mechanical protection against humidity and prevention of thermal damage to the substrate. The second is the optical enhancement by enlargement of absorption or reflective change. The

third one is the function of controlling of thermal condition during the writing and erasing processing.

In phase change optical disks, the design of each layer thickness is quite important, because all of the optical, thermo-mechanical characteristics are influenced by the layer structure.

1) Optically, those layers require large absorption efficiency of laser light and large signal amplitude corresponding to the reflectivity difference between amorphous and crystalline states.

2) Thermally, not only heating efficiency but also rapid quenching conditions for amorphization are important, thus, the design should fulfill these opposite requirements.

3) Mechanically, the material quality and the structure are required to endure the thermal stress caused by repeated heating and quenching cycles.

So a rapid quenching structure has been proposed to solve this issue. In this rapid quenching structure, the phase change layer and the dielectric layer between the phase change layer and reflective layer are sputtered thin. The thermal energy produced in the recording layer is rapidly diffused in this structure and it causes smaller damage for the other layers [16].

Using this kind of disk structure, it was reported that a million cycles of overwriting has been achieved [17]. The lifetime of the phase change optical disks is also estimated and it revealed to be sufficient long for commercial development. From the accelerated aging

test, the lifetime was estimated to be longer than 60 years in the environment of $32^{o}$C temperature and 80% relative humidity [18].

The ZnS-SiO2 thin film material for dielectric protective layer is made of mixture of small grains of ZnS and SiO2. ZnS is suitable material for phase change optical disk because it has a high refractive index of 2.4 and melting point of $1700^{o}$C. Adding of SiO2 into ZnS makes amorphous like structure is to decrease its internal stress. Figure 1-8 shows the structure of conventional DVDs.

z direction

Substrate
Al
Upper $SiO_2$-ZnS
Ge2Sb2Te5
Lower $SiO_2$-ZnS
Cover layer

Laser beam (650nm, NA=0.65)
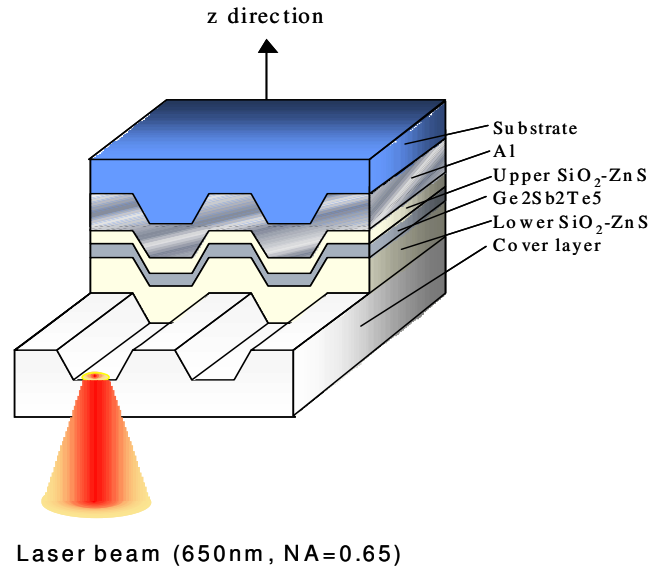
Figure 1-8 Conventional DVD disk structure

## 1.3.2    Structure of Blu-ray Disc

Figure 1-9 shows the structure of Blu-ray Disc. The structure of Blu-ray Disc is different from that of DVD. In order to make the data processing near to the laser head, the substrate is made thicker(1.1mm) while the cover layer is made thinner(0.1mm) . And the laser irradiates from the cover layer. So the Blu-ray Disc system is not compatible with

DVD system. A new optical disk drive has been designed specially for Blu-ray Disc by Sony, Philips, Hitachi, Sharp, Samsung and so on.
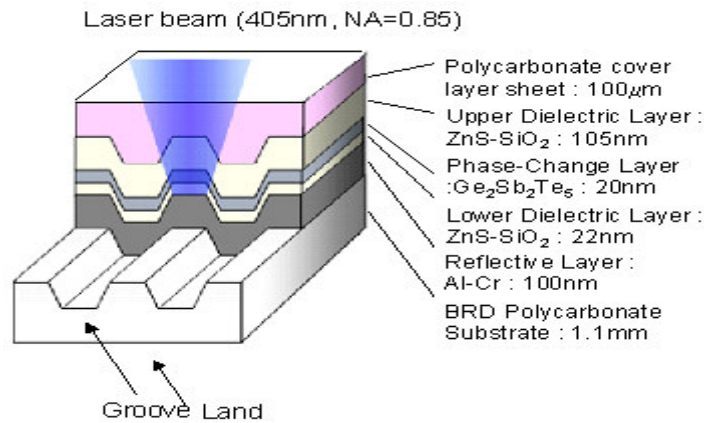
Figure 1-9 Blu-ray Disc structure

### 1.3.3    Structure of Advanced optical disks(AOD)

To compete with Blu-ray, Toshiba and NEC developed AOD. For compatibility with DVD, the structure of AOD is similar with that of DVD, applying two 0.6mm thickness layers as substrate bonded by UV-Resin. So the AOD is compatible with conventional DVD. The reflective layer material is substituted Aluminum with Silver. Figure 1-10 shows the structure of AOD.
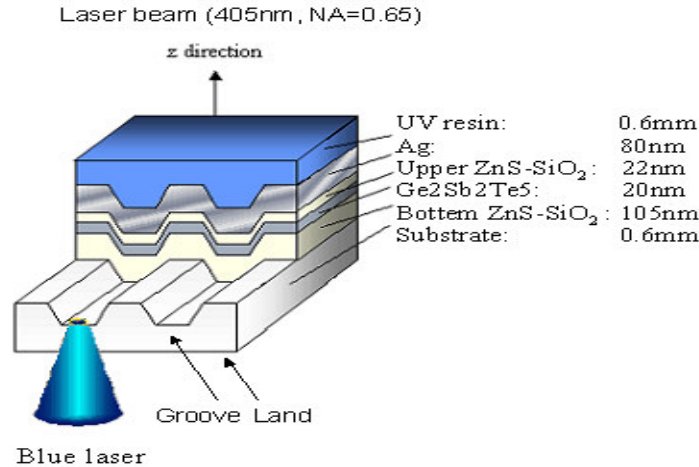
Figure 1-10 AOD disk structure

## 1.4  Motivations of the project

As development of high-definition television(HDTV) and digital movies TV, the phase change optical disks need high capacity to satisfy the demand. The easiest way to increase the data density is to utilize a shorter laser wavelength and a higher NA of objective lens to reduce the spot size. From DVD to Blu-ray Disc and AOD, the trend is very obvious [19][20]. These methods make the laser-beam spot size and the track pitches of the disks smaller and smaller. In this condition, any slight deformation in the disk will affect the data storage efficiency. As the high temperature appearing in the phase change optical disks when writing information, the thermal deformation becomes an important issue.

The working mechanism of phase change optical disk is to cause phase change under high temperature. The thermal issues of phase change optical disk are greatly concerned. Much work has been done in these areas [21]-[25]. However, very few reports are related to thermal deformation in phase change optical disk. Huh et al[26]reported the

relationships between the deformation of polycarbonate and the recording characteristics for CD. Tan et al[27] reported the substrate deformation studies on direct overwriting of phase change rewritable optical disk-DVD(Figure 1-11). From their research, it can be found that deformation affect the recording characteristics. Even worse, the deformation is accumulated and becomes larger with more writing cycle. Finally the deformation may become big enough to cause recording failed. So it is necessary to investigate the thermal deformation of phase change optical disks.
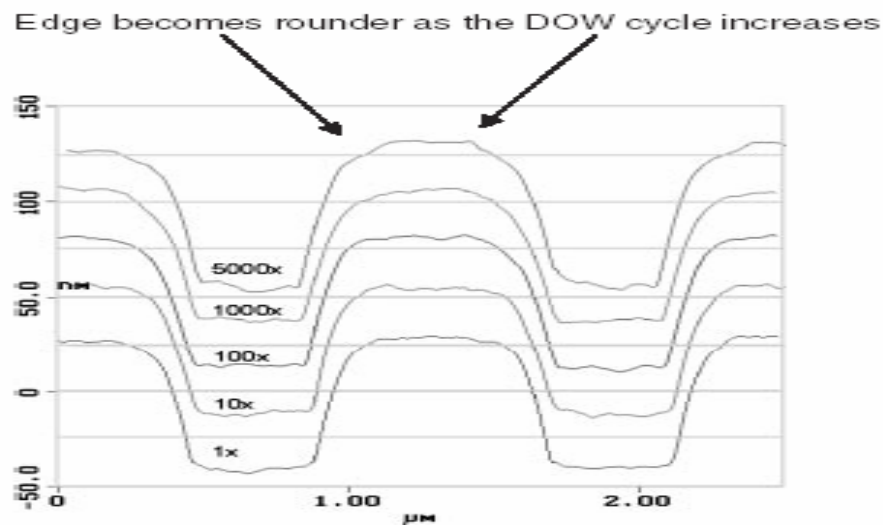
Figure 1-11 Land/Groove structure deformation after overwriting

The thermal deformation in optical disks includes elastic deformation and plastic deformation. Elastic deformation is reversible and plastic deformation is irreversible. Plastic deformation is related to elastic deformation. In general, the larger is the elastic deformation, the larger is the plastic deformation. So the plastic deformation can be decreased through decreasing the elastic deformation causing in optical disks. It is an effective method to investigate the transient elastic deformation in optical disks to find

17

the relationships between elastic deformation and optical, structure parameters. Then some methods can be found out to reduce elastic deformation to decrease the plastic deformation. In the following part, the deformation mentioned is elastic deformation without special explanation.

All previous research that was carried out on deformation of optical disks were based on the measured plastic deformation after overwriting. They did not reveal the mechanism of formation of deformation. And it is extremely difficult to physically measure the transient temperature and thermal deformation profiles within the disk as very small dimensions (less than 1µm) and very short time periods (less than 0.5s) are considered. In this research, simulation based on finite element method is chosen to analyze the thermal elastic deformation. To get deformation information of the phase change optical disk, it is very meaningful to develop a thermo-mechanical analysis simulator based on finite element method (FEM). Using this simulator, the thermal deformation of Blu-ray Disc and AOD during writing process can be calculated. The relationships between the thermal deformation and disk parameters, optical parameters can be investigated. The methods used to decrease the deformation will also be discussed.

## 1.5 Objectives

The objectives of the project are listed as follows:

1) Development of the finite element thermo-mechanical modeling and analysis simulator for high density phase change optical disks

2) Use the developed software to design and analyze the thermal properties of Blu-ray

Disc and AOD

3) Use the developed software to investigate the thermal deformation of Blu-ray Disc and AOD

## 1.6  Organization of Thesis

This thesis is organized as follows. The second chapter gives the thermo-mechanical modeling and the finite element solution for phase change optical disks. The algorithm is presented. Chapter three demonstrates the software design of thermo-mechanical analysis module. The fourth chapter focuses on the thermal modeling and analysis of Blu-ray Disc and AOD.  The fifth chapter investigates the thermal deformation of Blu-ray Disc and AOD. In the last chapter, the whole thesis is summarized and concluded. And possible future works are also mentioned in this chapter.

# Chapter 2 Thermo-mechanical modeling for Phase Change Optical Disks

In this chapter, the thermo-mechanical problem for phase change optical disks will be discussed. FEM modeling and solutions for those problems will be given.

## 2.1  Solutions for thermo-mechanical coupling problem

For thermo-mechanical coupling problem, there are two basic methods for solution. One is the direct solution method. The idea is to design coupling elements with extra freedom degrees, including displacement and temperature, and then to solve the coupling equations. For this kind of method, the algorithm is much complicated for design. And it waste too much computation time for solving the coupling equation. The other method is the sequential method.  The basic idea is that the thermal analysis is firstly performed and the temperature distribution is obtained and then the mechanical analysis is performed with the thermal strain as loads. The advantage of this method is that the algorithm is much easier than direct solution method. For the decoupling reason, the computation time for solving the equations is shorter.

So the second method was chosen to analyze the thermo-mechanical coupling problem in this research. Figure 2-1 is diagram of analysis process of the thermo-mechanical problems.
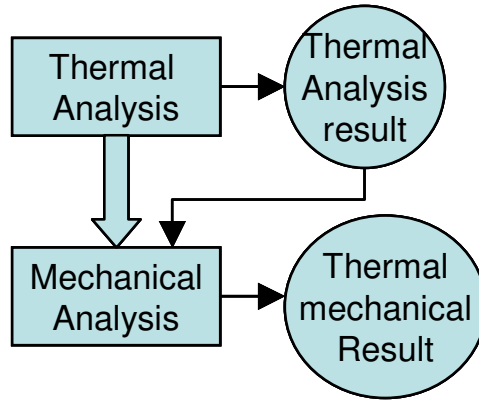
Figure 2-1 Analysis process of the thermo-mechanical problems

## 2.2  Thermal modeling for phase change optical disks

### 2.2.1     Modeling for the thermal simulation

Before 2000, all modeling and analysis of rewritable phase change optical disk do not take into consideration of the thermal effects caused by the laser light reflected by the reflective layer. Research carried out by Shi et al has shown that the thermal effect caused by the reflected laser light is significant. The differences have been found to be dependent on factors such as the wavelength, power, spot size of the laser light and the thickness of the phase change layer. So Shi et al have proposed the improved thermal model taking into consideration of both the incident and reflected laser light [28][29]. As the phase change optical disk consists of several layers, the laser light may reflect at each interface of all layers, not only the interface of reflective layer. Based on this consideration, Li et al have proposed the new thermal model [30]. In this research, the new thermal model proposed by Li et al was chosen.

## 2.2.2    Thermal modeling for phase change optical disks

Firstly, the thermal model for phase change optical disks proposed by Shi et al will be given. The thermal model can be expressed by the fundamental equations based on linear transient thermal conduction, as follows:

$$\nabla^2 T(r,t) + \frac{1}{k} g(r,t) = \frac{1}{\alpha} \frac{\partial T(r,t)}{\partial t}, \tag{2-1}$$

where $\alpha = \dfrac{k}{\rho C_p}$ is thermal diffusivity; $\rho$ is density; $C_p$ is specific heat, T is temperature, k is thermal conductivity coefficient; g(r,t) is the amount of heat energy per unit time and volume generated in the phase change layer.

The procedure for calculating heat generation g(r,t) is expressed as follows. The laser beam intensity distribution is assumed to be Gaussian:

$$I = I_0 \exp \left( - \frac{r^2}{r_0^2} \right), \tag{2-2}$$

where $I_0$ is the incident light intensity at the center of the laser beam,

$$I_0 = \frac{P}{\pi r_0^2}, \tag{2-3}$$

where P is the laser power; $r_0$ is the beam radius.

In this model, both the incident and reflected laser light are taken into consideration for the heating source. Then the heat generated in the phase change layer g(r, t) by the laser irradiation can be decomposed into two parts written as follows:

$$I_1 = A_1 I_0 s(t) \beta \exp\left[-\frac{(x-vt)^2 + y^2}{r_0^2}\right] \exp\left[-\beta(z - z_2)\right], \tag{2-4}$$

$$I_2 = A_2 I_0 s(t) \beta \exp\left[-\frac{(x-vt)^2 + y^2}{r_0^2}\right] \exp\left[-\beta(z_3 - z)\right] \exp\left[-\beta(z_3 - z_2)\right], \tag{2-5}$$

$$g(r,t) = \frac{I_1 + I_2}{\pi r_0^2}, \tag{2-6}$$

where $I_1$ and $I_2$ represent the contributions from the propagating and reflection light in the phase change layer respectively; $A_1$ and $A_2$ are the attenuation factors, which can be calculated by optical method; $\beta$ is the absorption coefficient given by $\beta=4\pi k/\lambda$ ; k is the optical extinction coefficient and $\lambda$ is the wavelength of the laser. z is the distance into the phase change disk measured from the surface of the substrate layer; z2 represents the distance to the interface of the phase change and first dielectric layer from the surface of the substrate; z3 is the distance to the interface of the phase change and second dielectric layer. Both of the decrease factor $A_1$ and $A_2$ can be calculated by using optical characteristic matrix method [14].

Then the thermal model proposed by Li et al will be given. The thermal model can be expressed by the fundamental equations based on linear transient thermal conduction, as follows:

$$\rho c \frac{\partial T}{\partial t} - \frac{\partial}{\partial x}\left(k_x \frac{\partial T}{\partial x}\right) - \frac{\partial}{\partial y}\left(k_y \frac{\partial T}{\partial y}\right) - \frac{\partial}{\partial z}\left(k_z \frac{\partial T}{\partial z}\right) - Q = 0, \tag{2-7}$$

where $\rho$ is density; $c$ is specific heat; $T$ is temperature; $k_x$, $k_y$, $k_z$ is thermal conductivity in three dimensions; $Q$ is heat density due to the irradiation of the incident laser beam; t is time; $x$, $y$, $z$ is coordinates.

Considering the interface effect of the thin films, $k_z$(z refers to thickness or z-direction of the thin films) is related to the bulk thermal conductivity, $k$, as:

$$k_z = \alpha k \ , \tag{2-8}$$

where $\alpha$ is a ratio within the range of [0, 1]. The ratio may be approximately estimated by the comparison of the readout waveforms of the marks from the experiment with the simulated marks.

Different recording technologies yield different heat generation. The heat generated, Q, is determined by the light intensity distribution. For a Gaussian laser beam, the heat density distribution Q(x, y, z, t) in the recording layer at a point (x, y, z) and time t with a focus point $(x_0, y_0, z_0)$ on the incident interface of the phase-change layer is given by:

$$Q(x,y,z,t) = \frac{\gamma \beta I_0(t)}{\pi r^2} \exp\left[ - \frac{(x - x_0 - vt)^2 + (y - y_0)^2}{r^2} \right] \exp[- \beta(z - z_0)], \tag{2-9}$$

where $I_0$ is the incident light intensity at the center of the laser beam,

$$I_0 = \frac{P}{\pi r^2} \ , \tag{2-10}$$

where P is the laser power; r is the laser beam radius; $\beta$ is the absorption coefficient given by $\beta = 4\pi k / \lambda$ ; k is the optical extinction coefficient; $\lambda$ is the wavelength of the laser; $\gamma$ is Ratio of the energy of the incident light reaching the incident interface of the phase change layer.

The parameter $\gamma$ may be determined by the optical characteristic matrix method as

follows:

$$\begin{bmatrix} B \\ C \end{bmatrix} = \left( \prod_{j}^{l} \begin{bmatrix} \cos \delta_j & \dfrac{i}{\eta_j} \sin \delta_j \\ i\eta_j \sin \delta_j & \cos \delta_j \end{bmatrix} \right) \begin{bmatrix} 1 \\ \eta_{l+1} \end{bmatrix},$$

(2-11)

where B and C are parameters for determining the admittance of the thin film assembly. $\eta_j$ and $\eta_{l+1}$ are the complex refractive indices of the thin film media and outgoing medium, respectively. If the incident light is normal to the surface of the medium, $\delta_j$ can be defined as follows:

$$\delta_j = \frac{2\pi}{\lambda}(n_j - ik_j)d_j,$$

(2-12)

where $n_j$ is the refractive index, $k_j$ is the extinction, $d_j$ is the film thickness, $\lambda$ is the wavelength of light.

The energy reflectance R and transmittance T of the incident light can be characterized in terms of B and C as follows:

$$R = \left( \frac{\eta_0 B - C}{\eta_0 B + C} \right) \left( \frac{\eta_0 B - C}{\eta_0 B + C} \right)^{*},$$

(2-13)

$$T = \frac{4\eta_0 \eta_{l+1}}{(\eta_0 B + C)(\eta_0 B + C)^{*}},$$

(2-14)

where * stands for a conjugated complex number. The energy absorbance A is therefore calculated from A=1-R-T. For the standard four-layer structure(dielectric/phase change layer/dielectric/reflective layer), the phase change layer mainly absorbs the energy of the incident laser beam. Thus it is reasonable to assume that the value of parameter $\gamma$ is equal to A.

### 2.2.3 Boundary condition

i) Boundary condition at the surface

The heat source is far from the surface and the surfaces of the optical disk are much lower than the heat generating area. To simplify the modeling, the effects caused by convection at the surface of the disk have been neglected. Thus the temperature on the top and bottom surface of the optical disk is fixed at constant room temperature at $27^{\circ}$C.

ii) Boundary condition at the interface

It is assumed that all the layers are in perfect thermal contact at the interface in the phase change optical disk. Thus the temperature and heat flux at the interface is continuous.

### 2.2.4 Initial condition

The initial temperature in the optical disks in specified to be the room temperature. And the room temperature is assumed to be $27^{\circ}$C.

$$T_0 \; = \; T_{room} \; = \; 27\,^{\circ}C. \qquad\qquad (2\text{-}15)$$

## 2.3 FEM solutions for 3D thermal conduction problem

### 2.3.1 Element chosen for thermal analysis based on FEM

The temperature in the element can be expressed by polynomial of coordinate. For

8-node element, the degree of polynomial should be equal to eight. The 3D 8-node
isoparametric element was chosen to perform the thermal analysis as Figure 2-2. The
shape functions for this type of element are listed as follows.
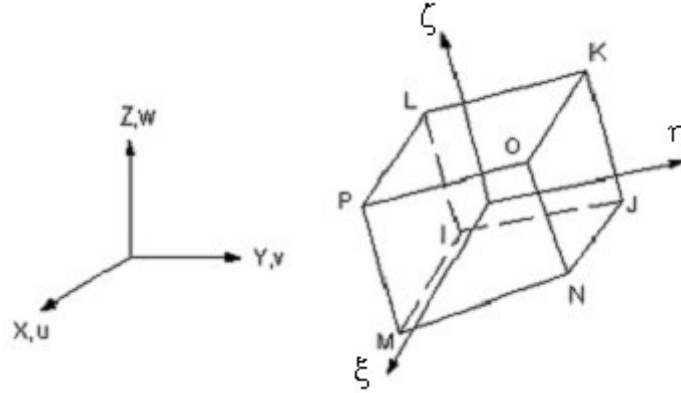


Figure 2-2  8-node 3D solid brick element for thermal analysis

The element is designed in natural coordinate

$$
\begin{aligned}
&N_1 = \frac{1}{8}(1-\xi)(1-\eta)(1-\zeta) && N_2 = \frac{1}{8}(1+\xi)(1-\eta)(1-\zeta) \\
&N_3 = \frac{1}{8}(1+\xi)(1+\eta)(1-\zeta) && N_4 = \frac{1}{8}(1-\xi)(1+\eta)(1-\zeta) \\
&N_5 = \frac{1}{8}(1-\xi)(1-\eta)(1+\zeta) && N_6 = \frac{1}{8}(1+\xi)(1-\eta)(1+\zeta) \\
&N_7 = \frac{1}{8}(1+\xi)(1+\eta)(1+\zeta) && N_8 = \frac{1}{8}(1-\xi)(1+\eta)(1+\zeta)
\end{aligned}
\tag{2-16}
$$

where $\xi$, $\eta$, $\zeta$ are natural coordinates.

So the temperature can be written in the following form:

$$
T = \sum_{i=1}^{8} N_i(x, y, z) \cdot T_i .
\tag{2-17}
$$

And then substituting the boundary conditions into the governing equation and we can get the Galerkin weighted residual

$$R_\Omega = \frac{\partial}{\partial x}\left(k_x \frac{\partial \tilde{T}}{\partial x}\right) + \frac{\partial}{\partial y}\left(k_y \frac{\partial \tilde{T}}{\partial y}\right) + \frac{\partial}{\partial z}\left(k_z \frac{\partial \tilde{T}}{\partial z}\right) + Q - \rho c \frac{\partial \tilde{T}}{\partial t}$$

$$.R_{\Gamma_2} = k_x \frac{\partial \tilde{T}}{\partial x}n_x + k_y \frac{\partial \tilde{T}}{\partial y}n_y + k_z \frac{\partial \tilde{T}}{\partial z}n_z - q \qquad . \qquad (2\text{-}18)$$

$$R_{\Gamma_3} = k_x \frac{\partial \tilde{T}}{\partial x}n_x + k_y \frac{\partial \tilde{T}}{\partial y}n_y + k_z \frac{\partial \tilde{T}}{\partial z}n_z - h\left(T_0 - \tilde{T}\right)$$

If the residual is reduced as close to zero as possible, the solution is accurate.

$$\int_\Omega R_\Omega w_1 d\Omega + \int_{\Gamma_2} R_{\Gamma_2} w_2 d\Gamma_2 + \int_{\Gamma_3} R_{\Gamma_3} w_3 d\Gamma_3 = 0, \qquad (2\text{-}19)$$

Choose the Galerkin weighted function

$$\begin{aligned} w_1 &= N_i \ (i = 1, 2, \cdots, 8) \\ w_2 &= w_3 = -w_1 \end{aligned}, \qquad (2\text{-}20)$$

so we can get the following equation

$$C\,\dot{T} + KT \ = \ P \ , \qquad (2\text{-}21)$$

where C is thermal capacity matrix; K is thermal conduction matrix; Both C and K are symmetrical positive definitely; P is temperature load vector; T is node temperature vector, where

$$K_{ij} = \sum_e K_{ij}^e + \sum_e H_{ij}^e$$

$$C_{ij} = \sum_e C_{ij}^e \qquad\qquad , \qquad (2\text{-}22)$$

$$P_i = \sum_e P_Q^e + \sum_e P_{q_i}^e + \sum_e P_{H_i}^e$$

and the element parameter

$$H_{ij}^e = \int_{\Gamma_3^e} h N_i N_j d\Gamma$$

$$C_{ij}^e = \int_{\Omega^e} \rho c N_i N_j d\Omega$$

$$P_Q^e = \int_{\Omega^e} Q N_i d\Omega \qquad , \qquad (2\text{-}23)$$

$$P_{q_i}^e = \int_{\Gamma_2^e} q N_i d\Gamma$$

$$P_{H_i}^e = \int_{\Gamma_3^e} h T_a N_i d\Gamma$$

And then we need to solve the one variable and one-degree differential equation,

$$C(T_{n+\alpha}, t_{n+\alpha}) \dot{T}_{n+\alpha} + K(T_{n+\alpha}, t_{n+\alpha}) = P(T_{n+\alpha}, t_{n+\alpha}), \qquad (2\text{-}24)$$

where

$$C_{n+\alpha} = C(T_{n+\alpha}, t_{n+\alpha})$$

$$K_{n+\alpha} = K(T_{n+\alpha}, t_{n+\alpha})$$

$$P_{n+\alpha} = P(T_{n+\alpha}, t_{n+\alpha})$$

$$T_{n+\alpha} = (1-\alpha)T_n + \alpha T_{n+1}$$

$$\dot{T}_{n+\alpha} = (T_{n+1} - T_n)/\Delta t = \Delta T / \Delta t$$

$$t_{n+\alpha} = t_n + \alpha \Delta t$$

Substituting these equations in the matrix equation, we obtain

$$\left[ \frac{C_{n+\alpha}}{\Delta t} + \alpha K_{n+\alpha} \right] \Delta T = P_{n+\alpha} - K_{n+\alpha} T_n . \qquad (2\text{-}25)$$

If the formula is defined as following,

$$K' = \left[ \frac{C_{n+\alpha}}{\Delta t} + \alpha K_{n+\alpha} \right],$$

$$P' = P_{n+\alpha} - K_{n+\alpha}T_n$$

(2-26)

Then the equations can be got

$$K' \cdot \Delta T = P'.$$

(2-27)

The method of Triangle decomposition method is used to solve the equations and ΔT is got. Then following the equation

$$T_{n+1} = T_n + \Delta T,$$

(2-28)

the temperature $T_{n+1}$ at t+Δt can be got.

## 2.3.2    Method to solve linear equations

There are two types of solution method for linear equations: direct method and iterative method [31]. Direct method includes: Gauss elimination method, Gauss and Jordan elimination method, Triangle decomposition method, Chase method, Block division method, and Wavefront method. Iterative method includes: Jacobi iterative method, Gauss-Sidel iterative method and Over relaxation method. Direct method is more efficient while iterative method is more precise when the equations are in huge orders.

In this research, the method of Triangular factorization [32] is used to solve the linear equations, as the coefficient matrices are symmetric. The algorithm shows as follows:

$$K \cdot \delta = P,$$

(2-29)

where K is the global stiffness matrix, $\delta$ is the vector to be solved, P is the global load

vector

Based on matrix decomposition theory,

$$K = L \cdot S, \tag{2-30}$$

where S is up-triangle matrix and L is sub-triangle matrix as follows:

$$L = \begin{bmatrix} 1 & & & \\ l_{21} & 1 & & \\ \vdots & \ddots & \ddots & \\ l_{n1} & l_{n2} & \cdots & 1 \end{bmatrix} \qquad S = \begin{bmatrix} S_{11} & S_{12} & \cdots & S_{1n} \\ & S_{22} & \ddots & S_{2n} \\ & & \ddots & \vdots \\ & & & S_{nn} \end{bmatrix}. \tag{2-31}$$

Then decomposition of K by L and S is done,

$$L \cdot S \cdot \delta = P, \tag{2-32}$$

and then multiply the reverse of L on both side,

$$S \cdot \delta = L^{-1} \cdot P. \tag{2-33}$$

set $L^{-1} \cdot P = V$, then

$$S \cdot \delta = V. \tag{2-34}$$

So two steps can be used to solve the equation

(1) Get the V

As $L \cdot V = P$ and L is sub-triangle matrix, so V can be gotten after solving the following equations.

$$L \quad V \quad = \quad P \tag{2-35}$$

(2) Get the variable $\delta$

As $S \cdot \delta = V$ and S is the up-triangle matrix, so $\delta$ can be obtained after solving the following equations.



$$S \quad \delta \quad = \quad V \tag{2-36}$$

Algorithm lists as follows:

Set $D \cdot L^T = S$, then $K = L \cdot D \cdot L^T$, so

$$K_{ij} = \sum_{r=1}^{i} l_{ri}^{\ T} d_{rr} l_{rj}^{\ T} = \sum_{r=1}^{i-1} l_{ri}^{\ T} d_{rr} l_{rj}^{\ T} + l_{ii}^{\ T} d_{ii} l_{rj}^{\ T}, \tag{2-37}$$

Noted:

$$l_{ii}^{T} = 1, \ D = \begin{bmatrix} d_{11} & 0 & \cdots & 0 \\ 0 & d_{22} & \ddots & \vdots \\ \vdots & \ddots & \ddots & 0 \\ 0 & \cdots & 0 & d_{NN} \end{bmatrix}, \tag{2-38}$$

then

$$d_{ii}l_{rj}^{T} = S_{ij} = K_{ij} - \sum_{r=1}^{i-1} l_{ri}^{T} d_{rr} l_{rj}^{T}$$

$$l_{ij} = S_{ij} / d_{ii} \tag{2-39}$$

$$d_{ii} = S_{ii}$$

Procedure used to realize the algorithms as follows:

$$i = 1$$

$$S_{1j} = K_{1j} (j \geq 1)$$

$$d_{11} = S_{11} = K_{11}$$

$$l_{1j}^{T} = S_{1j} / d_{11} (j > 1)$$

$$\dots \dots, \tag{2-40}$$

$$i = i$$

$$S_{ij} = K_{ij} (j \geq i)$$

$$d_{ii} = S_{ii}$$

$$l_{ij}^{T} = S_{ij} / d_{ii} (j > i)$$

## 2.4 Mechanical analysis for phase change optical disks

### 2.4.1    Principle of minimum potential energy

Firstly some basic relation among stress, strain and displacement will be given.

Hookean law gives the relation between stress $\{\sigma\}$, strain $\{\varepsilon\}$ and thermal strain $\{\varepsilon_o\}$ if

considered the thermal effects,

$$\{\sigma\} = [D](\{\varepsilon\} - \{\varepsilon_0\}), \tag{2-41}$$

where [D] is the isotropic elastic matrix,

$$[D] = \frac{E \cdot (1-v)}{(1+v)(1-2v)} \begin{bmatrix} 1 & \dfrac{v}{1-v} & \dfrac{v}{1-v} & 0 & 0 & 0 \\ \dfrac{v}{1-v} & 1 & \dfrac{1}{1-v} & 0 & 0 & 0 \\ \dfrac{v}{1-v} & \dfrac{1}{1-v} & 1 & 0 & 0 & 0 \\ 0 & 0 & 0 & \dfrac{1-2v}{2(1-v)} & 0 & 0 \\ 0 & 0 & 0 & 0 & \dfrac{1-2v}{2(1-v)} & 0 \\ 0 & 0 & 0 & 0 & 0 & \dfrac{1-2v}{2(1-v)} \end{bmatrix},$$

where E is Elastic modules, $v$ is Poisson Ratio.

The geometry equation demonstrates the relation between strain $\{\varepsilon\}$ and displacement $\{\delta\}$,

$$\{\varepsilon\} = [L] \times \{\delta\} = [L][N]\{f\} = [B]\{f\}, \tag{2-42}$$

where $\{f\}$ is the node displacement vector, $\{\delta\}$ is the displacement of any point, [L] is differential operator, [B] is the strain interpolation matrix, [N] is the shape function.

$$
[L] = \begin{bmatrix}
\dfrac{\partial}{\partial x} & 0 & 0 \\[8pt]
0 & \dfrac{\partial}{\partial y} & 0 \\[8pt]
0 & 0 & \dfrac{\partial}{\partial z} \\[8pt]
\dfrac{\partial}{\partial y} & \dfrac{\partial}{\partial x} & 0 \\[8pt]
\dfrac{\partial}{\partial z} & 0 & \dfrac{\partial}{\partial x} \\[8pt]
0 & \dfrac{\partial}{\partial z} & \dfrac{\partial}{\partial y}
\end{bmatrix},
$$

as $[B] = [L] \cdot [N]$, then

$$
[B] = \begin{bmatrix}
\dfrac{\partial N_1}{\partial x} & & & \dfrac{\partial N_2}{\partial x} & & \cdots & \dfrac{\partial N_2}{\partial x} & \\[8pt]
& \dfrac{\partial N_1}{\partial y} & & & \dfrac{\partial N_2}{\partial y} & \cdots & & \dfrac{\partial N_2}{\partial y} \\[8pt]
& & \dfrac{\partial N_1}{\partial z} & & \dfrac{\partial N_2}{\partial y} & \cdots & & \dfrac{\partial N_2}{\partial z} \\[8pt]
\dfrac{\partial N_1}{\partial y} & \dfrac{\partial N_1}{\partial x} & & \dfrac{\partial N_2}{\partial y} & \dfrac{\partial N_2}{\partial x} & \cdots & \dfrac{\partial N_2}{\partial y} & \dfrac{\partial N_2}{\partial x} \\[8pt]
\dfrac{\partial N_1}{\partial z} & & \dfrac{\partial N_1}{\partial x} & \dfrac{\partial N_2}{\partial z} & & \dfrac{\partial N_2}{\partial x} & \cdots & \dfrac{\partial N_2}{\partial z} & \dfrac{\partial N_2}{\partial x} \\[8pt]
& \dfrac{\partial N_1}{\partial z} & \dfrac{\partial N_1}{\partial y} & & \dfrac{\partial N_2}{\partial z} & \dfrac{\partial N_2}{\partial y} & \cdots & \dfrac{\partial N_2}{\partial z} & \dfrac{\partial N_2}{\partial y}
\end{bmatrix}_{6 \times 24}.
$$

To solve the displacement distribution, the principle of minimum potential energy [33][34] was used to perform the mechanical analysis.

$$
\partial \Pi_p / \partial \delta = 0, \tag{2-43}
$$

where $\delta$ is displacement, $\Pi_p$ is potential energy which is

$$
\Pi_p = U + W. \tag{2-44}
$$

The strain energy $U$ is

35

$$U = \frac{1}{2}\iiint_V (\{\varepsilon\}^T - \{\varepsilon_0\}^T) \cdot [D] \cdot (\{\varepsilon\}^T - \{\varepsilon_0\}^T)dV , \tag{2-45}$$

where thermal strain is

$$\{\varepsilon_0\} = \alpha(T - T_0)[1 \quad 1 \quad 1 \quad 0 \quad 0 \quad 0]^T , \tag{2-46}$$

where $\{\varepsilon\}$ is the total strain vector, $\{\varepsilon_0\}$, the thermal strain vector, $[D]$, the isotropic elastic matrix, $\alpha$, the coefficients of thermal expansion, $T$, the current temperature, and $T_0$, the initial temperature.

The work $W$ done due to external load is

$$W = -[\iiint_V \{\delta\}^T \{P_V\}dV + \iint_A \{\delta\}^T \{P_s\}dA + \{f\}^T \{F_c\}] , \tag{2-47}$$

where $\{\delta\}$ is the node displacement vector, $\{f\}$ is the displacement of any point; $\{P_v\}$ is the load in volume; $\{P_s\}$ is the load on surface; and $\{F_c\}$ is the load on node.

Substituting equations (2-43) and (2-45) to (2-41), then

$$\iiint_V [B]^T [D][B]dV \cdot \{\delta\} - \iiint_V [N]^T \{P_V\}dV - \iint_A [N]^T \{P_A\}dA - \{F_C\} - \iiint_V [B]^T [D]\{\varepsilon_0\}dV = 0 . \tag{2-48}$$

Assume

$$[K] = \iiint_V [B]^T [D][B]dV , \tag{2-49}$$

$$\{F\} = \iiint_V [N]^T \{P_V\}dV + \iint_A [N]^T \{P_A\}dA + \{F_C\} + \iiint_V [B]^T [D]\{\varepsilon_0\}dV , \tag{2-50}$$

the following equation can be got

$$[K] \cdot \{\delta\} = \{F\}. \tag{2-51}$$

## 2.4.2     Displacement boundary conditions

The top and bottom surface of the phase change optical disks are far from the recording layer, so the displacements are assumed to be constrained on the top and bottom surface. The displacements of nodes on top and bottom surface are specified to zero in three dimensions.

# 2.5   FEM solutions for thermo-mechanical problem

## 2.5.1     Element chosen for thermo-mechanical analysis based on FEM

The displacement in the element can be expressed by polynomial of coordinate. For 8-node 3-dimension solid brick element, the degree of polynomial should be equal to eight. The 3D 8-node isoparametric element is chosen to perform the mechanical analysis as Figure 2-3. The shape functions for this type of element are listed as follows.
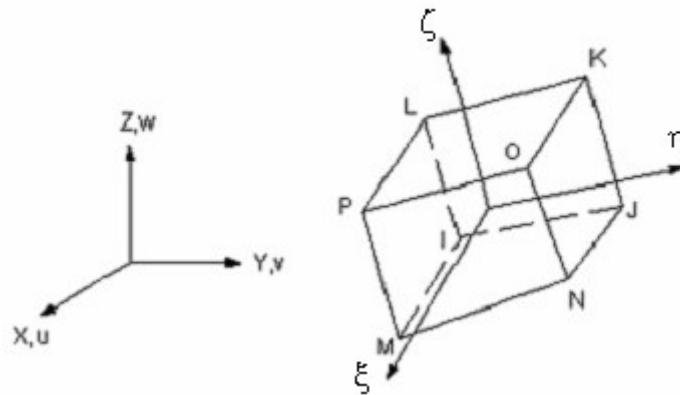


Figure 2-3 8-node 3D solid brick element for mechanical analysis

The element is designed in natural coordinate

$$N_1 = \frac{1}{8}(1-\xi)(1-\eta)(1-\zeta) \quad N_2 = \frac{1}{8}(1+\xi)(1-\eta)(1-\zeta)$$

$$N_3 = \frac{1}{8}(1+\xi)(1+\eta)(1-\zeta) \quad N_4 = \frac{1}{8}(1-\xi)(1+\eta)(1-\zeta)$$

$$N_5 = \frac{1}{8}(1-\xi)(1-\eta)(1+\zeta) \quad N_6 = \frac{1}{8}(1+\xi)(1-\eta)(1+\zeta)$$

$$N_7 = \frac{1}{8}(1+\xi)(1+\eta)(1+\zeta) \quad N_8 = \frac{1}{8}(1-\xi)(1+\eta)(1+\zeta)$$

(2-52)

where $\xi$, $\eta$, $\zeta$ are natural coordinates.

$$\{f\} = \{u \quad v \quad w\}^T$$

$$= \begin{bmatrix} N_1 & & & N_2 & & & \cdots & N_8 & & \\ & N_1 & & & N_2 & & & \cdots & & N_8 & \\ & & N_1 & & & N_2 & \cdots & & & & N_8 \end{bmatrix} \cdot \begin{Bmatrix} u_1 \\ v_1 \\ w_1 \\ \vdots \\ u_8 \\ v_8 \\ w_8 \end{Bmatrix},$$

(2-53)

The isoparametric element

$$x = \sum_{i=1}^{8} N_i \cdot x_i \quad y = \sum_{i=1}^{8} N_i \cdot y_i \quad z = \sum_{i=1}^{8} N_i \cdot z_i,$$

(2-54)

then

$$\begin{Bmatrix} \dfrac{\partial N_i}{\partial \xi} \\ \dfrac{\partial N_i}{\partial \eta} \\ \dfrac{\partial N_i}{\partial \zeta} \end{Bmatrix} = \begin{bmatrix} \dfrac{\partial x}{\partial \xi} & \dfrac{\partial y}{\partial \xi} & \dfrac{\partial z}{\partial \xi} \\ \dfrac{\partial x}{\partial \eta} & \dfrac{\partial y}{\partial \eta} & \dfrac{\partial z}{\partial \eta} \\ \dfrac{\partial x}{\partial \zeta} & \dfrac{\partial y}{\partial \zeta} & \dfrac{\partial z}{\partial \zeta} \end{bmatrix} \cdot \begin{Bmatrix} \dfrac{\partial N_i}{\partial x} \\ \dfrac{\partial N_i}{\partial y} \\ \dfrac{\partial N_i}{\partial z} \end{Bmatrix} = J \cdot \begin{Bmatrix} \dfrac{\partial N_i}{\partial x} \\ \dfrac{\partial N_i}{\partial y} \\ \dfrac{\partial N_i}{\partial z} \end{Bmatrix},$$

(2-55)

and Jacobi matrix J can be calculated by the derivation of shape function in natural

coordinate multiplied with node coordinates in global coordinates as follows:

$$
J \equiv
\begin{bmatrix}
\dfrac{\partial x}{\partial \xi} & \dfrac{\partial y}{\partial \xi} & \dfrac{\partial z}{\partial \xi} \\[2mm]
\dfrac{\partial x}{\partial \eta} & \dfrac{\partial y}{\partial \eta} & \dfrac{\partial z}{\partial \eta} \\[2mm]
\dfrac{\partial x}{\partial \zeta} & \dfrac{\partial y}{\partial \zeta} & \dfrac{\partial z}{\partial \zeta}
\end{bmatrix}
=
\begin{bmatrix}
\sum\limits_{i=1}^{8} \dfrac{\partial N_i}{\partial \xi} x_i & \sum\limits_{i=1}^{8} \dfrac{\partial N_i}{\partial \xi} y_i & \sum\limits_{i=1}^{8} \dfrac{\partial N_i}{\partial \xi} z_i \\[3mm]
\sum\limits_{i=1}^{8} \dfrac{\partial N_i}{\partial \eta} x_i & \sum\limits_{i=1}^{8} \dfrac{\partial N_i}{\partial \eta} y_i & \sum\limits_{i=1}^{8} \dfrac{\partial N_i}{\partial \eta} z_i \\[3mm]
\sum\limits_{i=1}^{8} \dfrac{\partial N_i}{\partial \zeta} x_i & \sum\limits_{i=1}^{8} \dfrac{\partial N_i}{\partial \zeta} y_i & \sum\limits_{i=1}^{8} \dfrac{\partial N_i}{\partial \zeta} z_i
\end{bmatrix}.
$$

$$
=
\begin{bmatrix}
\dfrac{\partial N_1}{\partial \xi} & \dfrac{\partial N_2}{\partial \xi} & \cdots & \dfrac{\partial N_8}{\partial \xi} \\[2mm]
\dfrac{\partial N_1}{\partial \eta} & \dfrac{\partial N_2}{\partial \eta} & \cdots & \dfrac{\partial N_8}{\partial \eta} \\[2mm]
\dfrac{\partial N_1}{\partial \zeta} & \dfrac{\partial N_2}{\partial \zeta} & \cdots & \dfrac{\partial N_8}{\partial \zeta}
\end{bmatrix}
\cdot
\begin{bmatrix}
x_1 & y_1 & z_1 \\
x_2 & y_2 & z_2 \\
\vdots & \vdots & \vdots \\
x_8 & y_8 & z_8
\end{bmatrix}
$$

(2-56)

Finally the derivation of shape function in global coordinate can be obtained,

$$
\begin{Bmatrix}
\dfrac{\partial N_i}{\partial x} \\[2mm]
\dfrac{\partial N_i}{\partial y} \\[2mm]
\dfrac{\partial N_i}{\partial z}
\end{Bmatrix}
= J^{-1} \cdot
\begin{Bmatrix}
\dfrac{\partial N_i}{\partial \xi} \\[2mm]
\dfrac{\partial N_i}{\partial \eta} \\[2mm]
\dfrac{\partial N_i}{\partial \zeta}
\end{Bmatrix} .
$$

(2-57)

For integration, the relationship between global coordinate system and natural coordinate system can be described as follows:

$$
dV =
\begin{vmatrix}
\dfrac{\partial x}{\partial \xi} & \dfrac{\partial y}{\partial \xi} & \dfrac{\partial z}{\partial \xi} \\[2mm]
\dfrac{\partial x}{\partial \eta} & \dfrac{\partial y}{\partial \eta} & \dfrac{\partial z}{\partial \eta} \\[2mm]
\dfrac{\partial x}{\partial \zeta} & \dfrac{\partial y}{\partial \zeta} & \dfrac{\partial z}{\partial \zeta}
\end{vmatrix}
\cdot d\xi d\eta d\zeta = |J| \cdot d\xi d\eta d\zeta .
$$

(2-58)

## 2.5.2    Element stiffness matrix

The element stiffness matrix is

$$[K]^e = \iiint_V [B]^T [D][B] dV \ ,$$

as the [D] matrix is only related to material properties and not related to the coordinates,

the [B] matrix should be gotten firstly to get the integration. [B] matrix shows as follows:

$$[B] = \begin{bmatrix} \frac{\partial N_1}{\partial x} & & & & \frac{\partial N_2}{\partial x} & & & \cdots & \frac{\partial N_2}{\partial x} & \\ & \frac{\partial N_1}{\partial y} & & & & \frac{\partial N_2}{\partial y} & & \cdots & & \frac{\partial N_2}{\partial y} \\ & & \frac{\partial N_1}{\partial z} & & & & \frac{\partial N_2}{\partial y} & \cdots & & \frac{\partial N_2}{\partial z} \\ \frac{\partial N_1}{\partial y} & \frac{\partial N_1}{\partial x} & & \frac{\partial N_2}{\partial y} & \frac{\partial N_2}{\partial x} & & & \cdots & \frac{\partial N_2}{\partial y} & \frac{\partial N_2}{\partial x} \\ \frac{\partial N_1}{\partial z} & & \frac{\partial N_1}{\partial x} & \frac{\partial N_2}{\partial z} & & \frac{\partial N_2}{\partial x} & & \cdots & \frac{\partial N_2}{\partial z} & \frac{\partial N_2}{\partial x} \\ & \frac{\partial N_1}{\partial z} & \frac{\partial N_1}{\partial y} & & \frac{\partial N_2}{\partial z} & \frac{\partial N_2}{\partial y} & & \cdots & \frac{\partial N_2}{\partial z} & \frac{\partial N_2}{\partial y} \end{bmatrix}_{6 \times 24} \quad (2\text{-}59)$$

With the following equations, the derivation of shape function in global coordinate can be

gotten by inverse of Jacobi matrix multiplied with derivation of shape function in natural

coordinate. The [B] can be gotten.

$$\begin{bmatrix} \frac{\partial N_1}{\partial x} & \frac{\partial N_2}{\partial x} & \frac{\partial N_3}{\partial x} & \frac{\partial N_4}{\partial x} & \frac{\partial N_5}{\partial x} & \frac{\partial N_6}{\partial x} & \frac{\partial N_7}{\partial x} & \frac{\partial N_8}{\partial x} \\ \frac{\partial N_1}{\partial y} & \frac{\partial N_2}{\partial y} & \frac{\partial N_3}{\partial y} & \frac{\partial N_4}{\partial y} & \frac{\partial N_5}{\partial y} & \frac{\partial N_6}{\partial y} & \frac{\partial N_7}{\partial y} & \frac{\partial N_8}{\partial y} \\ \frac{\partial N_1}{\partial z} & \frac{\partial N_2}{\partial z} & \frac{\partial N_3}{\partial z} & \frac{\partial N_4}{\partial z} & \frac{\partial N_5}{\partial z} & \frac{\partial N_6}{\partial z} & \frac{\partial N_7}{\partial z} & \frac{\partial N_8}{\partial z} \end{bmatrix} =$$

$$J^{-1} \cdot \begin{bmatrix} \frac{\partial N_1}{\partial \xi} & \frac{\partial N_2}{\partial \xi} & \frac{\partial N_3}{\partial \xi} & \frac{\partial N_4}{\partial \xi} & \frac{\partial N_5}{\partial \xi} & \frac{\partial N_6}{\partial \xi} & \frac{\partial N_7}{\partial \xi} & \frac{\partial N_8}{\partial \xi} \\ \frac{\partial N_1}{\partial \eta} & \frac{\partial N_2}{\partial \eta} & \frac{\partial N_3}{\partial \eta} & \frac{\partial N_4}{\partial \eta} & \frac{\partial N_5}{\partial \eta} & \frac{\partial N_6}{\partial \eta} & \frac{\partial N_7}{\partial \eta} & \frac{\partial N_8}{\partial \eta} \\ \frac{\partial N_1}{\partial \zeta} & \frac{\partial N_2}{\partial \zeta} & \frac{\partial N_3}{\partial \zeta} & \frac{\partial N_4}{\partial \zeta} & \frac{\partial N_5}{\partial \zeta} & \frac{\partial N_6}{\partial \zeta} & \frac{\partial N_7}{\partial \zeta} & \frac{\partial N_8}{\partial \zeta} \end{bmatrix} \ . \quad (2\text{-}60)$$

And then the element stiffness matrix can be calculated

$$[K]^e = \iiint_V [B]^T [D][B] dV = \iiint_V [B]^T [D][B]\cdot|J|\cdot d\xi d\eta d\zeta.$$  (2-61)

Gauss Integration method is applied to transform the integration into numerical computation. It is assumed the function

$$G(\xi,\eta,\zeta) = [B]^T \cdot [D]\cdot[B]\cdot|J|.$$  (2-62)

The 3 Gauss points integration is used to calculate the $[K]^e$.

Gauss points $\xi_i, \eta_j, \zeta_m$:

-0.7745966692415, 0, 0.7745966692415

Corresponding weight function value $H_i$, $H_j$, $H_m$:

5/9,  8 /9, 5/9

Then element stiffness matrix $[K]^e$ can be obtained

$$[K]^e = \iiint_V [B]^T [D][B] dV = \iiint [B]^T [D][B]\cdot|J|\cdot d\xi d\eta d\zeta$$
$$= \sum_{m=1}^{8}\sum_{j=1}^{8}\sum_{i=1}^{8} H_i H_j H_m \cdot G(\xi_i,\eta_j,\zeta_m)$$  (2-63)

## 2.5.3    Global stiffness matrix

All the element stiffness matrices assemble the global stiffness matrix. The algorithm is shown as follows,

$$[K] = \sum_{N}^{e} [G]^{T} \cdot [K]^{e} \cdot [G] \, , \tag{2-64}$$

where N is number of elements. [G] is the assemble matrix,

$$[G]^{T} = \begin{array}{c} 1 \\ \vdots \\ i \\ \vdots \\ j \\ \vdots \\ k \\ \vdots \\ l \\ \vdots \\ m \\ \vdots \\ n \\ \vdots \\ o \\ \vdots \\ p \\ \vdots \\ N \end{array} \begin{bmatrix} 0 & 0 & 0 & 0 & 0 & 0 & 0 & 0 \\ 0 & 0 & 0 & 0 & 0 & 0 & 0 & 0 \\ I & 0 & 0 & 0 & 0 & 0 & 0 & 0 \\ 0 & 0 & 0 & 0 & 0 & 0 & 0 & 0 \\ 0 & I & 0 & 0 & 0 & 0 & 0 & 0 \\ \vdots & 0 & 0 & & & & & \\ & 0 & I & 0 & & & & \\ & & 0 & 0 & & & & \\ & & 0 & I & 0 & & & \\ & & & 0 & 0 & & & \\ & & & 0 & I & 0 & & \\ & & & & 0 & 0 & & \\ & & & & 0 & I & 0 & \\ & & & & & 0 & 0 & \\ & & & & & 0 & I & 0 \\ & & & & & & 0 & 0 \\ & & & & & & 0 & I \\ & & & & & & & 0 \end{bmatrix} . \tag{2-65}$$

## 2.5.4    Element equivalent loads

As the force from outside is zero, only load resulted from the thermal strain generated from the laser irradiation is considered.  The thermal strain is

$$\{\varepsilon_{0}\} = \alpha(\phi - \phi_{0})\begin{bmatrix} 1 & 1 & 1 & 0 & 0 & 0 \end{bmatrix}^{T} .$$

The load generated is

$$\{F_h\}^e = \iiint_V [B]^T [D]\{\varepsilon_0\} dV = \iiint_V [B]^T [D]\{\varepsilon_0\} \cdot |J| \cdot d\xi d\eta d\zeta , \quad (2\text{-}66)$$

The 3 Gauss points integration is used to calculate the $\{F_h\}^e$.

Gauss points $\xi_i, \eta_j, \zeta_m$ are:

$$-0.7745966692415, 0, 0.7745966692415$$

Corresponding weight function value $H_i$, $H_j$, $H_m$:

$$5/9, 8/9, 5/9$$

It is assumed

$$W(\xi, \eta, \zeta) = [B]^T \cdot [D] \cdot \{\varepsilon_0\} \cdot |J|$$

Then

$$\{F_h\}^e = \iiint_V [B]^T [D]\{\varepsilon_0\} dV = \iiint_V [B]^T [D]\{\varepsilon_0\} \cdot |J| \cdot d\xi d\eta d\zeta$$

$$. \quad (2\text{-}67)$$

$$= \sum_{m=1}^{n} \sum_{j=1}^{n} \sum_{i=1}^{n} H_i H_j H_m \cdot W(\xi_i, \eta_j, \zeta_m)$$

## 2.5.5    Global equivalent loads vector

After getting the element equivalent load vector $\{F_h\}^e$, it should be assembled to the global equivalent load vector $\{F_h\}$. The algorithm is described as following:

$$\{F_h\} = \sum_{N}^{e} [G]^T \cdot \{F_h\}^e . \quad (2\text{-}68)$$

### 2.5.6 Boundary conditions

Assuming the boundary condition for node j is:

$$\delta_j = \bar{\delta}_j \tag{2-69}$$

Setting $\alpha$ as a large number about $10^{10}$, then the boundary conditions can be realized by multiplying $\alpha$ with corresponding elements in global stiffness matrix and global equivalent load vector as follows,

$$
\begin{aligned}
k_{jj} &= \alpha \cdot k_{jj} \quad \& \ k_{ij} = 1 \, (i \neq j) \\
F_i &= \alpha \cdot k_{ij} \cdot \bar{\delta}_j
\end{aligned}
\tag{2-70}
$$

Then the revised equations can be obtained

$$K' \cdot \delta = F' . \tag{2-71}$$

### 2.5.7 Method to solve the linear equations

Similar with the thermal analysis, the method of Triangle decomposition was used to solve the equations (2-71). The algorithm has been described in section 2.3.2. Then the displacement can be gotten.

## 2.6 The diagram of finite element solution for thermo-mechanical analysis

Figure 2-4 shows the diagram of the finite element solution for thermo-mechanical analysis. From the figure, the algorithm and computation steps can be seen clearly. Our thermo-mechanical analysis simulator is designed according to the diagram. The partial

programming codes in Fortran Language can be found in the Appendix.
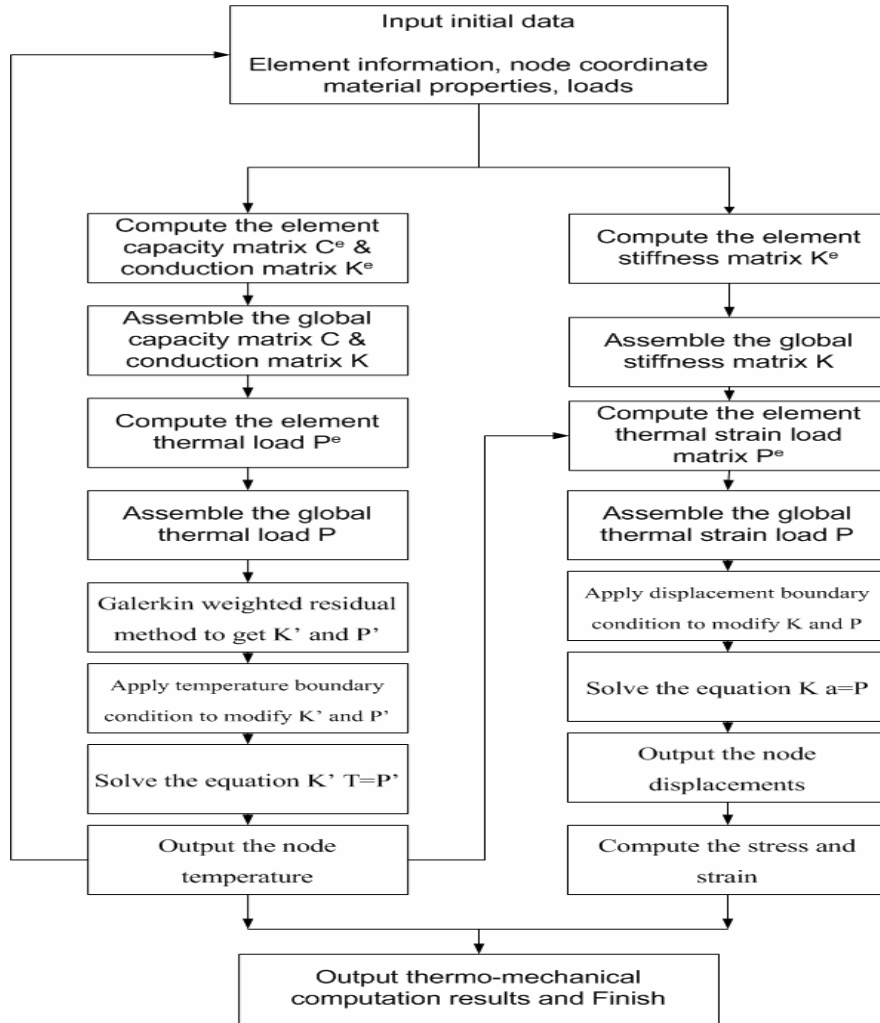


Figure 2-4 Diagram of the thermo-mechanical analysis

## 2.7 Summary

In this chapter, the basic theory and physical equations for thermo-mechanical analysis in phase change optical disks have been outlined. The method used to solve the equations has been described. The finite element solution for thermo-mechanical problems has been introduced. Finally the analysis procedure is given.

# Chapter 3  Software Development for phase change optical disk design

## 3.1  Introduction

Nowadays the competitive companies are trying to develop new generation phase change optical disks. The product development cycle is very critical. Those who first develop the better products with lower cost and less development time will dominate the market. And they can design the standard if their products are accepted by the world in advance, which can bring them much more income. All these benefits drive competitive companies to decrease the product development time so that their product will emerge in the market beforehand.

In phase change optical disks, recording and erasing are achieved by laser heating to shift the media in two states: crystalline and amorphous. The difference in reflectivity of crystalline and amorphous states denotes the different stored information. Hence the optical, thermo-mechanical performance under the laser irradiation on the disk need to be investigated during the development of the new generation phase change optical disks. To realize the goal of designing better product with lower cost and less development time, the computer aided engineering (CAE) is a good method to perform computer simulation and analysis of phase change optical disks.

Many reports mentioned the numerical simulations of the phase change optical disks.

Some of them focused on the optical performance analysis of optical disk with software named DIFFRACT. Other reports focused on the thermal issues of optical disks. Multi-physics commercial software such as ANSYS (based on finite element method) is often used in the design and analysis of optical disks [28]. As these software are not designed specially for phase change optical disks, some complicated processes like the amorphization and crystallization process of the phase change phenomenon cannot be easily simulated. H. Kando et al [35] developed a mark simulator for phase change optical disks. With this simulator, the time-dependent temperature distribution in 3-dimensional structure was analyzed by solving the heat conduction equation based on finite difference method(FDM). With the limitation of constructed mesh for FDM, the simulator is not suitable for handling complicated geometry, such as the land and groove structure.

In practice, optical and thermo-mechanical designs of phase change optical disks are coupled. To optimize the performance of the phase change optical disks, the software with the investigation of optical and thermo-mechanical analysis module is needed. But till now, there is no software tools that can supply the integrated functions of the three aspects. And the software designed by our lab named PCODD(phase change optical disk design) can only support the integrated analysis of optical and thermal aspects for phase change optical disks. So it is very necessary to develop a design and analysis software tools for phase change optical disks that provides an integrated design environment allowing users to carry out optical, thermo-mechanical analysis of rewritable phase change optical disks accurately and efficiently. As the former designed software PCODD

can only provide the optical and thermal analysis functions, a mechanical analysis module needs to be implemented.

## 3.2  Design and development of the PCODD software

The PCODD software is designed based on Microsoft Windows 95/98/NT/XP. The hardware platform requirements should be at least Intel Pentium II 450MHz class CPU with 128MB of RAM and a 5GB SCSI hard disk. It allows users to freely design and modify the phase change optical disk with multi-layer structure, as well as land and groove structures. There is no limitation on the number of layers to be included and the geometry sizes of the land and groove. A resource data library is implemented for the commonly used and prospective materials in optical and thermal aspects, where these data are obtained from the publications as well as in-house experimentation.

Users may also specify the properties for new materials and add into the standby data library. Currently alloy materials are commonly used in optical disks where their optical parameters are usually obtained from experiments. To save time, this software provides a powerful function to calculate alloy materials' optical index instead of experiments. Based on the Effective Media Approximation Theory [36], the relationship between the component ratio of alloys and their optical index can be calculated from the corresponding pure materials, which are stored in the data library. With this function, the alloy's optical index can be adjusted by their component in order to optimize the optical performance of the disk.
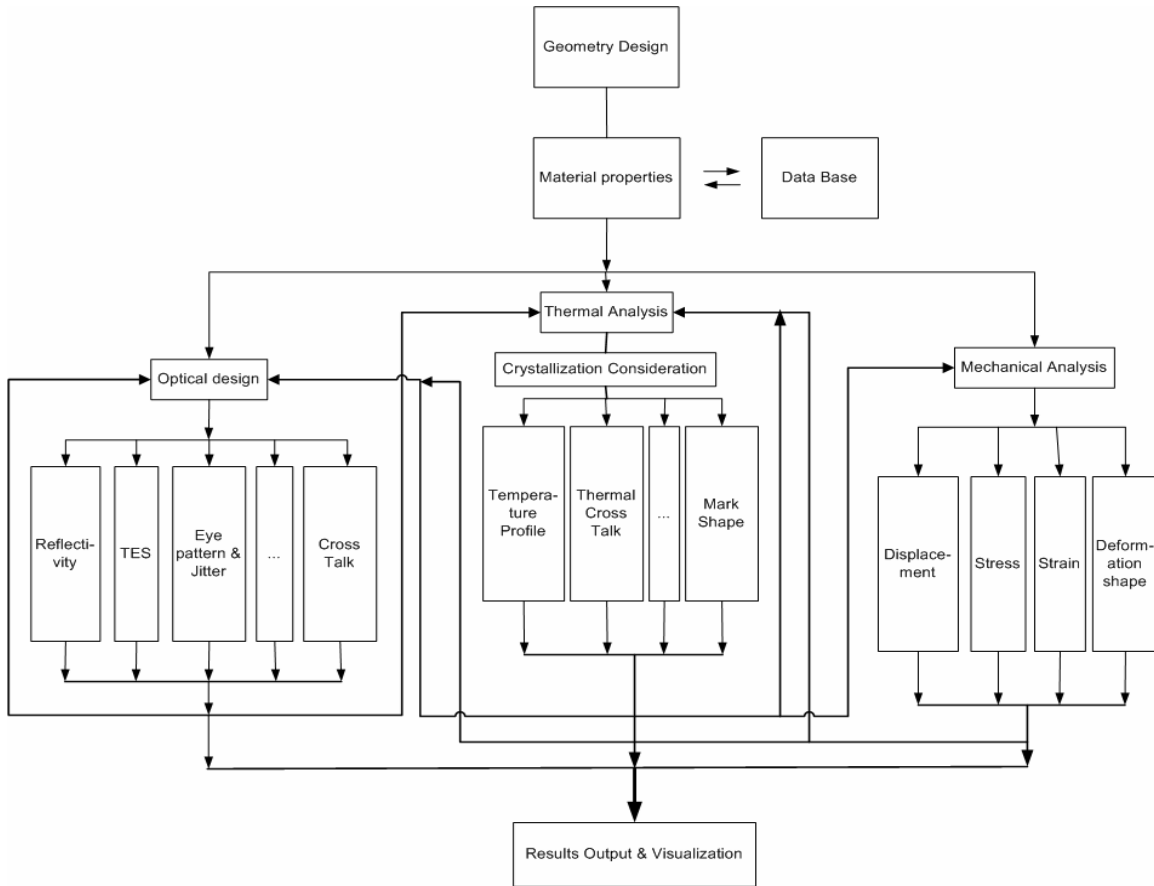
Figure 3-1 Structure of PCODD software

The design of phase change optical disk can be performed from multi-layer disk structure with varying land and groove structures under different laser irradiation to obtain the desired optical properties. This software is capable of simulating both static and dynamic cases. Various parameters such as the media, laser wavelength, duration of laser irradiation, laser spot, disk structure and disk tilt can be varied according to the will of the users to obtain the required final optical effects.

In recent years, FDTD method has been regarded as one of the most powerful methods in vector diffraction computation because of its good accuracy, simple formulization and applicability to complicated structures [37][38]. The option to use the method of scalar

49

theory is also available. After designing the optical disk structure, the software can accordingly calculate and graphically provide information like the disk reflectivity, modulation amplitude, cross-talk, track error signal, eye-patterns, carrier-to-noise ratio, pupil baseball patterns and so on.

The thermal process in 3-dimensional optical disks is simulated based on FEM. The greatest advantages of FEM are its abilities to handle truly arbitrary geometry and to deal with general boundary conditions. FEM is also well adapted to the cases when geometrical deformation may be resulted from the physical process. FEM is thus an effective and reliable approach to solving heat transfer problem with high level of effective and reliable approach to solving heat transfer problem with high level of temperature gradient extremity. The interactive graphical user interface of the software allows users to specify the optical and thermal parameters conveniently, such as rotation speed of disk, laser power, laser pulse waveform, thermal convection and so on.

With the use of FEM, the transient thermal and thermal expansion process resulting from single pulse, multiple pulses or any combination of them can be simulated and analyzed. Thermal effects and thermal deformation through the laser irradiation can also be evaluated. All the results can be graphically displayed, including temperature distribution profiles, temperature contour displays, heating and cooling rates, heat flux distribution profiles, displacement profile, displacement contour distribution, stress, strain, animation of time dependent temperature and displacement distribution and other useful information.

## 3.3  Functions of PCODD software

Figure 3-1 shows the whole structure of PCODD software. The typical steps involved in the thermo-mechanical coupling modeling and analysis of phase change optical disks are listed as follows:

Pre-processing $\left\{\begin{array}{l} \end{array}\right.$
1)  Geometrical modeling of the disk structure (including material choice)

2)  Finite element modeling (Including mesh design)

Solutions $\left\{\begin{array}{l} \end{array}\right.$
3)  Considerations of loads, boundary condition, initial condition, rotation speed et al

4)  Solutions for static, dynamic analysis for thermo-mechanical  analysis

Post-processing $\left\{\begin{array}{l} \end{array}\right.$
5)  Visualization and analysis of results

### 3.3.1      PCODD software interface

The objectives of PCODD are to simplify the entire process listed above as much as possible and to allow for maximum design flexibility. So any phase change optical disk designer without any finite element analysis experience can use this software easily to perform thermo-mechanical analysis.

To meet the objectives, the interface of the software has been made familiar and friendly to those who can use windows operating system. So those who exposed to the software for the first time can grasp the software in a short learning cycle. The overall interface of PCODD can be seen in Figure 3-2.
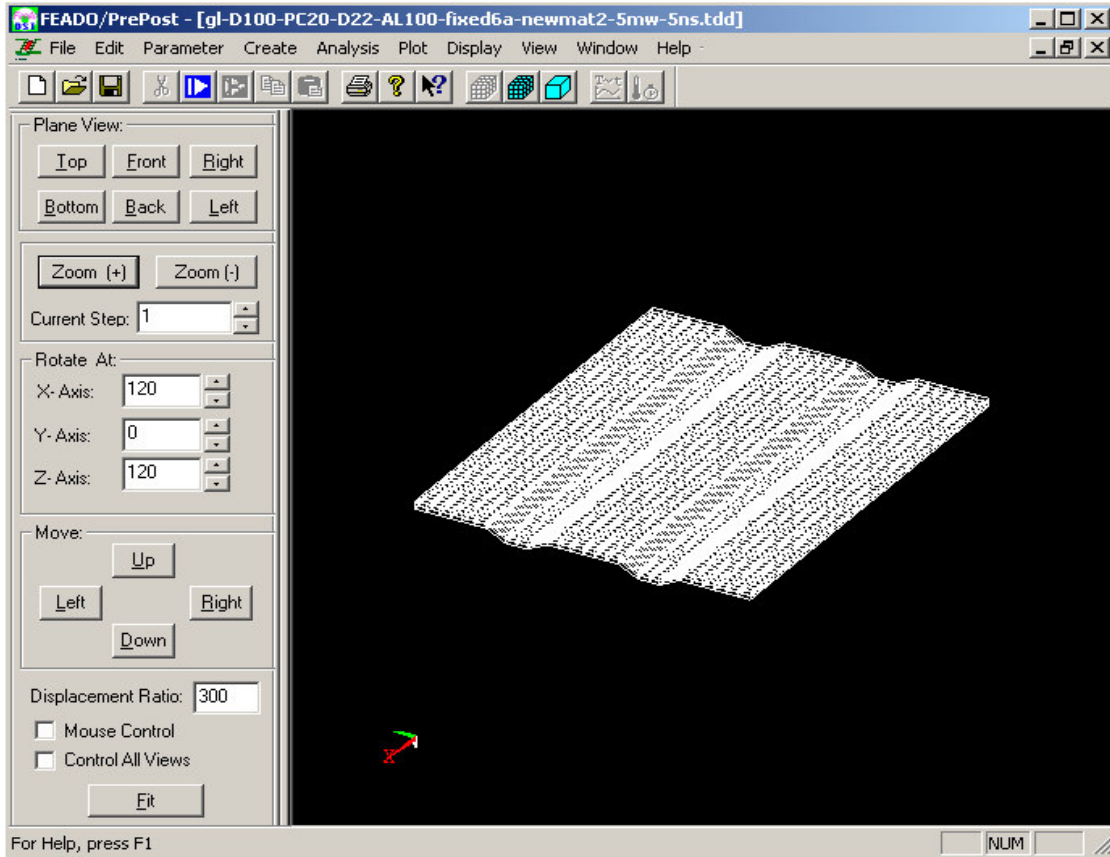
Figure 3-2 PCODD software interface

## 3.3.2    Design of the phase change optical disk structure

Figure 3-3 shows the dialog for the input of substrate structure's dimension. From the dialog, the substrate can be chosen between plane and groove structure. After specifying the type of substrate, the land width, groove depth, groove width, sidewall angle as well as the sample size can be designated.

The thermal parameter input dialog is shown in Figure 3-4. With this dialog, the four types of information can be specified. The first is the layer number of the phase change optical disks. After specifying the layer number, the rest parameters can be loaded from the model designed before. The second is the layer thickness and material parameters.

52

Whether the layer is phase change layer or not can be specified. The material properties, including optical and thermal parameters, can be input by hand or loaded from database. Figure 3-5 shows the dialog of database. The third is the laser system information. The laser wavelength and numerical aperture of objective lens can be specified. The laser light is Gaussian beam and can be chosen between circular and ellipse. And the laser can be chosen to irradiate from substrate or top layer. The last one is to make the modification of the layer properties easy. Layers can be added, removed or changed.
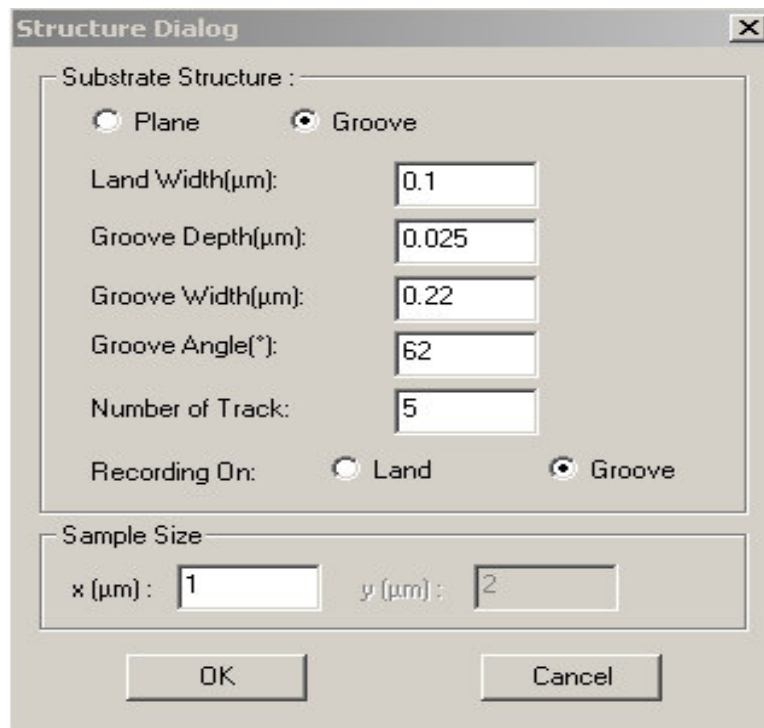


Figure 3-3 Optical disk structure input interface
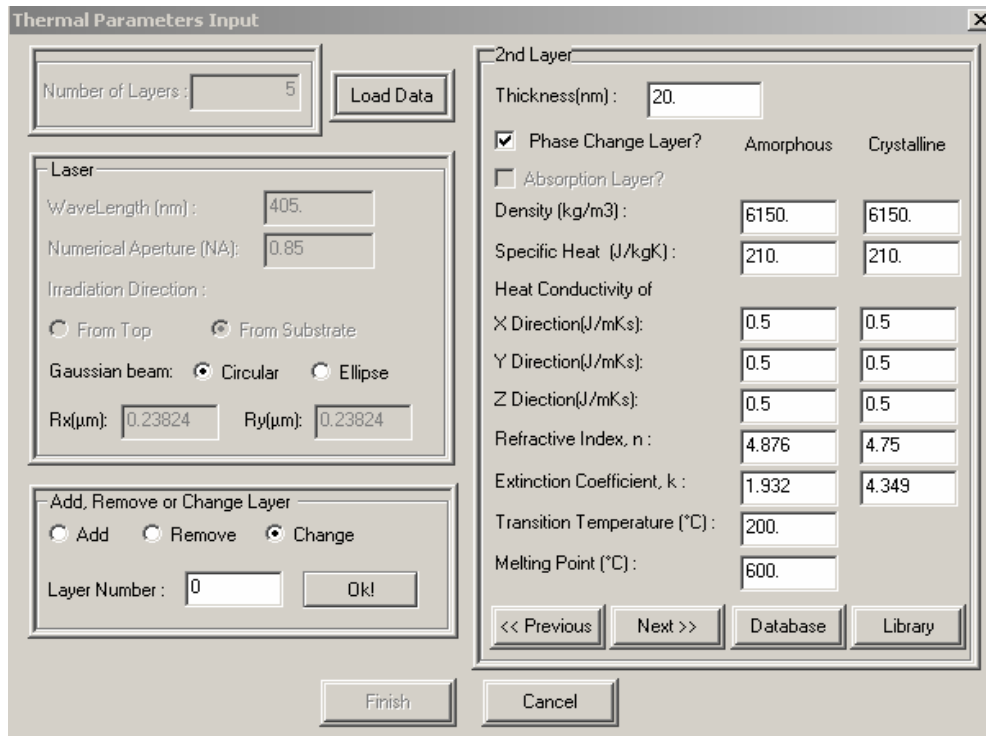
Figure 3-4 Input interface of material properties, laser information et al
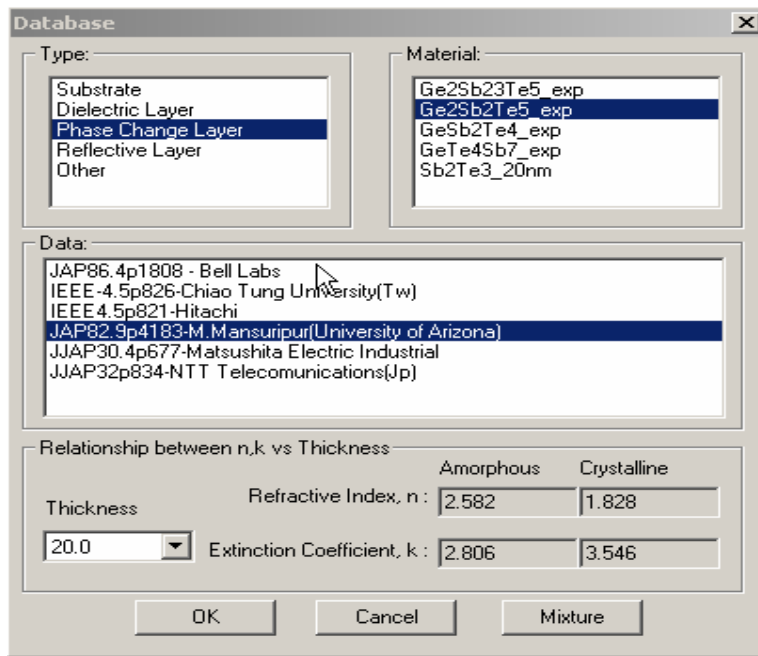


Figure 3-5 Interface of database for material properties

The mesh setting can be designated from the dialog shown in Figure 3-6. The number of

elements along x axis, on land, on groove and along z axis can be specified. Actually the results are more precise with more elements. But the computation time is much longer with more elements. So both the precision and computation time should be considered when designing the finite element model. After specifying the mesh properties, the discrete model can be seen in Figure 3-7.
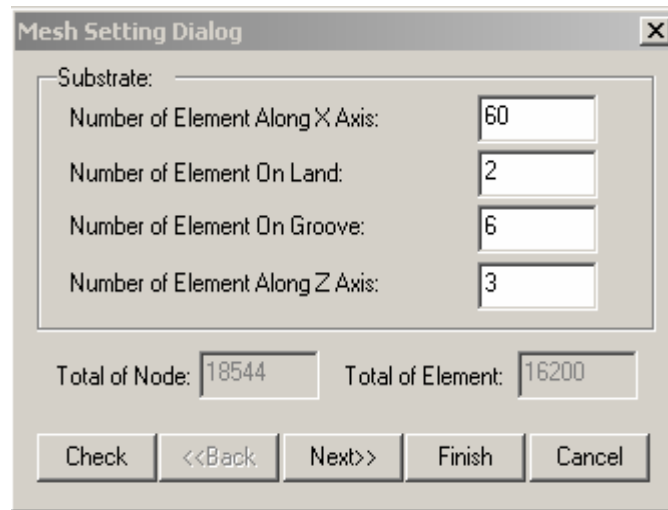


Figure 3-6 Interface of mesh setting
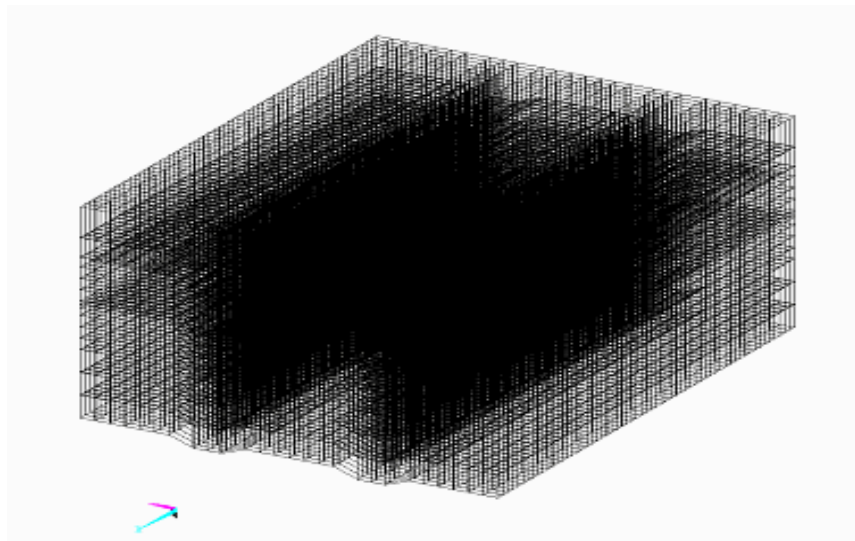


Figure 3-7 Finite element model

### 3.3.3 Parameters for solution

The information of the loading and other simulation conditions can be input from the dialog illustrated in Figure 3-8. With this dialog, three main types of information can be specified. The first is the load information. The laser power and laser pulse can be set here. So many kinds of write or rewrite strategies can be designed in this dialog. The second is the simulation condition and type. Simulation condition includes the initial temperature and time step size for analysis. The type of simulation involves type of analysis and type of process. These are special for analysis of phase change optical disk. There are two choices for type of analysis: static and dynamic analysis. And three types of process are considered: write, rewrite and multi-track. The third is the linear rotation speed of the phase change optical disks and the starting point of the laser irradiation.
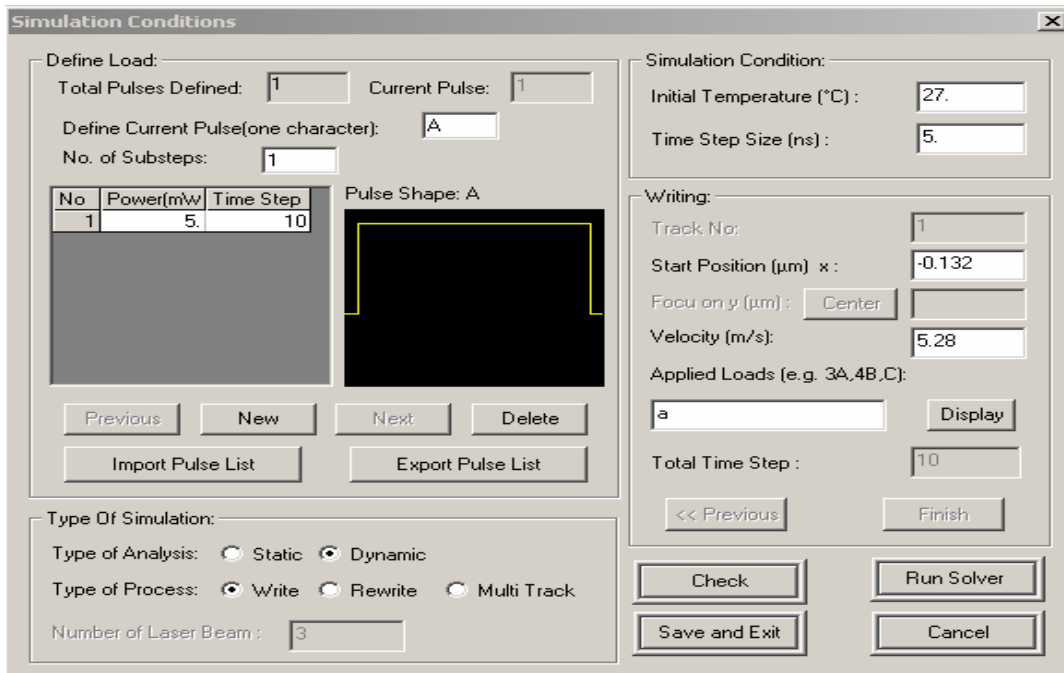


Figure 3-8 Input interface for laser pulse, initial condition and analysis type

Figure 3-9 shows the dialog for the parameters input of the thermal expansion

56

analysis. The boundary conditions can be specified in the left column. And the material properties including Young's modulus, Poisson ratio and coefficients of thermal expansion, can be specified in this dialog. Once all these parameters are specified, the analysis of the thermo-mechanical model can be commenced.
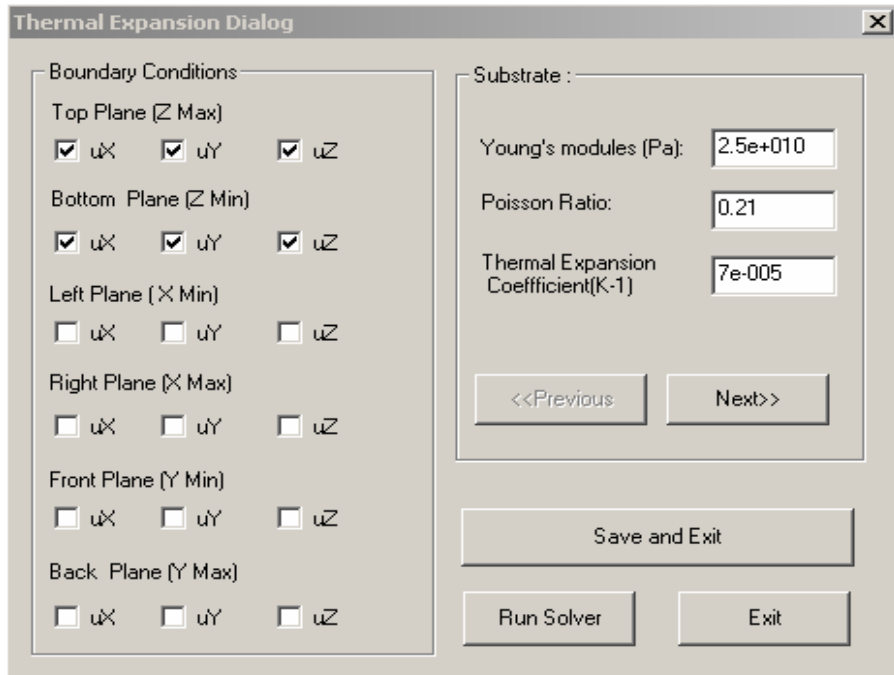


Figure 3-9 Mechanical properties and boundary conditions

### 3.3.4    Post-processing of Results

After the solution of the thermo-mechanical analysis, the temperature, mark shape, displacement (including the three components and vector sum of displacement), stress (including normal, shear and Von Mises stress) and strain (including normal, shear and Von Mises strain) profiles can be easily extracted with any of the numerous post-processing functions available. The contour of these variables can be displayed in the software. Figure 3-10 is the contour for temperature. Figure 3-11, Figure 3-12 and Figure

3-13 show the contour for mark shape, displacement in z direction and shear stress xy respectively. And the curve of these variables profiles along all directions can be plotted. Figure 3-14 plots the displacement Z profile along the thickness direction of the phase change optical disk.
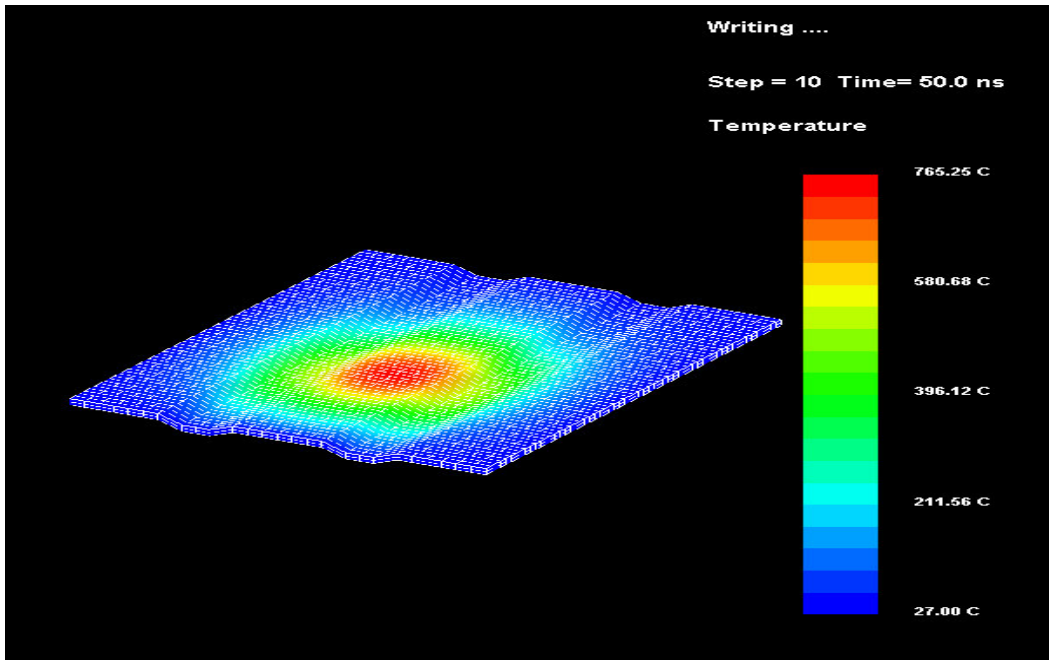


Figure 3-10 Temperature contour
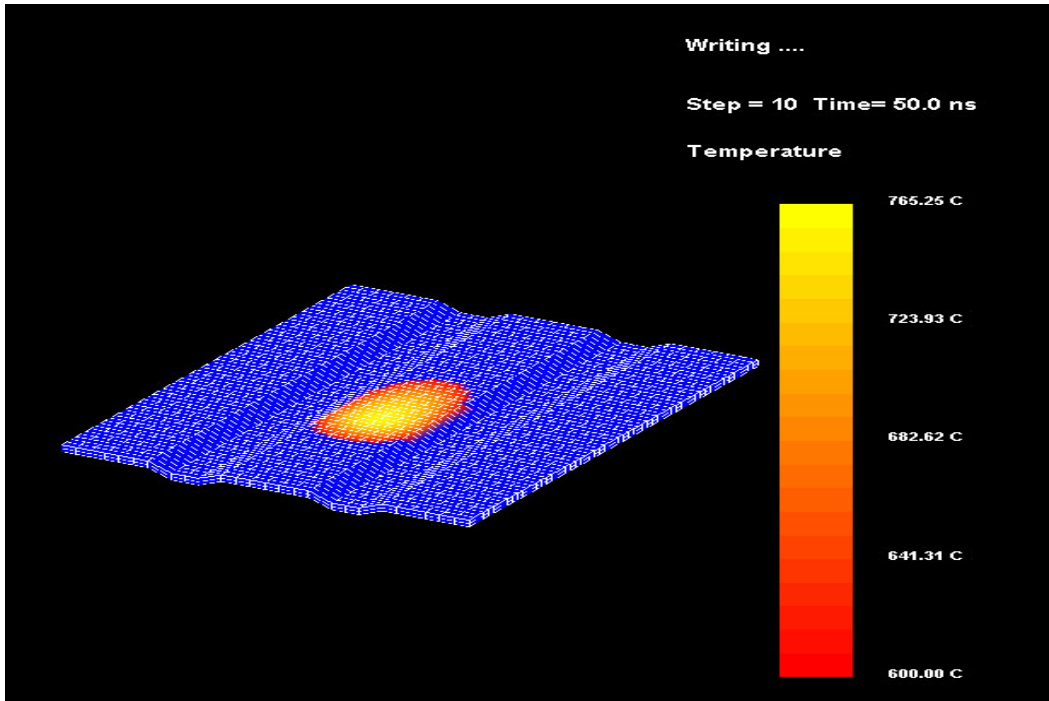
Figure 3-11 Mark shape
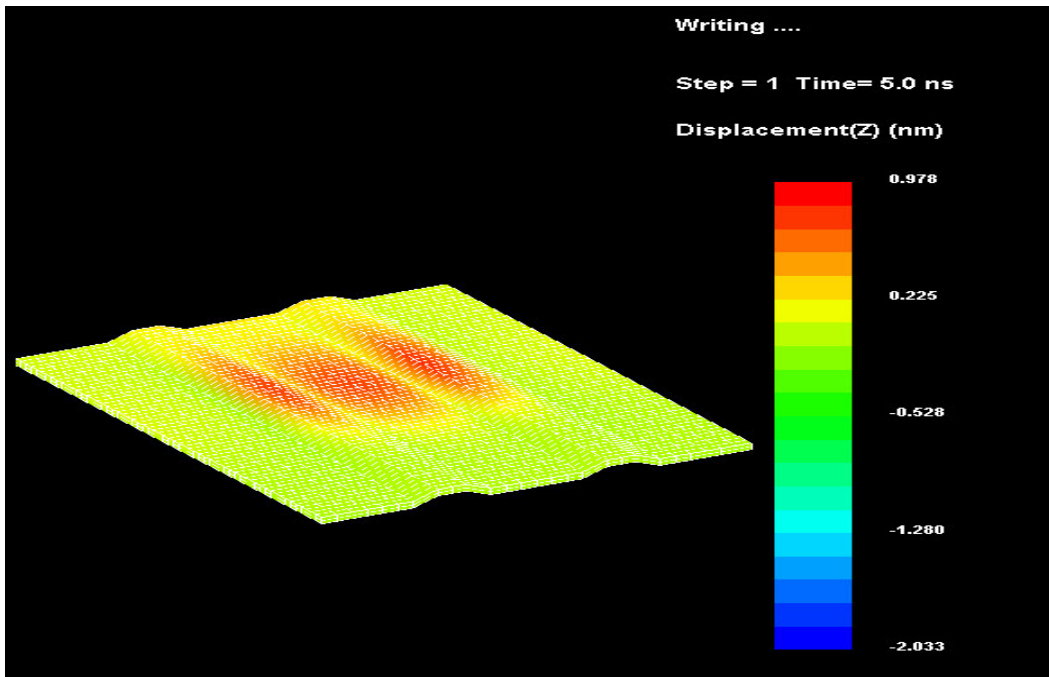


Figure 3-12 Displacement contour
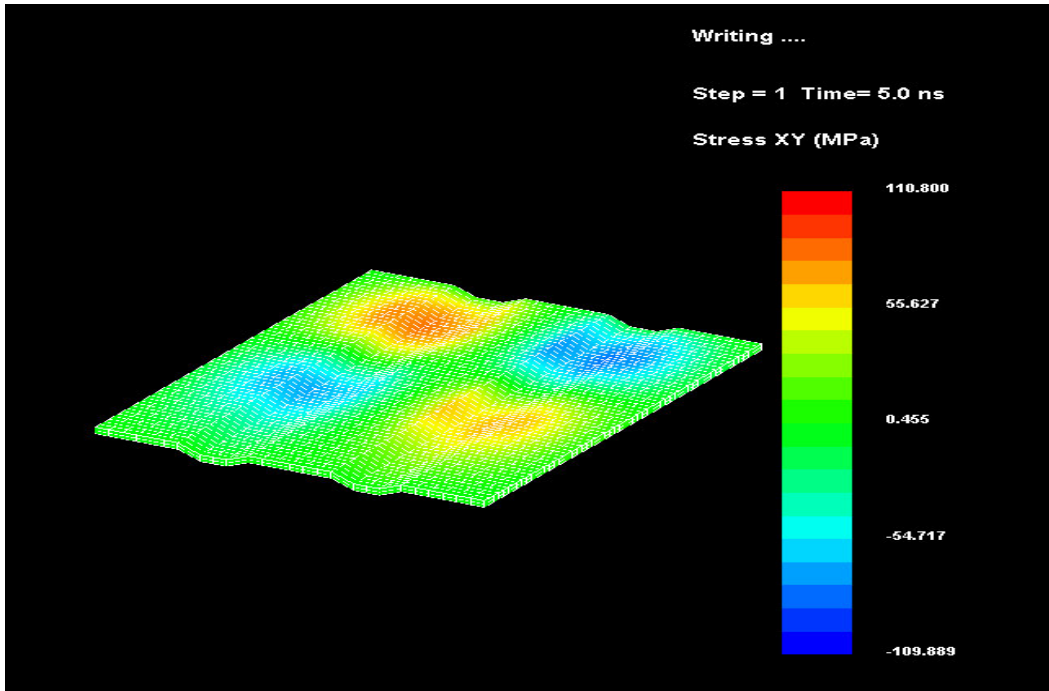
Figure 3-13 Stress contour
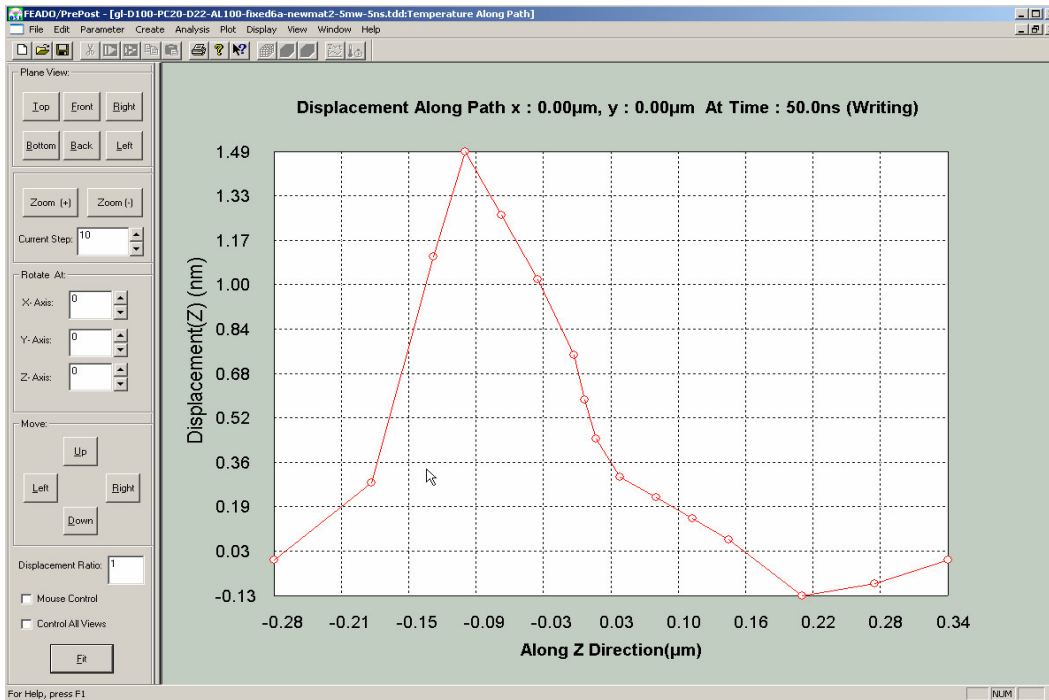


Figure 3-14 Displacement profile

## 3.4 Summary

In this chapter, the reasons behind the development of dedicated rewritable phase change optical disk thermo-mechanical modeling and analysis software were given out. The development process of the software was then described in detail. Then, the software interface for pre-processing, solution, post-processing was illustrated. And the functions and capabilities of PCODD software were introduced.

# Chapter 4  Thermal modeling and analysis of Blu-ray Disc and AOD

## 4.1  Introduction

Blu-ray Disc and AOD are two hot competitive candidates for next generation phase change optical disks. So the thermal deformation analysis of Blu-ray Disc and AOD is very useful to supply reference to optimize the disk structure from the point of deformation. In this chapter, the thermal modeling and analysis of Blu-ray Disc and AOD will be investigated. The thermal deformation of them will be analyzed in chapter 5.

## 4.2  Geometry modeling for phase change optical disks

The multi-layer phase change optical disk was modeled as a rectangular section, made up of the respective thin films material, namely the polycarbonate substrate, the $ZnS\text{-}SiO_2$ dielectric, the $Ge_2Sb_2Te_5$ phase change layer, the reflective layer, polycarbonate cover layer sheet. The choice of using a rectangular section for the geometric model was based on the assumption that the heating effect caused by an incident laser beam, with a beam radius in the range of 0.5μm will be well contained within the perimeter of the chosen dimension.

One important point to note is that the substrate is modeled as having a thickness of 0.5μm instead of its actual thickness of 1.1mm and 0.1mm. The reasons for the

simplification are as follows:

1) Through numerous simulations, it has been discovered that the thermo-mechanical effects within the disk do not extend beyond 0.5μm into the substrate and cover layer.

2) The software is not able to model the huge difference in the order of magnitude between the thickness of the deposited thin films ($10^{-9}$m) and that of the substrate ($10^{-3}$m).

Based on the above two considerations, it is safe to state that the use of a 0.5μm thick substrate for the simulation will not affect the results obtained. The disk properties are assumed to be isotropic, homogenous and independent of temperature.

## 4.2.1    Blu-ray Disc modeling

The multi-layer phase change optical disk is modeled as a rectangular section with a length of 1μm and width of approximately 0.8μm, made up of the respective thin films material, namely the polycarbonate substrate, the ZnS-SiO$_2$ dielectric, the Ge$_2$Sb$_2$Te$_5$ phase change layer, the aluminum alloy reflective layer and polycarbonate cover layer sheet. Figure 4-1 shows the geometry model of Blu-ray Disc used in the calculations. The material for the phase change layer is Ge$_2$Sb$_2$Te$_5$.

The blue-laser optical system of wavelength 405nm and NA 0.85 [19][39] was used. The land and groove disk structure is used: track pitch 0.32μm, land width 0.22μm, groove width 0.1μm, groove depth 0.025μm and sidewall angle 28$^o$. Sizes of the sampled region are: length is 1 μm and 5 tracks were used.    The    disk    rotates    with    constant    linear

velocity of 5.28m/s. The material properties in the simulation are listed in Table 4-1.

## 4.2.2 AOD modeling

The multi-layer phase change optical disk is modeled as a rectangular section with a length of 2μm and width of approximately 1μm, made up of the respective thin films material, namely the polycarbonate substrate, the ZnS-SiO$_2$ dielectric, the Ge$_2$Sb$_2$Te$_5$ phase change layer, the silver reflective layer, UV resin. Figure 4-2 shows the geometry model of AOD used in the calculations.

The blue-laser optical system of wavelength 405nm and NA 0.65 was used. The land and groove disk structure was used: track pitch 0.34(m, land width 0.12(m, groove width 0.22(m, groove depth 0.026(m and sidewall angle 28o. Sizes of the sampled region were: length is 2 (m and 7 tracks were used. The disk rotates with constant linear velocity of 5.28m/s. The material properties in the simulation are listed in Table 4-1.

Table 4-1 Material properties for Blu-ray Disc and AOD

| Material type | | Density (Kg/m$^3$) | Heat Conductivity (J/mKs) | Heat Capacity (J/KgK) | Refractive Index n | Extinction Coefficient k |
|---|---|---|---|---|---|---|
| Cover layer | | 1200 | 0.22 | 1172 | 1.569 | 0.03 |
| Dielectric | | 3650 | 0.6 | 560 | 2.129 | 0 |
| Phase change | Amorphous | 6150 | 0.5 | 210 | 4.8756 | 1.932 |
| | Crystalline | 6150 | 0.5 | 210 | 4.75 | 4.349 |
| Reflective layer - Al-Ar | | 2750 | 25 | 890 | 1.438 | 5.035 |
| Reflective layer - Ag | | 10500 | 429 | 235 | 1.0003 | 1.496 |
| UV Resin | | 1200 | 0.22 | 1172 | 1.569 | 0.03 |
| Substrate | | 1200 | 0.22 | 1172 | 1.569 | 0.03 |

CTE: coefficients of thermal expansion
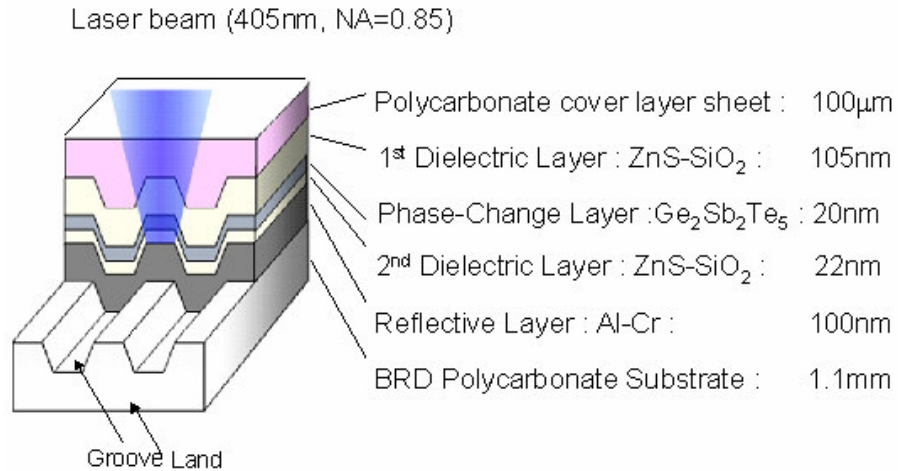
Figure 4-1 Blu-ray Disc structure
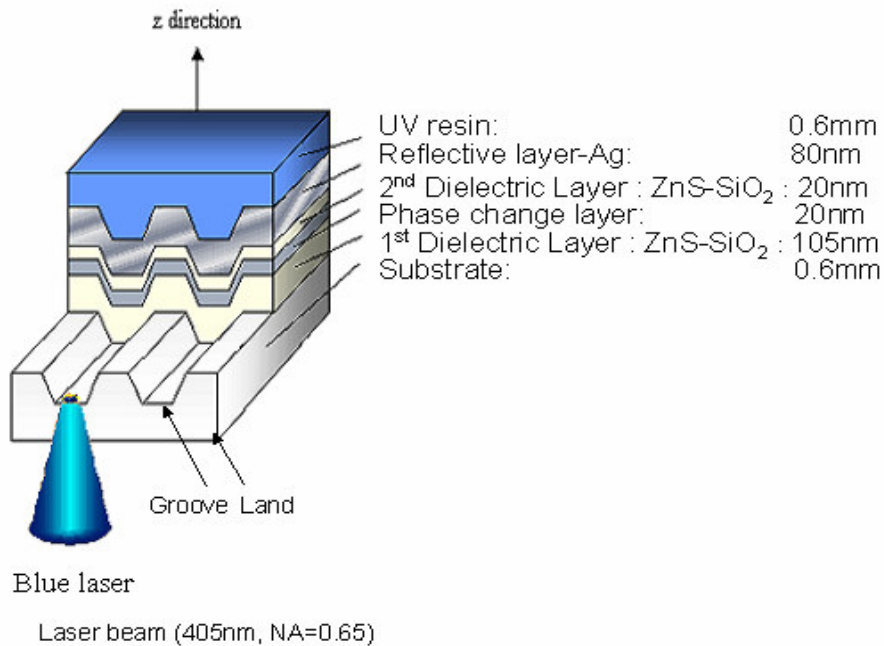


Figure 4-2 AOD structure

## 4.3 Finite element modeling

The finite element model was created based on the completed geometric model using the meshing function available in the program. While meshing the geometric model, a balance had to be made between having a very finely meshed finite-element model

versus the computation time. Thus the layers within the geometric model, namely the phase change and dielectric layers, which are of greater interest are more closely meshed, while those which are far away from the phase change layer-substrate, reflective layer, cover layer, are meshed more loosely.

A compromise was made by using a finite-element model that was sufficiently meshed for accuracy and yet had a simulation time of less than 4 hours for each transient thermo-mechanical analysis. And the computation precision versus element numbers of different meshes was listed in Table 4-2 for Blu-ray Disc and Table 4-3 for AOD.

From Table 4-2, it can be seen that the computation results is very precise when the element number is 16200 for Blu-ray Disc model. So the element number for finite element model for Blu-ray Disc model is chosen with 16200 in this research. Figure 4-3 shows the finite element model for Blu-ray Disc.

Table 4-2 The precision versus number of elements for Blu-ray Disc FEM model

| Element number | Peak temperature (℃) | Error (%) | Z displacement(nm) | Error (%) |
|---|---|---|---|---|
| 2700 | 471.70 | \ | 2.038 | \ |
| 8100 | 461.32 | 2.2 | 2.036 | 0.098 |
| 16200 | 461.27 | 0.011 | 2.033 | 0.15 |
| 31200 | 461.28 | 0.002 | 2.032 | 0.049 |

Error: the result error between current FEM model with FEM model with less element number
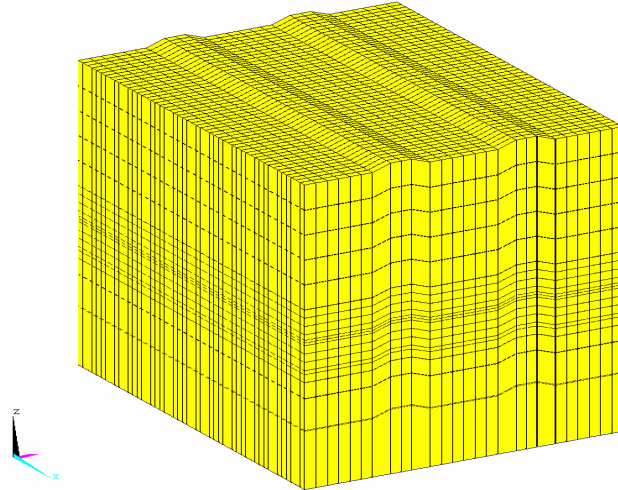
Figure 4-3 Finite element model for Blu-ray Disc

From Table 4-3, it can be seen that the computation results is very precise when the element number is 15400 for AOD model. So the element number for finite element model for AOD model is chosen with 15400 in this research. Figure 4-4 shows the finite element model for AOD.

Table 4-3 The precision versus number of elements for AOD FEM model

| Element number | Peak temperature (℃) | Error (%) | Z displacement(nm) | Error (%) |
|----------------|----------------------|-----------|---------------------|-----------|
| 2800 | 568.11 | \ | 2.141 | \ |
| 6160 | 525.39 | 7.5 | 2.261 | 5.6 |
| 9240 | 520.92 | 0.85 | 2.283 | 0.97 |
| 15400 | 518.66 | 0.43 | 2.289 | 0.26 |
| 30200 | 518.56 | 0.0019 | 2.290 | 0.0043 |

Error: the result error between current FEM model with FEM model with less element number
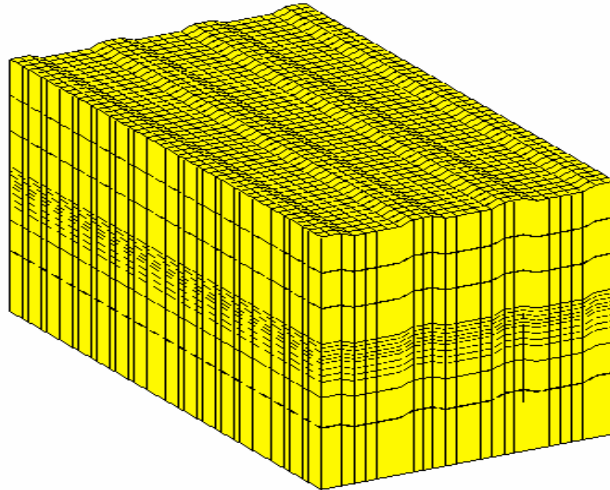
Figure 4-4 Finite element model for AOD

## 4.4 Simulation conditions

The simulation conditions used for thermo-mechanical analysis for Blu-ray Disc and AOD are listed in Figure 4-4. From the table, it can be seen that two main categories of parameters, optical and disk parameters, are varied to investigate their effects on the disk performance. The values for these parameters are chosen carefully to meet the phase change optical disk standards so that the results obtained form this research can be referred to the commercial design of Blu-ray Disc and AOD.

Table 4-4 Optical system and disk information

| Simulation conditions | Blu-ray Disc | AOD |
|---|---|---|
| **Optical Parameters** | | |
| Laser Wavelength (nm) | 405 | 405 |
| Numerical Aperture | 0.85 | 0.65 |
| Laser power (mW) | 1~8 | 5~20 |
| **System Parameters** | | |
| Rotation speed (m/s) | 5.28 | 5.28 |
| **Disk Parameters** | | |
| Track pitch (µm) | 0.32 | 0.34 |
| $1^{st}$ dielectric thickness (nm) | 90~120 | 80~120 |
| Phase change thickness (nm) | 15~30 | 15~30 |
| $2^{nd}$ dielectric thickness (nm) | 15~25 | 15~25 |
| Reflective thickness (nm) | 90~110 | 60~100 |
| Groove depth (nm) | 20~30 | 20~30 |
| Sidewall angle ($^{o}$) | 25~35 | 25~35 |

In all simulations, the disk properties were assumed to be isotropic, homogenous and independent of temperature. It was assumed that the laser energy is only absorbed in the phase change layer, which means that heat is only generated in that layer. A 100ns rectangular laser pulse was applied. The initial and boundary temperature were set as room temperature $27^{o}$C.

## 4.5 Temperature contour and profiles

### 4.5.1 Temperature contour and profiles for Blu-ray Disc

The condition of disk structure: Cover layer /$SiO_2$-ZnS (105nm)/ $Ge_2Sb_2Te_5$ (20nm)/

SiO$_2$-ZnS (22nm) /Al(100nm)/Substrate, Laser power: 5mW, groove depth: 25nm and sidewall: 28$^o$ has been investigated for Blu-ray Disc. Laser irradiates from the direction of cover layer.

Figure 4-5 shows the temperature contour of phase change layer from top view. The land and groove structure of the disk are distinguishable. This plot together with the bottom view as shown in Figure 4-6 are very useful to visualize the temperature distribution in the phase change layer of the disk. It can be observed that the temperature of the top surface of phase change layer is much higher than that of the bottom surface. And the temperature of the adjacent grooves is relatively high, which maybe erase the information stored on adjacent grooves. The peak temperature is 460.57$^o$C at 5ns.
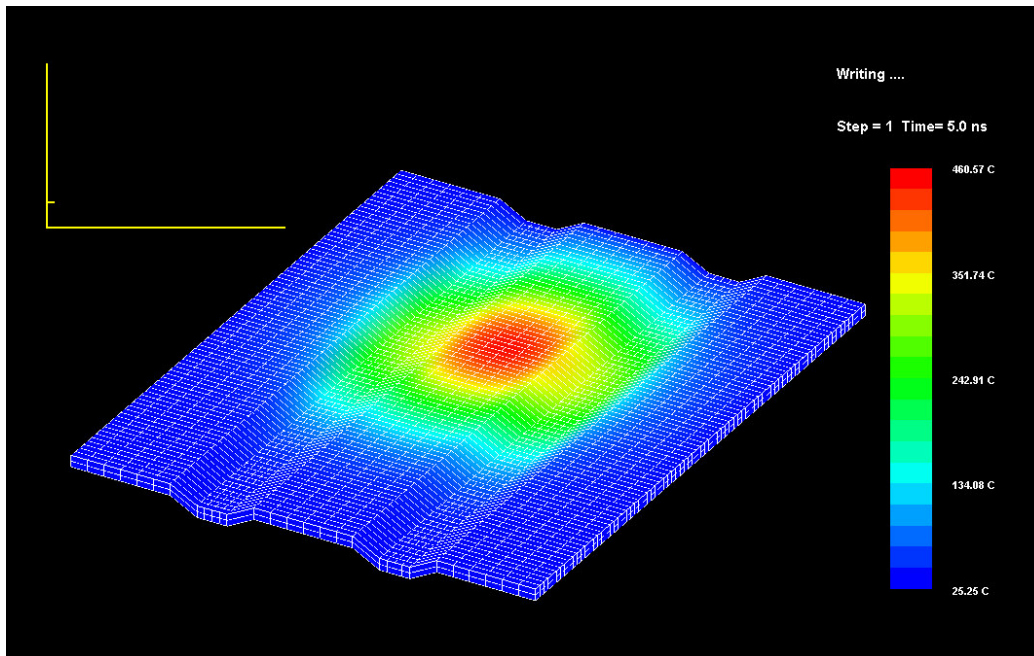


Figure 4-5 Top view temperature contour of phase change layer
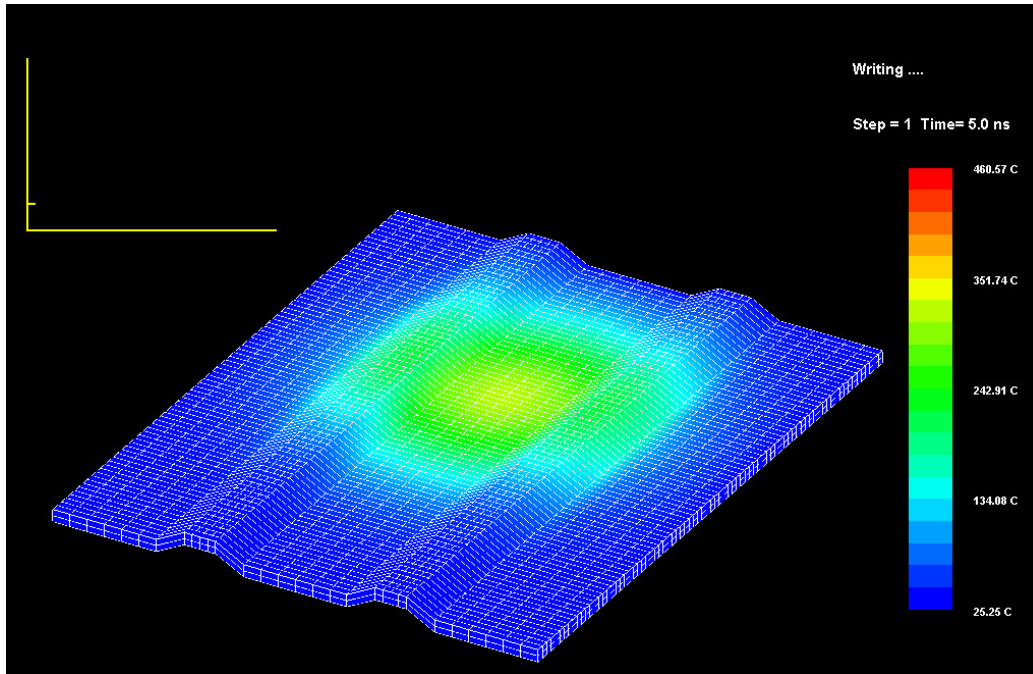
Figure 4-6 Bottom view temperature contour of phase change layer

Figure 4-7 illustrates the temperature profile in the direction of rotation during different time periods at the phase change layer. The profiles are Gaussian, corresponding to the assumed Gaussian nature of the irradiating laser. The peak temperature increases with time. And the peak temperature is moving forwards. This is attributable to the forward motion of the irradiation laser in the x direction.
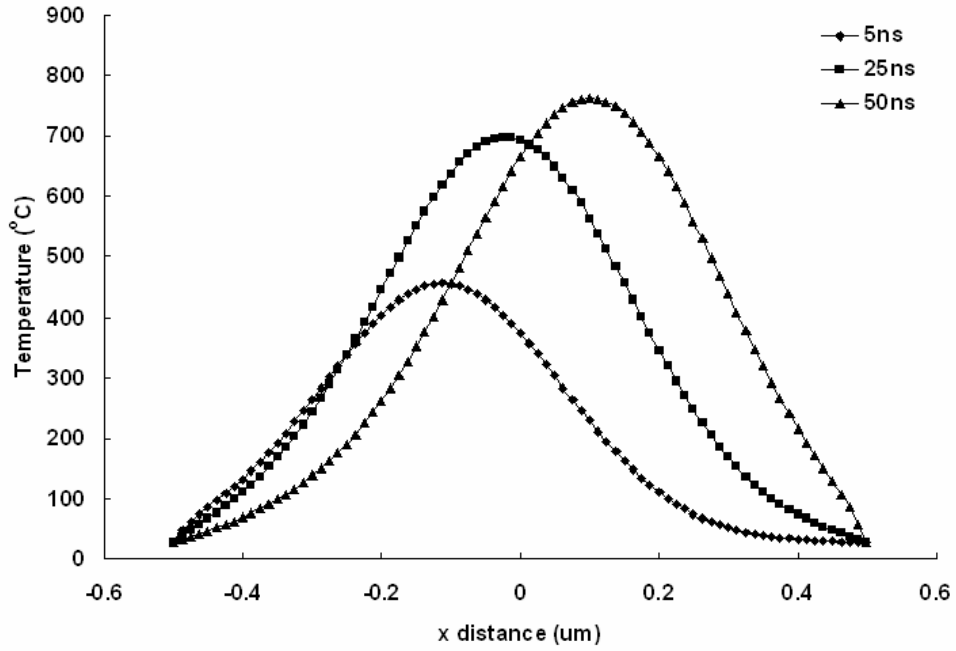
Figure 4-7 Temperature profile in the direction of rotation

during different time periods at the phase change layer
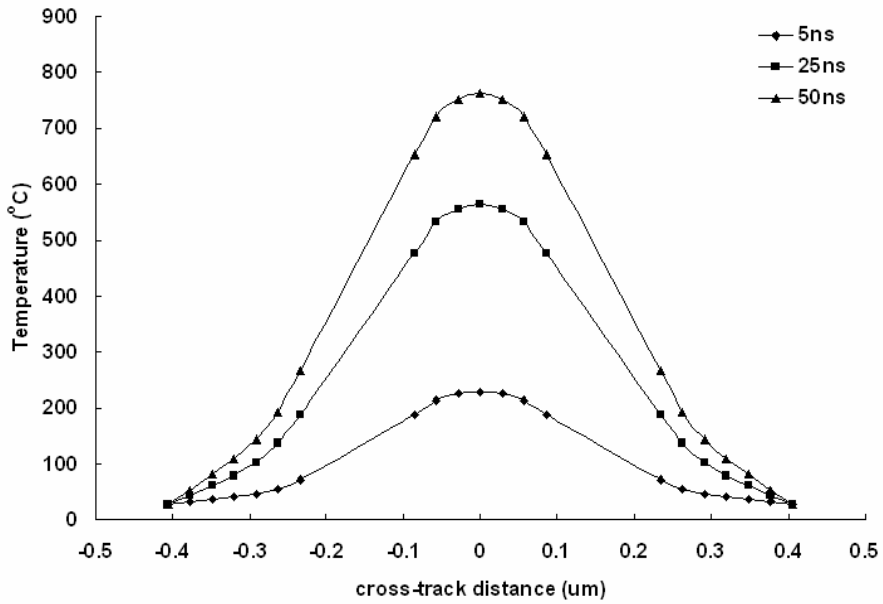


Figure 4-8 Temperature profile in the cross-track direction

during different time periods at the phase change layer

Figure 4-8 presents the temperature profile across the track during different time periods at phase change layer. The cross-track direction is perpendicular to rotation direction. From the figure, it can be concluded that the profiles are Gaussian. The curves obtained are symmetrical about the origin because the irradiating laser does not move in this direction.
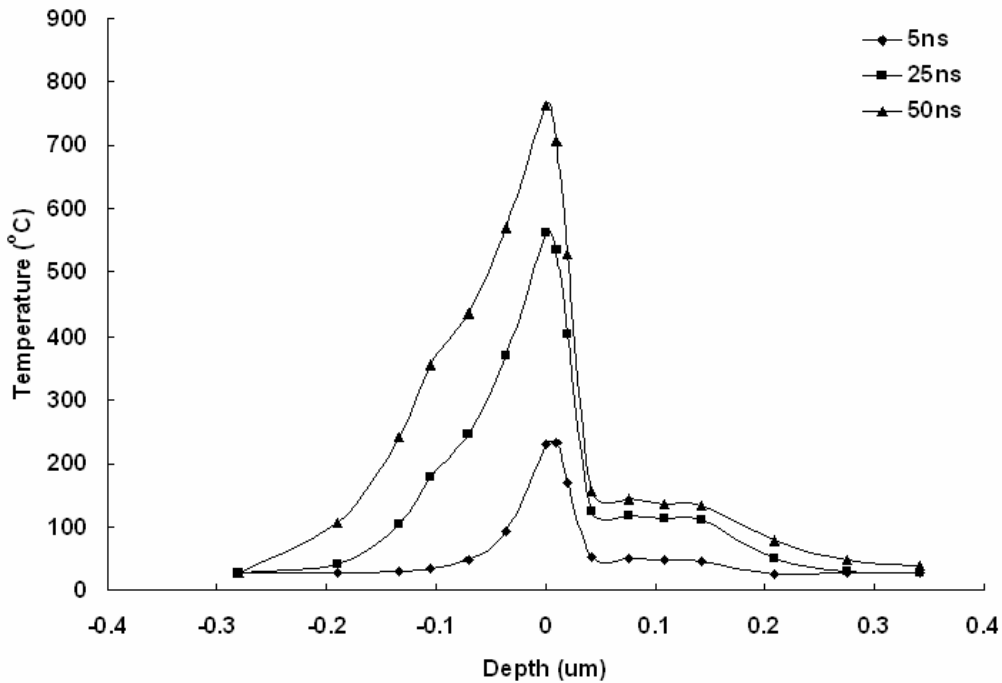


Figure 4-9 Temperature profile in the depth direction

during different time periods

Figure 4-9 shows the temperature profile in the depth direction at different time. It is observed that the temperature gradient is greatest in the lower dielectric layer(z=0.020 μm to 0.042μm). This implies that most of the heat generated in the recording layer conducted to bottom surface of the disk through the lower dielectric layer. The lower dielectric layer has two conflicting functions. One is to keep sufficient heat within the

phase change layer so that the temperature in phase change can rise to the desired extent. So it should be thick enough. The second function is to assist in the dissipation of excess heat energy into the ambient. Then it should be thin.

As the dielectric layer between the phase change layer and reflective layer plays a very important role in the recording process for phase change optical disk, the relationship between the peak temperature with respect to the thickness of this layer for both Blu-ray Disc and AOD have been investigated in following sections.

## 4.5.2    Temperature contour and profiles for AOD

The condition of disk structure: Cover layer /SiO$_2$-ZnS (105nm)/ Ge$_2$Sb$_2$Te$_5$ (20nm)/ SiO$_2$-ZnS (20nm) /Ag(80nm)/Substrate, Laser power: 12mW, groove depth: 26nm and sidewall: 28$^o$ has been investigated for AOD. Laser irradiates from the direction of substrate.

The temperature contour of phase change layer from bottom view can be seen in Figure 4-10. And Figure 4-11 shows the temperature contour of phase change layer from top view. It can be observed that the temperature of the bottom surface of phase change layer is much higher than that of the top surface. This is because the laser irradiating from the bottom direction. The peak temperature is 510.92$^o$C at 5ns. The same problem as Blu-ray Disc, the temperature on adjacent track is also high, which maybe causes the information stored lose.
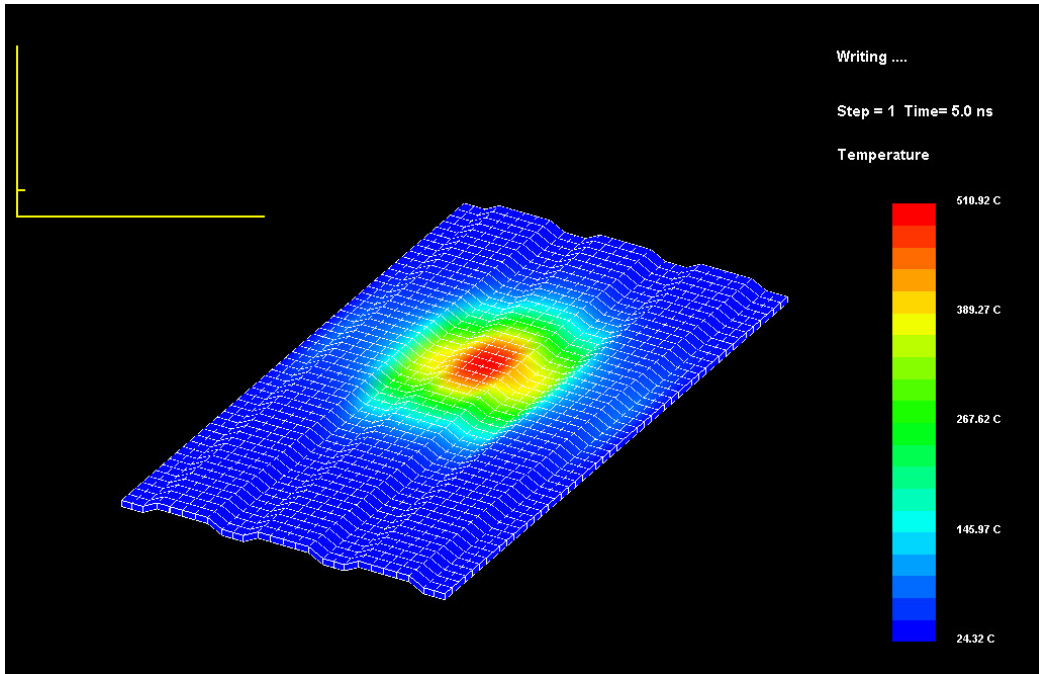
Figure 4-10 Temperature contour for bottom of phase change layer of AOD
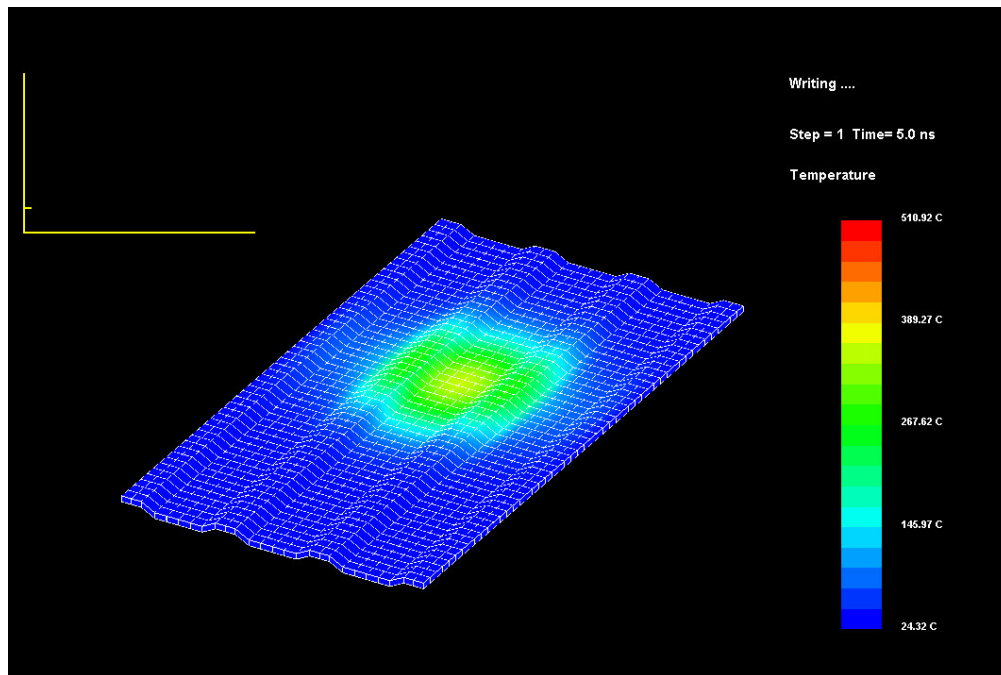


Figure 4-11 Temperature contour for top of phase change layer of AOD
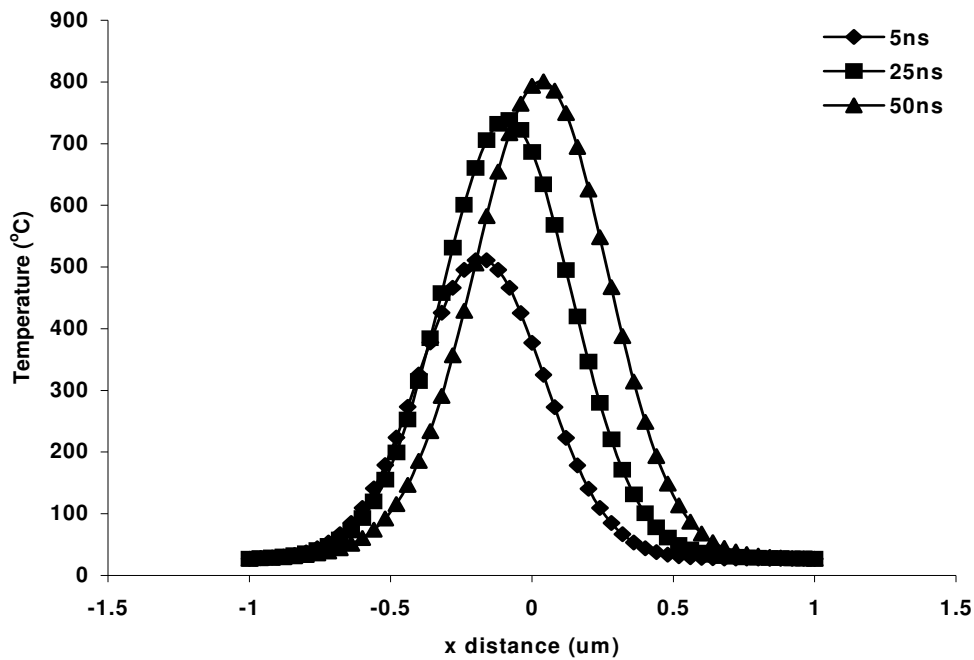
Figure 4-12 Temperature profile in the direction of rotation

at different time on the phase change layer

Figure 4-12 shows the temperature profile in the direction of rotation during different time periods at the phase change layer. The results are similar with that of Blu-ray Disc.

Figure 4-13 presents the temperature profile across the track during different time periods at phase change layer. The results are similar with that of Blu-ray Disc.
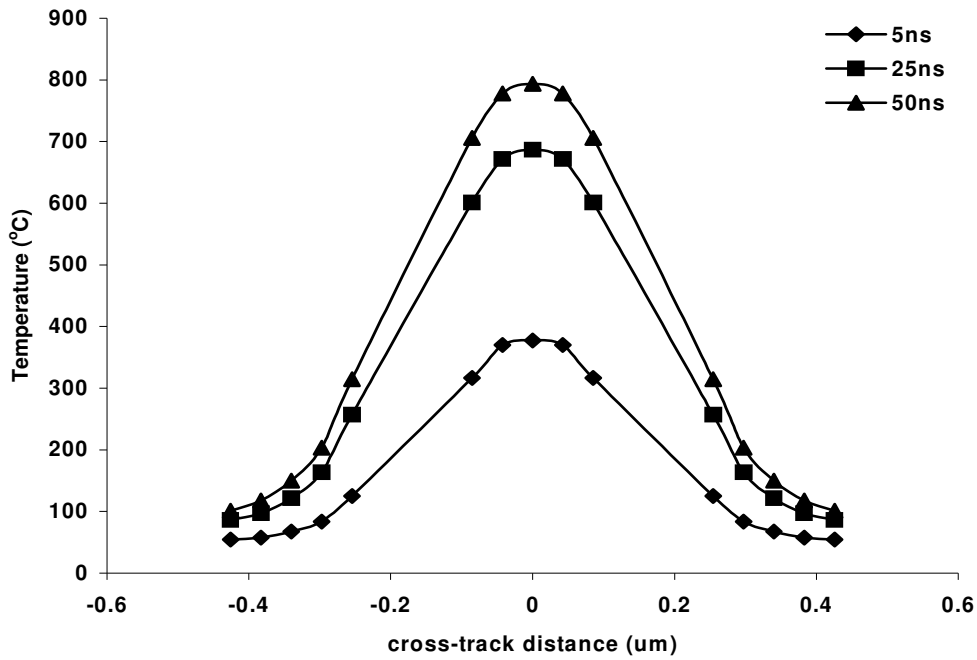
Figure 4-13 Temperature profile in the cross-track direction

at different time on the phase change layer

Figure 4-14 shows the temperature profile in the depth direction at different time.  It is observed that the temperature gradient is greatest in the $2^{nd}$ dielectric layer($z=0.020$ μm to $0.042$μm). As the dielectric layer between the phase change layer and reflective layer plays a very important role in the recording process for phase change optical disk, the relationship between the peak temperature with respect to the thickness of this layer for both Blu-ray Disc and AOD have been investigated in following sections.
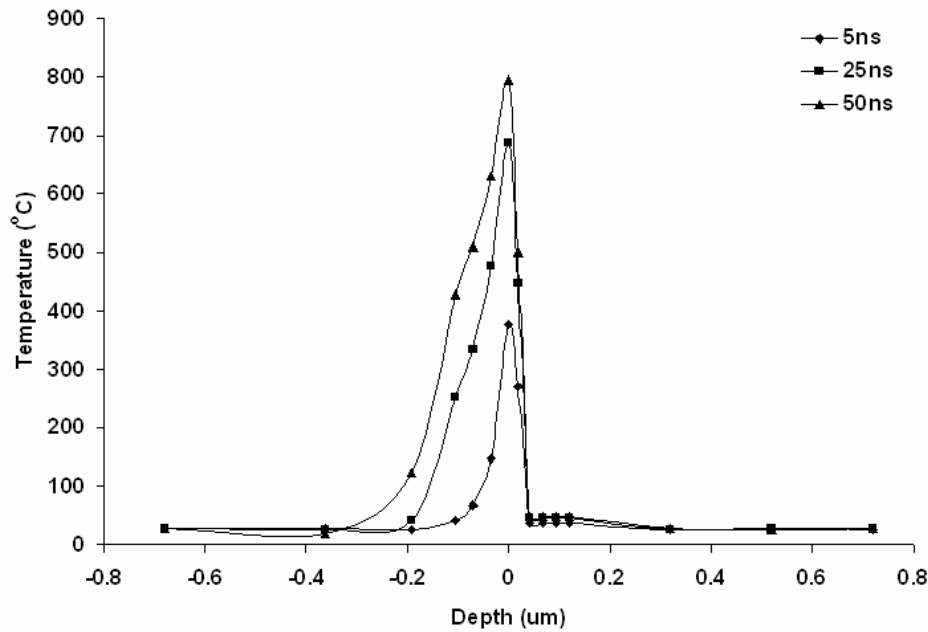
Figure 4-14 Temperature profile in the depth direction at different time

## 4.6 The effects of optical parameters on temperature profiles

In this section, the relationship between the temperature and the optical parameters was investigated for Blu-ray Disc and AOD, which can be referred to help disk designers to calibrate the operating laser power required for the write process. Three main optical aspects of phase change recording were investigated, including the laser power, laser wavelength and NA of objective lens. The simulated writing laser power ranged from 1-8mW for Blu-ray Disc and 5-20mW for AOD. The laser wavelength is 405nm for both Blu-ray Disc and AOD. And the NA is set as 0.85 for Blu-ray Disc and 0.65 for AOD.

Figure 4-15 illustrates the peak temperature versus laser power for Blu-ray Disc during the write process and Figure 4-16 shows that for AOD.

The peak temperature increases with laser power. Higher irradiation laser power

makes more optical energy absorbed in the recording layer, which generates more thermal heat. Thus it leads to higher temperature. From the figures, it can be seen that the relationship between peak temperature and laser power is almost linear for the given range of laser power.
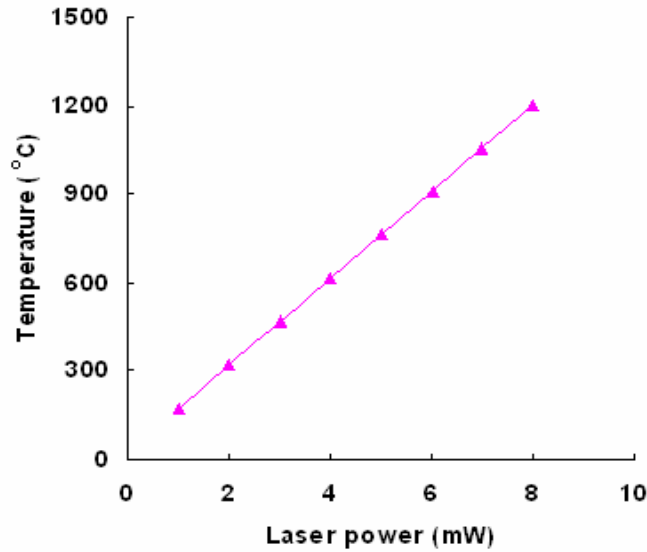


Figure 4-15 Peak temperature versus Laser power for Blu-ray Disc
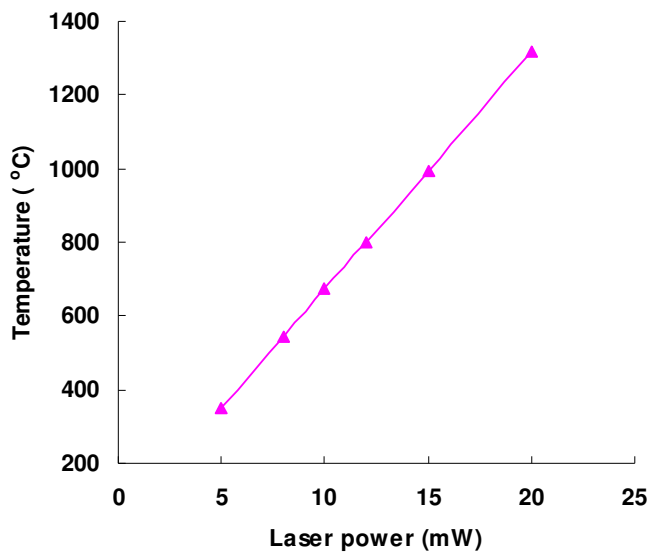


Figure 4-16 Peak temperature versus Laser power for AOD

79

## 4.7 The effects of disk parameters on temperature profiles

The disk parameters include the thickness of two dielectric layers, phase change layer and reflective layer, groove depth, sidewall angle. The relationship between peak temperature and disk parameters was investigated in this section, which will allow disk designers to optimize the disk parameters.

### a) Variation of 1st dielectric layer thickness

The thickness of the 1st dielectric layer was varied ranging from 90 to 120nm for both Blu-ray Disc and AOD. Figure 4-17 presents the results obtained from the simulations done.
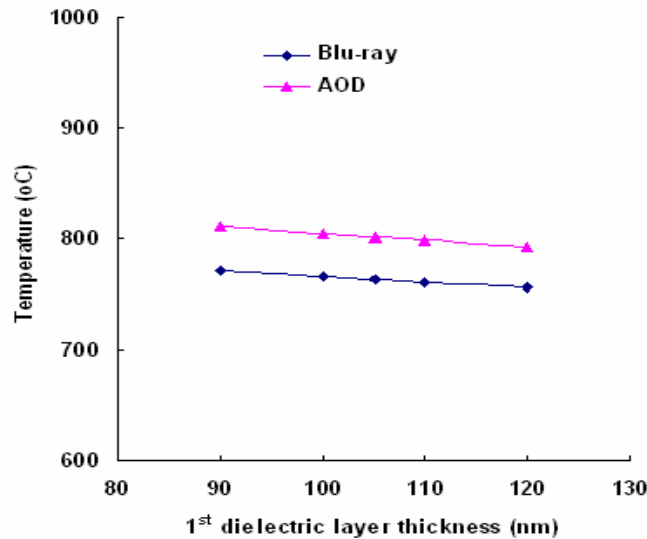


Figure 4-17 Peak temperature versus 1st dielectric layer thickness

From the figure, it can be observed that peak temperature decreases with the thickness of the 1st dielectric layer. But the effect is not obvious because the values of peak temperature change slightly with the increase of the thickness of the 1st dielectric layer

for both Blu-ray Disc and AOD. Thus it is possible to vary the thickness of $1^{st}$ dielectric layer without affecting the thermal properties of the phase change disk obviously.

## b) Variation of phase change layer thickness

Figure 4-18 shows the relationship between peak temperature during writing and the phase change layer thickness ranging from 15 to 28nm. From the figure, it is seen that the peak temperature reached during writing process increases with the phase change layer thickness. It can be explained that more laser energy can be absorbed with the thicker phase change layer at the specific disk configuration and optical parameters. The higher energy absorption generates more heat to rise the peak temperature within the phase change layer. And the peak temperature of AOD increases more quickly than that of Blu-ray Disc with the phase change layer thickness. It can be explained that the laser power employed for AOD is larger than that of Blu-ray Disc.
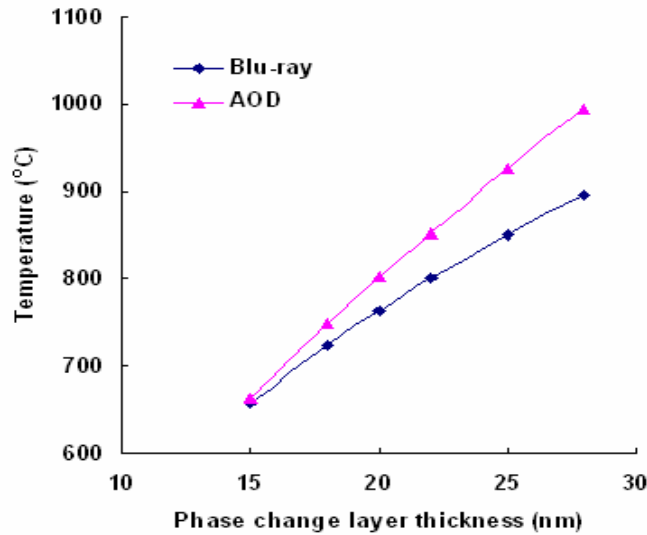


Figure 4-18 Peak temperature versus Phase change layer thickness

## c) Variation of 2$^{nd}$ dielectric layer thickness

In this section, the writing processes were simulated varying with respect to 2$^{nd}$ dielectric layer thickness ranged from 15 to 30nm. Figure 4-19 illustrates the variation of the peak temperature reached with respect to the 2$^{nd}$ dielectric layer thickness. From this figure, it is seen that the peak temperature attained increase almost linearly with changes in the 2$^{nd}$ dielectric layer thickness for both Blu-ray Disc and AOD. The explanation for this phenomenon would be that the 2$^{nd}$ dielectric plays a role as a thermal insulation due to its low thermal conductivity, which prevents the heat flowing out of the phase change layer. Hence, the thicker the 2$^{nd}$ dielectric layer is, the harder the heat generated in the phase change layer flows out, resulting in a higher peak temperature obtained in the same heating time.
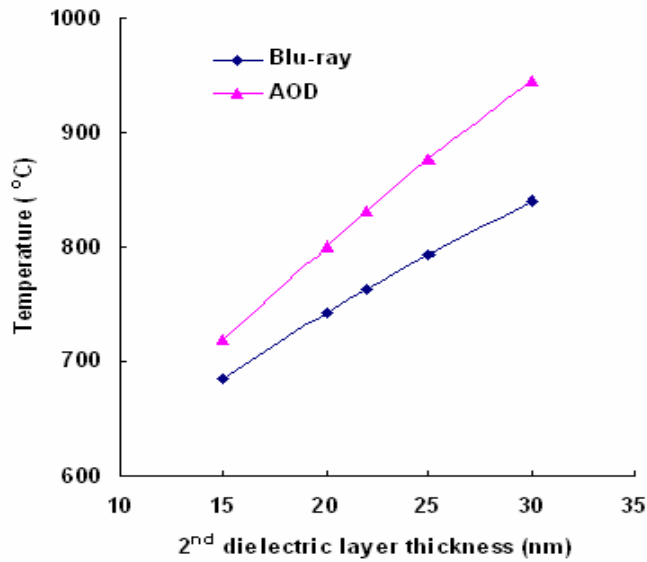


Figure 4-19 Peak temperature versus 2$^{nd}$ dielectric layer thickness

## d) Variation of reflective layer thickness

Figure 4-20 presents the peak temperature reached during writing versus reflective layer thickness ranged from 60 to 110nm. For Blu-ray Disc, the material used as the reflective layer is Al-Ar alloy while AOD employs silver as reflective layer.

From Figure 4-20, it is realized that the peak temperature reached decreased with increasing thickness of the reflective layer. The explanation should be that the reflective layer has a relatively higher thermal conductivity compared to that of phase change layer and dielectric layer. The reflective layer behaves to conduct away the heat generated within the phase change layer. With a thicker reflective layer, more heat can be conducted away and the peak temperature is lower.
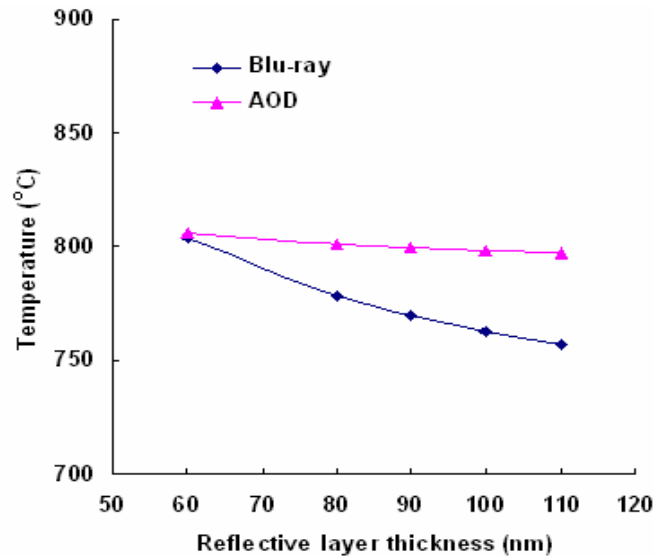


Figure 4-20 Peak temperature versus Reflective layer thickness

## e) Variation of groove depth

This section of the simulation investigates the effects that the groove depth ranged from 20 to 30nm has on the peak temperature reached.
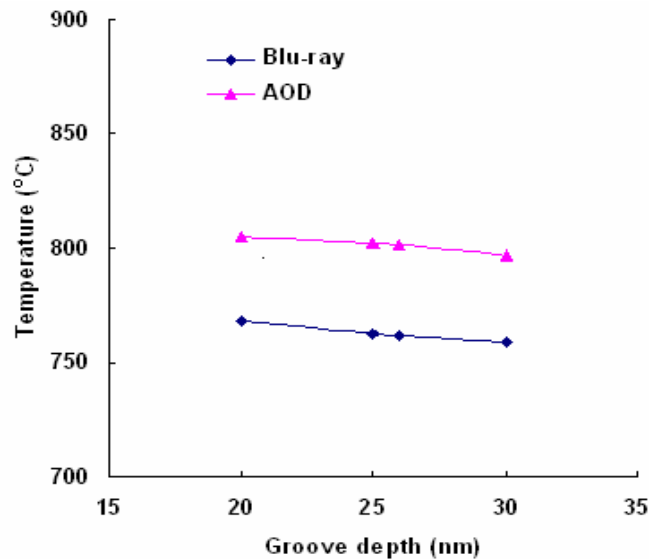


Figure 4-21 Peak temperature versus Groove depth

Figure 4-21 illustrates the results obtained. From this figure, it is observed that the peak temperature attained is smaller with respect to the groove depth increasing. Thus, it is possible to increase the groove depth so as to decrease the peak temperature in the Blu-ray Disc and AOD.

## f) Variation of sidewall angle

Figure 4-22 presents the peak temperature reached during writing process versus the sidewall angle varying from $25^{o}$ to $35^{o}$. From this figure, it is observed that the peak temperature attained is almost constant with respect to the sidewall angle. Thus, it is possible to vary the sidewall angle without affecting the thermal properties of the phase

change optical disks.
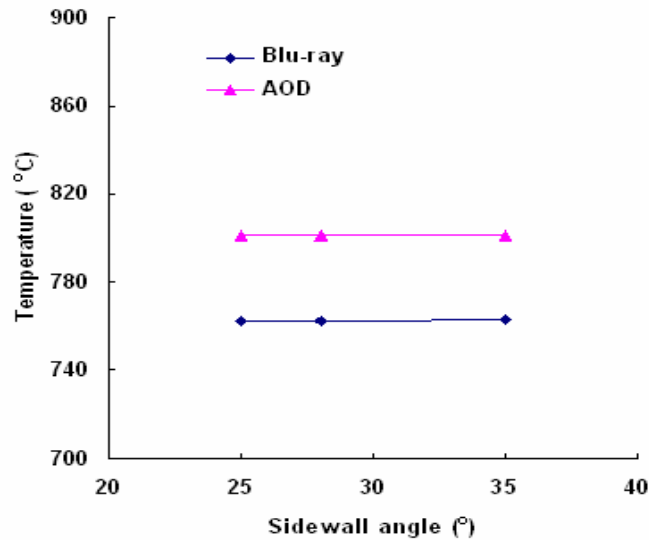


Figure 4-22 Peak temperature versus Sidewall angle

## 4.8 Summary

In this chapter, the thermal modeling and analysis for blu-ray and AODs has been conducted. The temperature distribution and profiles within the blu-ray and AODs have been got. From the preceding discussions, it is found that various aspects of the phase change recording system affects the thermal profiles within the disk. They are categorized as optical parameters and disk parameters. The optical parameters considered the irradiating laser wavelength, laser power and NA of objective lens employed. While the disk parameters took into consideration of thickness of the various thin film layers used in the disk, the groove depth and sidewall angle of the phase change optical disk.

The relationship between the peak temperature reached during writing process and the

various parameters for Blu-ray Disc and AOD are summarized as follows:

1) Laser power: Higher laser power, higher peak temperature

2) $1^{st}$ dielectric layer: Peak temperature almost constant with variations of $1^{st}$ dielectric layer thickness

3) Phase change layer: Thicker phase change layer, higher peak temperature

4) $2^{nd}$ dielectric layer: Greater thickness, higher peak temperature

5) Reflective layer: Thicker reflective layer, lower peak temperature

6) Groove depth: Peak temperature decreases with increasing of groove depth

7) Sidewall angle: Peak temperature almost constant with change of sidewall angle

The detail of above results can be gotten in previous section of this chapter. These results can benefit the design of Blu-ray Disc and AOD.

# Chapter 5  Thermal Deformation of Blu-ray Disc and AOD

## 5.1  Introduction

 As mentioned in the motivations of this project, the deformation of phase change optical disks affects the recording characteristics. Even worse, the deformation is accumulated and becomes larger with more writing cycle. Finally the deformation may reach the extent making recording failure in advance of its designed lifetime. That means the deformation may reduce the overwriting cycle or lifetime of phase change optical disks. In this chapter, the thermal deformation of Blu-ray Disc and AOD will be investigated.

## 5.2  Modeling for Blu-ray Disc and AOD

The geometry modeling and FEM modeling for Blu-ray Disc and AOD are the same as section 4.2 and section 4.3. The detail can be seen in these parts. Figure 4-3 shows the finite element model for Blu-ray Disc. Figure 4-4 shows the finite element model for AOD. The mechanical properties of materials can be seen in Table 5-1.

## 5.3  Simulation conditions

The simulation conditions used for thermo-mechanical analysis for Blu-ray Disc and AOD are listed in Table 4-4. The displacement boundary condition is assumed that the top and bottom surface is constrained for   convenience.

Table 5-1 Thermo-mechanical properties of materials for Blu-ray Disc and AOD

| Material type | | Density $(Kg/m^3)$ | Heat Conductivity (J/mKs) | Heat Capacity (J/KgK) | Refractive Index n | Extinction Coefficient k | Elastic Modulus E (GPa) | Poisson Ration ν | CTE $(10^{-6}/K)$ |
|---|---|---|---|---|---|---|---|---|---|
| Cover layer | | 1200 | 0.22 | 1172 | 1.569 | 0.03 | 25 | 0.21 | 70 |
| Dielectric | | 3650 | 0.6 | 560 | 2.129 | 0 | 20 | 0.18 | 6.3 |
| Phase change | Amorphous | 6150 | 0.5 | 210 | 4.8756 | 1.932 | 30 | 0.19 | 18 |
| | Crystalline | 6150 | 0.5 | 210 | 4.75 | 4.349 | 30 | 0.19 | 18 |
| Reflective layer - Al-Ar | | 2750 | 25 | 890 | 1.438 | 5.035 | 69 | 0.33 | 23.6 |
| Reflective layer - Ag | | 10500 | 429 | 235 | 1.0003 | 1.496 | 75.84 | 0.37 | 18.9 |
| UV Resin | | 1200 | 0.22 | 1172 | 1.569 | 0.03 | 25 | 0.21 | 70 |
| Substrate | | 1200 | 0.22 | 1172 | 1.569 | 0.03 | 25 | 0.21 | 70 |

CTE: coefficients of thermal expansion

## 5.4  Deformation contour

The deformation in thickness direction is the most concerned. So the deformation in thickness direction will be focused in the following sections. For convenience, deformation in thickness direction is named Z displacement in the following sections.

### 5.4.1     Deformation contour and profiles for Blu-ray Disc

The condition of disk structure: Cover layer /SiO$_2$-ZnS (105nm)/ Ge$_2$Sb$_2$Te$_5$ (20nm)/ SiO$_2$-ZnS (22nm) /Al(100nm)/Substrate, Laser power: 5mW, groove depth: 25nm and sidewall: 28$^o$ has been investigated for Blu-ray Disc. Laser irradiates from the direction of cover layer.

Figure 5-1 shows the deformation in each layer of blu-ray at 5ns and Figure 5-2 shows that at 50ns. From the two figures, it is seen that the deformation in phase change layer is the largest at 5ns while the deformation in   cover layer is the largest at 50ns.
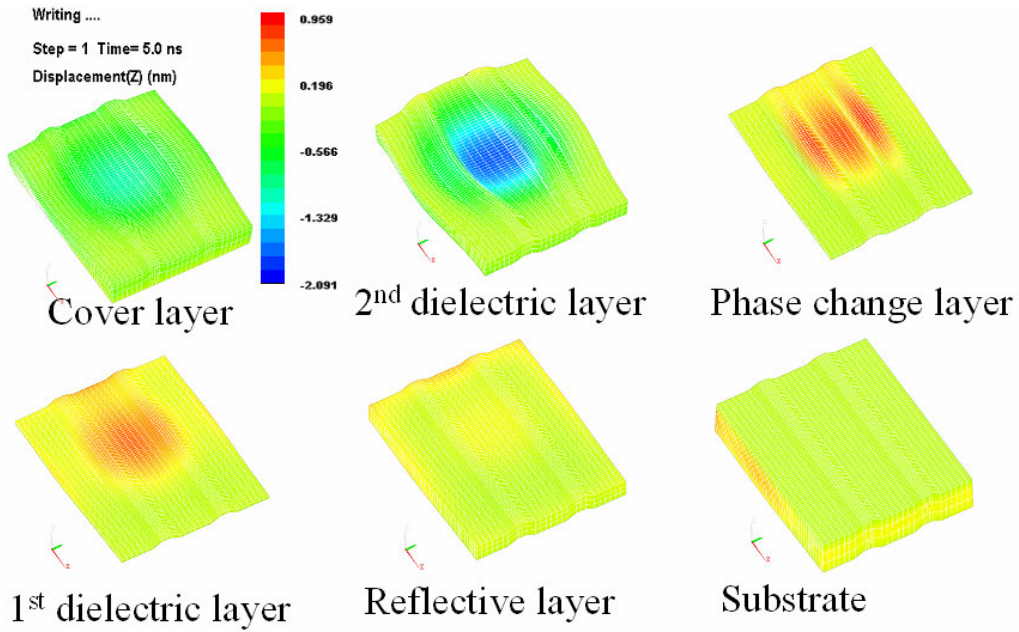
Figure 5-1 Deformation shape of each layer of blu-ray at 5ns
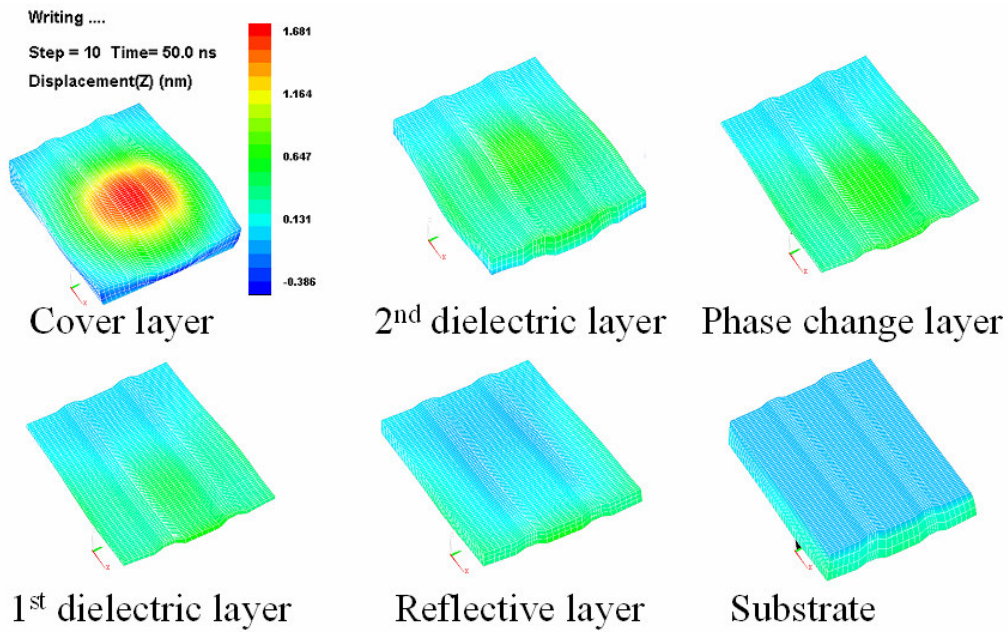


Figure 5-2 Deformation shape of each layer of blu-ray at 50ns

Figure 5-3 shows the displacement in thickness direction in the cover layer. The peak deformation is 1.581nm on the laser irradiation point. It can be seen that the deformation is spread to adjacent grooves. The shape of the deformation area seems like a bump.

From the results obtained, it can be observed that the deformations in the adjacent tracks are large. This kind of deformation has made the groove and land width expand or shrink. So the groove land structure can be changed after many times overwriting.
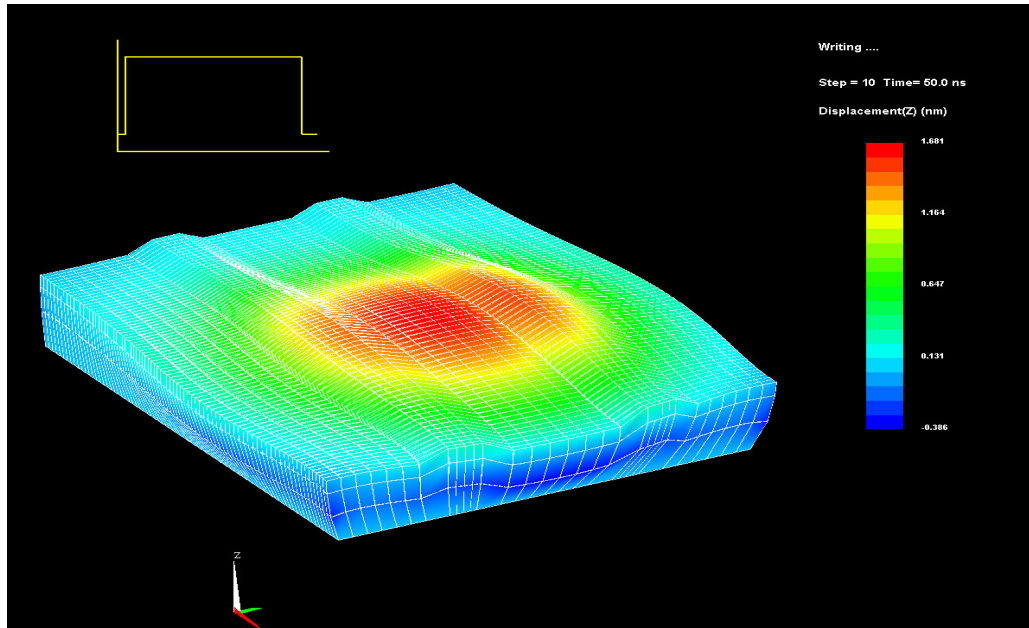


Figure 5-3 Deformation in cover layer at 50ns

## 5.4.2 Deformation contour and profiles for AOD

The condition of disk structure: Cover layer /SiO$_2$-ZnS (105nm)/ Ge$_2$Sb$_2$Te$_5$ (20nm)/ SiO$_2$-ZnS (20nm) /Ag(80nm)/Substrate, Laser power: 12mW, groove depth: 26nm and sidewall: 28$^o$ has been investigated for AOD. Laser irradiates from the direction of substrate.

Figure 5-4 shows the deformation in each layer of AOD at 5ns and Figure 5-5 shows that at 50ns. From the two figures, it can be observed that the deformation in phase change layer is the largest at 5ns while the deformation in substrate is the largest at 50ns.
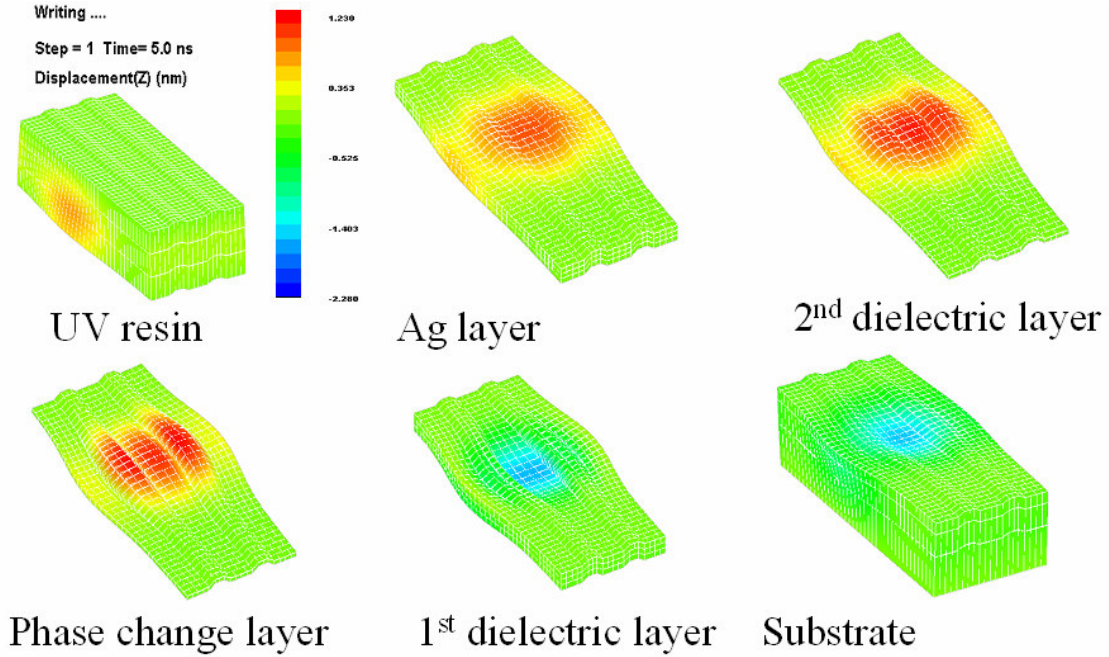
Figure 5-4 Deformation shape of each layer of AOD at 5ns
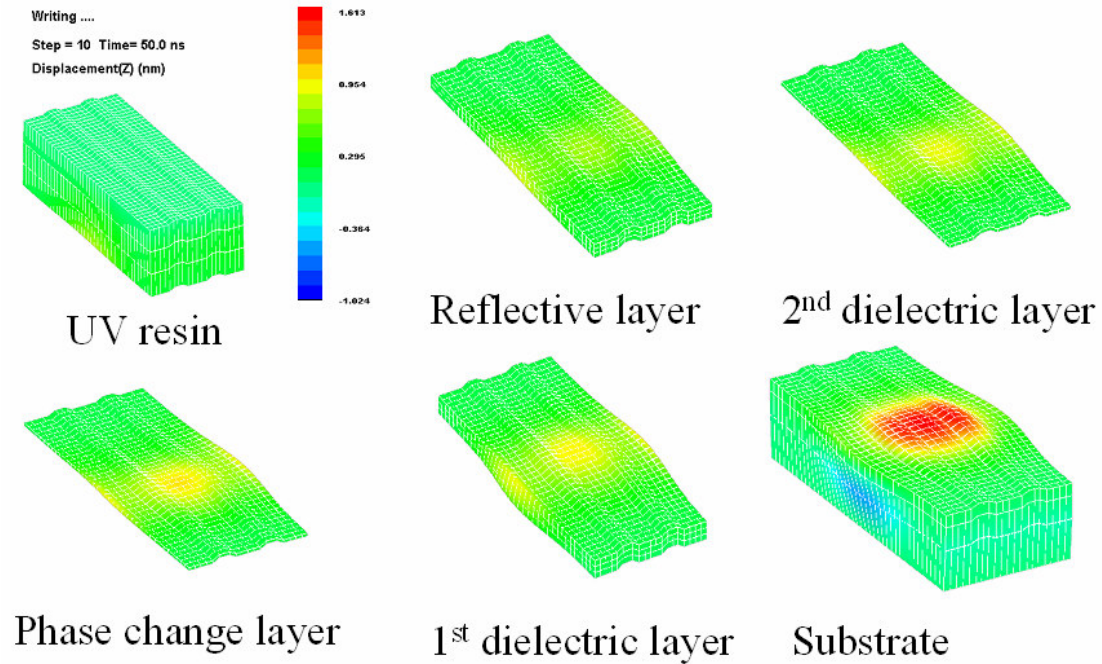


Figure 5-5 Deformation shape of each layer of AOD at 50ns
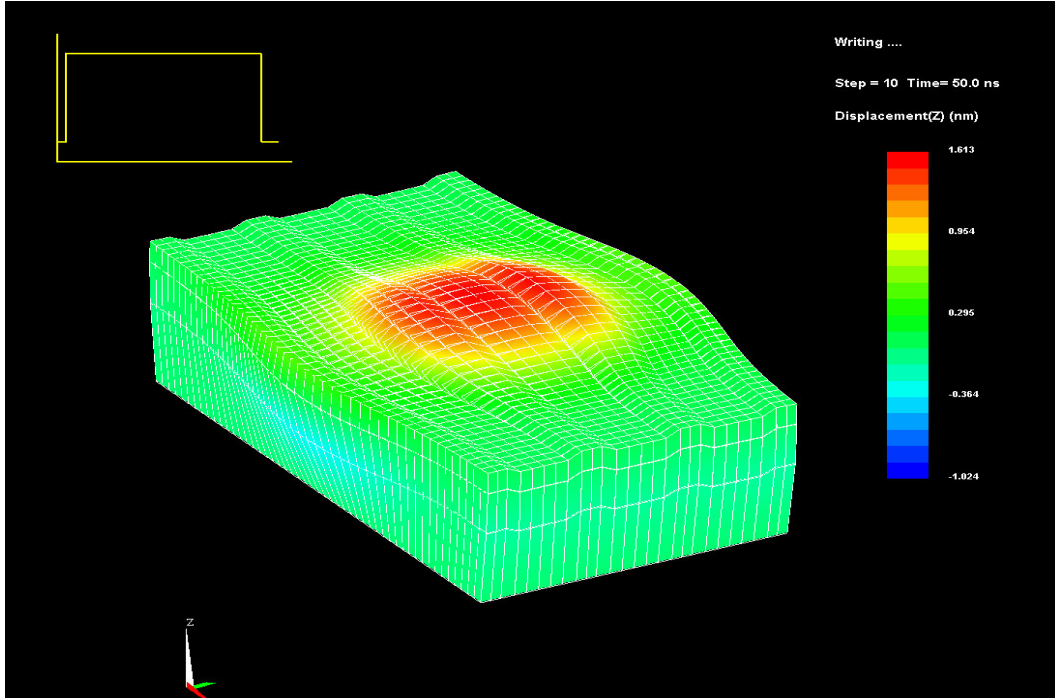
Figure 5-6 Deformation in substrate at 50ns for AOD

Figure 5-6 shows Z displacement in the substrate. The peak deformation is 1.613nm on the laser irradiation point in the substrate layer. The deformation distribution in the substrate of AOD is similar with that in the cover layer of Blu-ray Disc.

## 5.5 Comparison between peak temperature and peak deformation

Figure 5-7 shows the temperature and deformation along thickness direction at 50ns for Blu-ray Disc and Figure 5-8 for AOD. It can be seen that the peak temperature and peak deformation are emerging in different layers. The peak temperature always exists in the phase change layer while the peak deformation exists in the other layers. At 5ns, the peak deformation lies in phase change layer and the peak deformation goes to the cover layer At 50ns for Blu-ray Disc. For AOD, the situation is similar with cover layer replaced by

92

substrate. It can be explained that the heat are restricted in dielectric layer and phase change layer at the beginning. Then the heat spread to other layers and the temperature gets stable. Although the temperature in the cover layer (substrate for AOD) is smaller than phase change layer and dielectric layer, the peak deformation exists in the cover layer or substrate as the coefficients of thermal expansion(CTE) of cover layer (substrate for AOD) are much larger than that of other layers. One method to solve this problem is to add thermal shielded layers between the dielectric layer and cover layer (substrate for AOD) to decrease the temperature in cover layer. The other method is to find some other materials with low CTE to substitute this kind of cover layer(substrate for AOD).
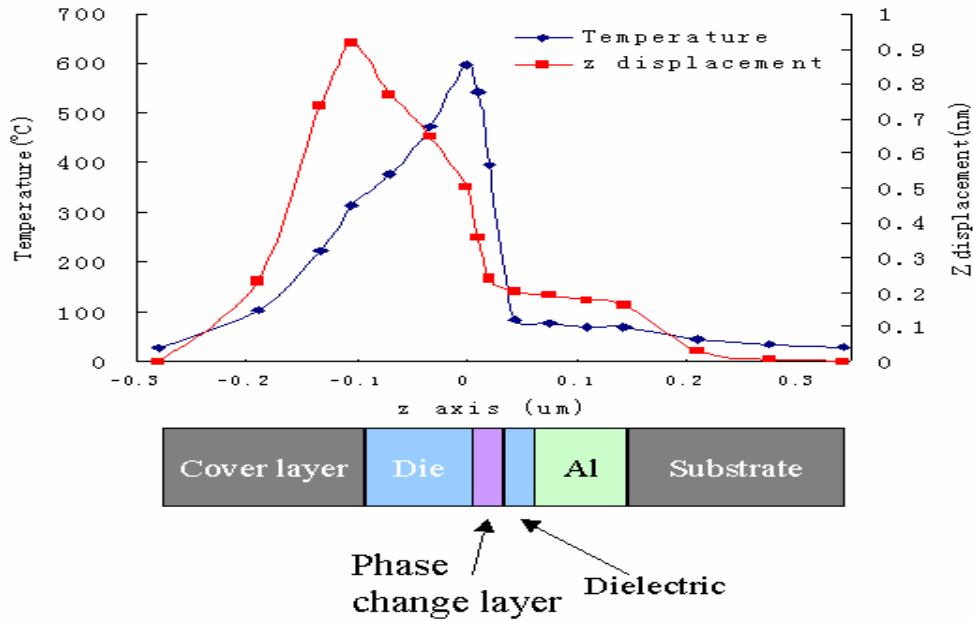


Figure 5-7 Temperature and deformation along thickness direction for Blu-ray Disc

93
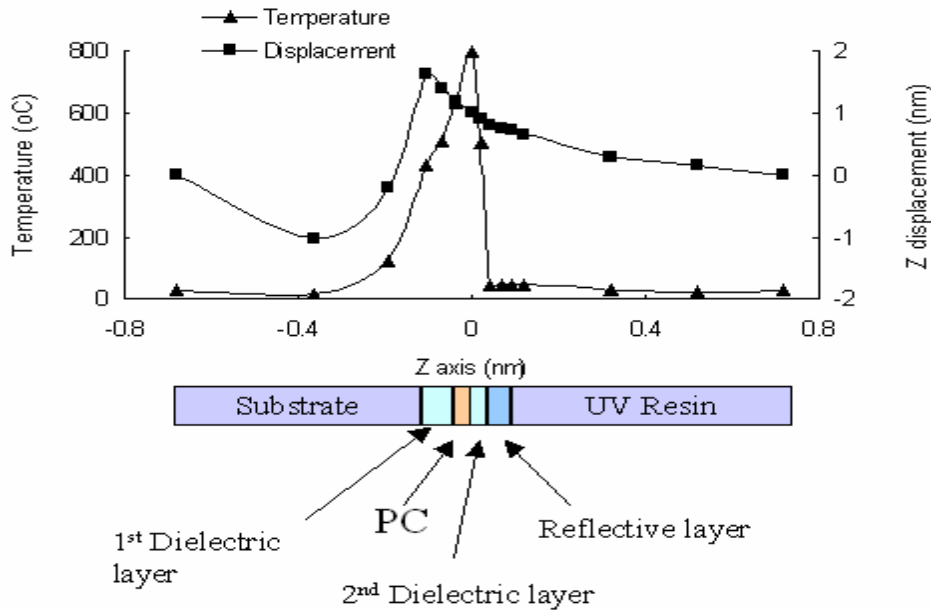
Figure 5-8 Temperature and deformation along thickness direction for AOD

## 5.6 The effects of optical parameters on deformation profiles

In this section, the relationship between the deformation and the optical parameters was investigated for blu-ray and AOD. Three main optical aspects of phase change recording were investigated, including the laser power, laser wavelength and NA of objective lens. The simulated writing laser power ranged from 1-8mW for Blu-ray and 5-20mW for AOD. The laser wavelength is 405nm for both Blu-ray and AOD. And the NA is set as 0.85 for Blu-ray and 0.65 for AOD.

Figure 5-9 illustrates the peak deformation versus laser power for Blu-ray Disc during the write process and Figure 5-10 shows that for AOD. From these two figures, it is found that the peak deformation increases with laser power. Higher irradiation laser power makes more optical energy absorbed in the recording layer, which generates more thermal heat. Thus it leads to higher temperature. Under higher temperature, the

thermal deformation is surely larger. From the figures, it can be seen that the relationship between peak deformation and laser power is almost linear for the given range of laser power.
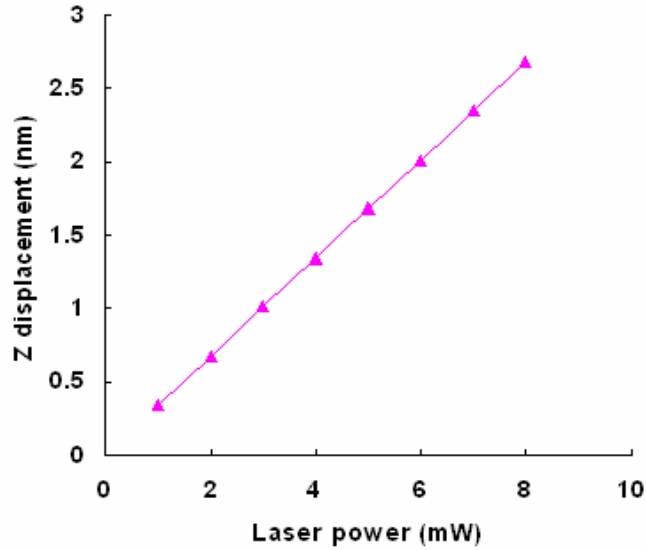


Figure 5-9 Peak deformation versus Laser power for Blu-ray Disc
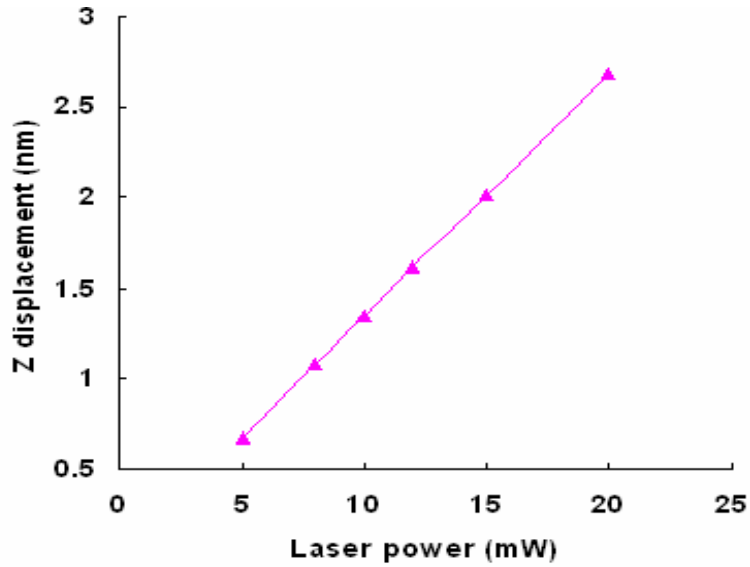


Figure 5-10 Peak deformation versus Laser power for AOD

## 5.7  The effects of disk parameters on deformation profiles

The disk parameters include the thickness of two dielectric layers, phase change layer and reflective layer, groove depth, sidewall angle. The relationship between peak deformation and disk parameters was investigated in this section, which will allow disk designers to optimize the disk parameters.

### a) Variation of 1st dielectric layer thickness

The thickness of the 1st dielectric layer was varied ranging from 90 to 120nm for both blu-ray and AOD. Figure 5-11 presents the results obtained from the simulations done.
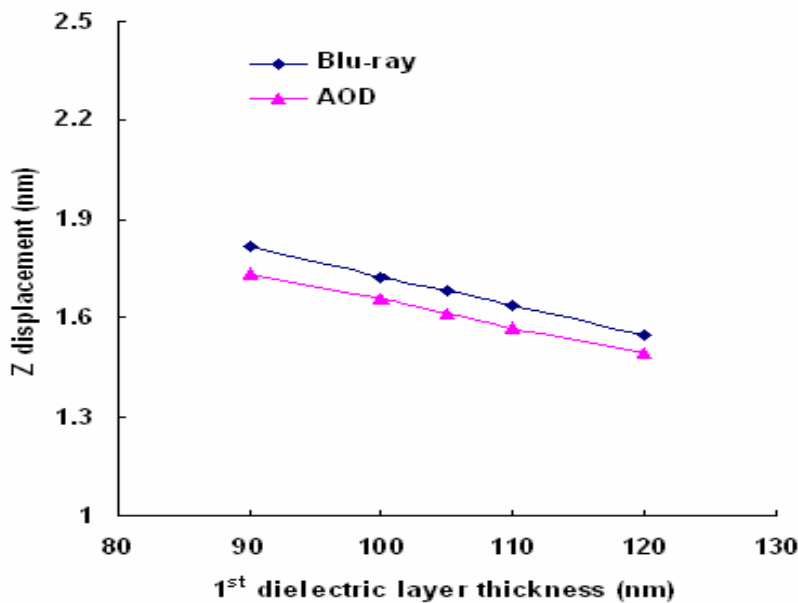


Figure 5-11 Peak deformation versus 1st dielectric layer thickness

From the figure, it can be observed that peak deformation decreases with the thickness of the 1st dielectric layer for both Blu-ray and AOD. The explanation should be that the coefficient of thermal expansion of dielectric layer is smaller than other layers. From previous section 4.7, the thermal properties   are almost not affected by the change of 1st

dielectric layer thickness. Hence the deformation in Blu-ray and AOD can be decreased by increasing the thickness of 1ˢᵗ dielectric layer without affecting the thermal properties.

## b) Variation of phase change layer thickness

Figure 5-12 shows the relationship between peak deformation during writing and the phase change layer thickness ranged from 15 to 28nm. From the figure, it can be seen that the peak deformation reached during writing process increases with the phase change layer thickness. It can be explained that more laser energy can be absorbed with the thicker phase change layer at the specific disk configuration and optical parameters. The higher energy absorption generates more heat to rise the temperature within the disks. Under higher temperature for the same disk, the thermal deformation is surely larger.
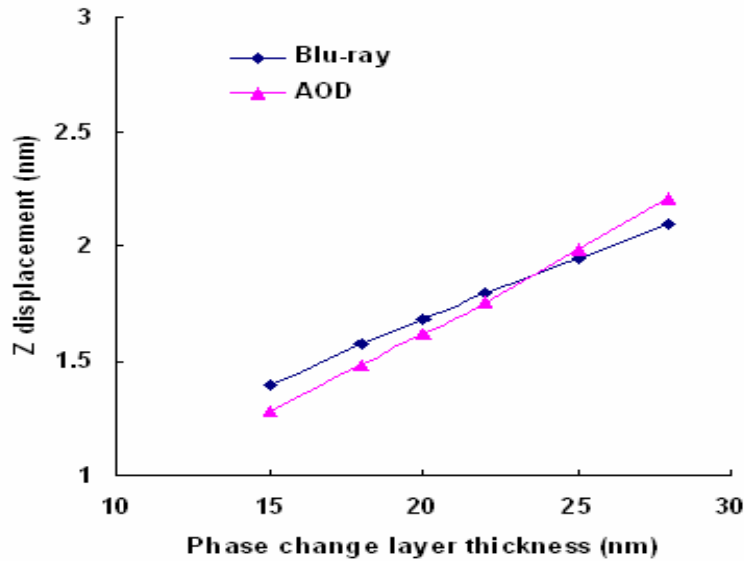


Figure 5-12 Peak deformation versus Phase change layer thickness

## c) Variation of 2$^{nd}$ dielectric layer thickness

In this section, the writing processes were simulated varying with respect to 2$^{nd}$ dielectric layer thickness ranged from 15 to 30nm.
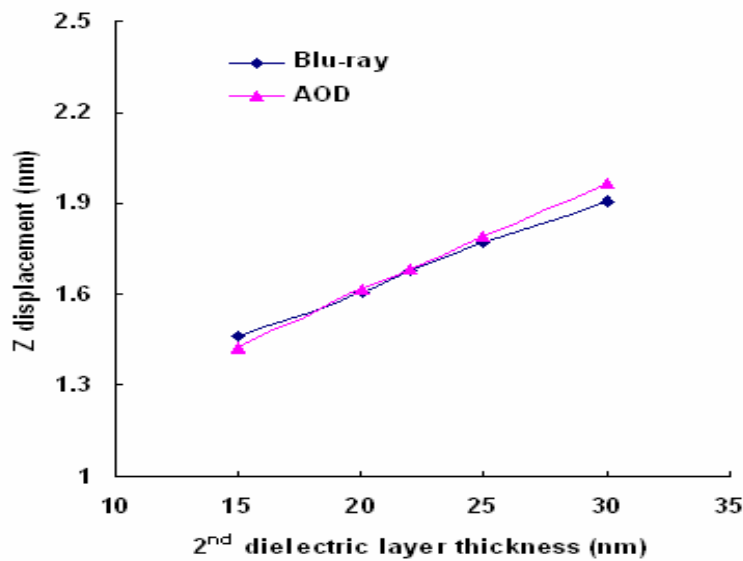


Figure 5-13 Peak deformation versus 2$^{nd}$ dielectric layer thickness

Figure 5-13 illustrates the variation of the peak deformation reached with respect to the 2$^{nd}$ dielectric layer thickness. From this figure, it is seen that the peak deformation attained increase almost linearly with changes in the 2$^{nd}$ dielectric layer thickness for both Blu-ray and AOD. Serving as a thermal insulation, thicker 2$^{nd}$ dielectric layer results in higher temperature within the disks. And the thermal expansion will be heavier.

## d) Variation of reflective layer thickness

Figure 5-14 presents the peak deformation reached during writing versus reflective layer thickness ranged from 60 to 110nm. For Blu-ray Disc, the material used as the reflective layer is Al-Ar alloy while AOD employs silver as reflective layer.

From Figure 5-14, it is realized that the peak deformation reached decreased with increasing thickness of the reflective layer. The explanation should be that the reflective layer serves as thermal conductor. The Thicker is the reflective layer, the lower is the temperature in the disks. The thermal deformation is smaller under lower temperature.
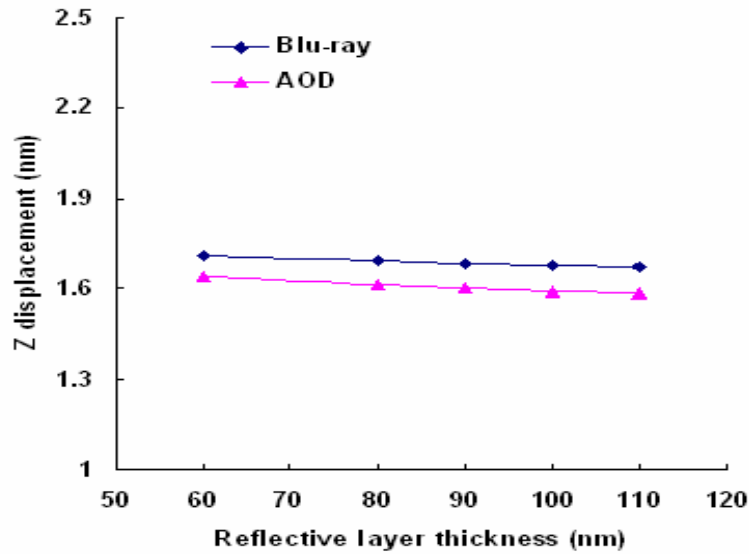


Figure 5-14 Peak deformation versus Reflective layer thickness

## e) Variation of groove depth

This section of the simulation investigates the effects that the groove depth ranged from 20 to 30nm has on the peak deformation reached. Figure 5-15 illustrates the results obtained. From this figure, it is observed that the peak deformation attained decrease with respect to the groove depth. Thus, it is possible to increase the groove depth to decrease the deformation of the phase change optical disks.
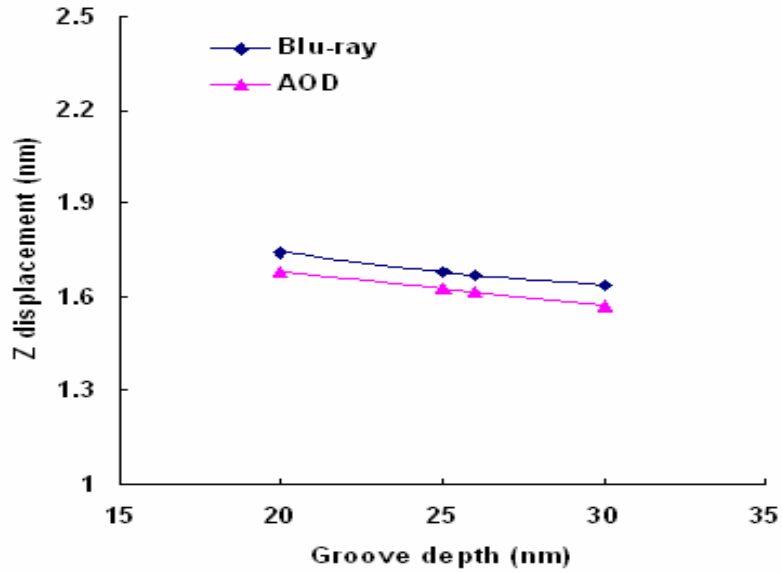
Figure 5-15 Peak deformation versus Groove depth

## f) Variation of sidewall angle

Figure 5-16 presents the peak deformation reached during writing process versus the sidewall angle varying from $25^o$ to $35^o$.
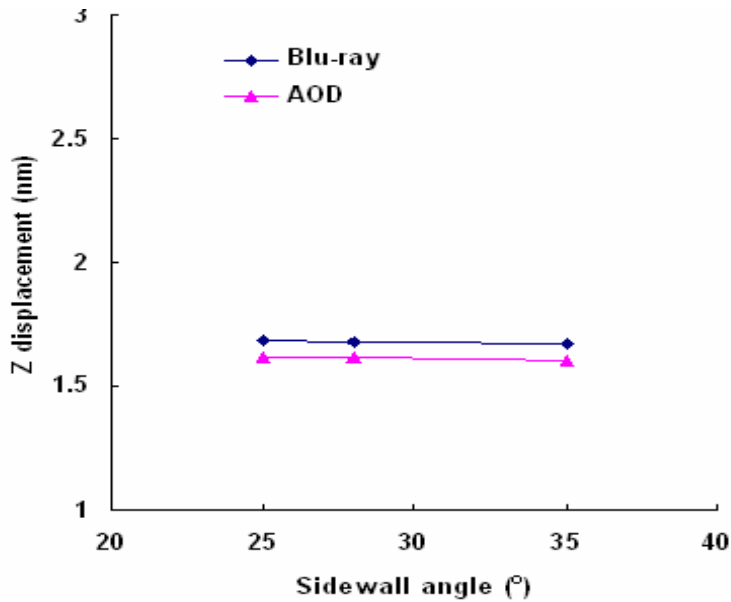


Figure 5-16 Peak deformation versus Sidewall angle

100

From this figure, it is observed that the peak deformation attained is almost constant with respect to the sidewall angle. Hence, the variation of the sidewall angle does not affect the thermal deformation of the phase change optical disks.

## 5.8  Summary

In this chapter, the thermal deformation for Blu-ray Disc and AOD has been investigated. The deformation distribution and profiles within the Blu-ray Disc and AOD have been gotten. The deformed area seems like a bump and the deformation in adjacent tracks are large. The peak deformation and peak deformation lies in different layers.  It is found that various aspects of the phase change recording system affect the thermal deformation within the disk. They are categorized as optical parameters and disk parameters. The optical parameters considered the irradiating laser wavelength, laser power and NA of objective lens employed. While the disk parameters took into consideration of thickness of the various thin film layers used in the disk, the groove depth and sidewall angle of the phase change optical disk.

The relationship between the peak deformation reached during writing process and the various parameters for Blu-ray Disc and AOD are summarized as follows:

1) Laser power: Higher laser power, larger peak deformation

2) $1^{st}$ dielectric layer: Larger thickness, smaller peak deformation

3) Phase change layer: Thicker phase change layer, larger peak deformation

4) $2^{nd}$ dielectric layer: Greater thickness, larger peak deformation

5) Reflective layer: Thicker reflective layer, smaller peak deformation

6)  Groove depth: Peak deformation decreases with increasing of groove depth

7)  Sidewall angle: Peak deformation almost constant with change of sidewall angle

The detail of above results can be gotten in previous section of this chapter. These results can benefit the design of Blu-ray Disc and AOD to decrease the thermal deformation in phase change optical disks. To decrease the thermal deformation in phase change optical disks, thinner phase change layer and smaller laser power are two most effective methods. Increasing the thickness of $1^{st}$ dielectric layer and reflective layer, decreasing the thickness of $2^{nd}$ dielectric layer, and increasing the groove depth are some other effective methods to decrease the thermal deformation.

# Chapter 6 Conclusion and Future Works

The thermo-mechanical theory was used to analyze the thermo-mechanical problem in phase change optical disks. Thermo-mechanical modeling was proposed and thermo-mechanical analysis module was established successfully applying finite element method. The module was implanted into DSI developed thermal analysis software for phase-change optical disks - PCODD. Now PCODD contained the capability of both thermal and mechanical analysis for phase change optical disks.

With this software, the thermal analysis of Blu-ray Disc and AOD had been done. The temperature contour and profile for those two kinds of phase change optical disks had been obtained and analyzed. The effects of optical and disk structure parameters on temperature profiles in Blu-ray Disc and AOD had been investigated. The results shows: Higher laser power, higher peak temperature; Peak temperature almost constant with variations of $1^{st}$ dielectric layer thickness; Thicker phase change layer, higher peak temperature; Greater thickness of $2^{nd}$ dielectric layer, higher peak temperature; Thicker reflective layer, lower peak temperature; Peak temperature decrease with larger groove depth; Peak temperature is almost constant with change of sidewall angle

Following the thermal analysis, the thermal deformation in Blu-ray Disc and AOD was investigated with PCODD. The thermal deformation distribution had been acquired and discussed. The effects of optical and disk structure parameters on thermal deformation in

Blu-ray Disc and AOD had been investigated. The results demonstrated: Higher laser power, larger peak deformation;: Larger thickness of 1$^{st}$ dielectric layer, smaller peak deformation; Thicker phase change layer, larger peak deformation;: Greater thickness of 2$^{nd}$ dielectric layer, larger peak deformation. Thicker reflective layer, smaller peak deformation; Peak deformation decreases with increasing of groove depth; Peak deformation is almost constant with change of sidewall angle.

In Summary, thinner phase change layer and lower laser power are two most effective methods to decrease the thermal deformation in Blu-ray and AOD. Increasing thickness of 1$^{st}$ dielectric layer and reflective layer, increasing the groove depth, and decreasing 2$^{nd}$ dielectric layer thickness are some other effective methods to decrease the thermal deformation in Blu-ray and AOD. These results can be referenced for the design of Blu-ray Disc and AOD.

The temperature profiles and deformation profiles had been compared. It was found that the peak temperature and peak deformation existed in different layers for both Blu-ray disc and AOD. The peak temperature lay in phase change layer while the peak deformation lay in substrate for AOD and cover layer for Blu-ray Disc.

Now the elastic thermal deformation of high-density phase change optical disks, such as Blu-ray Disc and AOD, has been investigated. Then the next step should focus on the plastic thermal deformation simulation of the write and rewrite processes using future versions of the software. Other future works, including the investigation of thermal deformation of new structures of Blu-ray Disc and AOD, Super-RENS optical disks and

new generation phase change optical disks, can be conducted.

In conclusion, the objectives of this project have been achieved. A new version of the three-dimensional thermo-mechanical FEM modeling and analysis software for high-density phase change optical disks named PCODD, have been developed. The thermal deformation of Blu-ray Disc and AOD has been investigated using this software. The effects of optical parameters and disk parameters on thermal deformation also have been got. Some methods have been proposed to decrease the thermal deformation in Blu-ray Disc and AOD.

# References

[1]     D.J. Parker: DVD, the update for CD-ROM Professional. 9 (8) 68 (1996)

[2]     Lee Purcell. CD-R/DVD: Disc Recording Demystified. New York: McGraw-Hill, 2000

[3]     G. Bouwhuis: Principles of Optical Disc Systems, edited by Dr E.R Pike RSRE, Adam Hilger Publisher, USA, 7 (1985)

[4]     Toshiaki Iwanaga: Advanced signal processing for high-density recording using blue-violet laser. Optical Data Storage, 2004, 231

[5]     S. R. Ovshinsky: Reversible Electrical Switching Phenomena in Disordered Structure, Phys. Rev. Lett., 21(20), 1450-1453 (1968)

[6]     T. Ohta, M. Birukawa, N. Yamada, K. Hirao: Optical Recording; Phase-change and Magneto-optical recording. Journal of Magnetism and Magnetic Materials 242-245 (2002), 108-115

[7]     H.J. Borg, R.V. Woudenberg: Trends in Optical Recording. Journal of Magnetism and Magnetic Materials 193 (1999), 519

[8]     N. Akahira, N. Miyagawa, K. Nishiuchi, Y. Skaue and E. Ohno: High Density Recording on Phase Change Optical disks. SPIE. 2514, 294

[9]     N. Yamada, E. Ohno, K. Nishiuchi and N. Akahira: Rapid-phase Transitions of GeTe-Sb2Te3 Pseudobinary Amorphous Thin Films for an Optical Disk Memory, J. Appl. Phys., 69 (5), 2849-2856 (1991)

[10]    T. Nishida, M. Terao, Y. Miyauchi and N. Akahira: Single-beam Overwrite

Experiment using In-Se based Phase-change Optical Media, Appl. Phys. Lett. 50 (11), 667-669 (1987)

[11]   G.F. Zhou: Material Aspects in Phase Change Optical Recording. Materials Science & Engineering A304-306 (2001) 73-80

[12]   N. Miyagawa, Y. Gotoh, E. Ohno, K. Nishiuchi and N. Akahira: Land and Groove Recording for High Track Density on Phase-Change Optical Disks. Jpn. J. Appl. Phys. 32No. 11B (1993) 5324

[13]   H. Yamazaki, R. Chiba and I. Hatakeyama: Crystallization Time of the Ternary Ge-Sb-Te Alloys and Their Aptitude to Optical Disk Media at Higher Linear Velocity. Trans. Mat. Res. Soc. Jpn., 15B (1993) 1031

[14]   S. Morita, M. Nishyawa and T. Ueda: Super-High-Density Optical Disk Using Deep Groove Method. Jpn. J. Appl. Phys. 36 No. 1B (1997) 444

[15]   T. Kurumizawa, M. Takao, K. Kimura and K. Nagata: Extended Abstracts of the 35th Spring Meeting, 1988; The Japan Society of Apply Physics and Related Societies, No. 3, 28p-ZQ-3, 839 (1988)

[16]   T. Ohta, K. Inoue, M. Uchida, K. Yoshioka, T. Akiyama, S. Furukawa, K. Nagata and S. Nakamura: Phase Change Disk Media having Rapid Cooling Structure, Proc. Int. Symp. on Optical Memory, 1989, Jpn. J. Appl. Phys. 28 (suppl. 28-3, 123-128 (1989).

[17]   T. Ohta, M. Uchida, K. Yoshioka, K. Inoue, T. Akiyama, S. Furukawa, K. Kotera and S. Nakamura: Million Cycle Overwritable Phase Change Optical Disk Media, Proc. SPIE 1078 (Optical Data Storage Topical Meeting), 27-34 (1989).

[18]   T. Ohta, S. Furukawa, K. Yoshioka, M. Uchida, K. Inoue, T. Akiyama, K. Nagata

and S. Nakamura: Accelerated Aging Studies for Phase Change Type Disc Media, Proc. SPIE 1316 (Optical Data Storage), 367-373 (1990)

[19]    H. Hofmann, S. Dambach and H. Richter: Blue Laser Phase Change Recording System. Journal of Magnetism and Magnetic Materials **249** (2002) 499

[20]    T. Higuchi, H. Kobayashi, K.Takahashi and T.Imai: System Stability against Fingerprints on Blu-ray Disc System. Jpn. J. Appl.  Phys. **43** (2004) 4884

[21]    T. Ishizuka, S. Ohshima and Y. Iriye: Three-dimensional Thermal Calculation of Phase Change Optical Disks Using Internal Energy. Computer Aided Innovation of New Materials II (1993) 775

[22]    C.A.Volkert and M. Wutting: Modeling of Laser Pulsed Heating and Quenching in Optical Data Storage Media. Journal of Applied Physics **86** (1999) 1808

[23]     C.B. Peng, L. Cheng and M. Mansuripur: Experimental and Theoretical Investigations of Laser-induced Crystallization and Amorphization in Phase-Change Optical Recording Media. J. Appl. Phys. 82, No. 9 (1997) 4183

[24]    M. Mansurifur, G. A. Gonnell and J. W. Goodman: Laser-induced Local Heating of Multilayers . Appl. Opt. 21, No. 6 (1982) 1106

[25]    J.J. Ho, T.C. Chong, L.P. Shi, Z.J. Liu and J.C Lee: Thermal Modeling of Grooved Phase Change Optical Recording Disk. Jpn. J. Appl. Phys. 38, No. 3B (1999) 1604

[26]    Y.J. Huh, J.S. Kim, T.Y. Nam and S.C. Kim: Deformation and Recording Characteristics of Compact Disc-Recordables. Jpn. J. Appl.  Phys Vol. **36** (1997) 403

[27]    P.K. Tan, L.P. Shi, X.S. Miao, H. Meng, K.P. Wong, K.G. Lim and T.C. Chong:

Substrate Deformation Studies on Direct Overwriting of Phase-Change Rewritable Optical Disc with Germanium Nitride Interface Layer. Jpn. J. Appl. Phys. **43,** No. 7B (2004) 5024

[28]    L.P. Shi, T.C. Chong, J.J. Ho, Z.J. Liu, B.X. Xu, X.S. Miao, Y.M. Huang: Optical Data Storage, 1998, 71

[29]    L.P. Shi and C.T. Chong: New Structures of the Super-Resolution Near-Field Phase-Change Optical Disk and a New Mask-Layer Material. J.Tominaga and D.P. Tsai (Eds.): Optical Nanotechnologies, Topics Appl. Phys. 88, 87-107 (2003)

[30]    J.M. Li, L.P. Shi, X.S. Miao, K.G. Lim, H.X. Yang and T.C. Chong. Integrated thermal and optical analyses of phase-change optical disk. Jpn. J. Appl. Phys. 43 (2004), 4724-4729

[31]    Giorgio Pauletto. Computational solution of large-scale macroeconometric models. Kluwer Academic Publishers, 1997

[32]    R.J. Hosking et al. First steps in numerical analysis 2nd ed**.** London: Arnold, 1996.

[33]    M.Kleiber. Handbook of Computational Solid Mechanics. New York: Springer, 1998

[34]    Noboru Kikuchi. Finite Element Methods in Mechanics. New York: Cambridge University Press, 1986.

[35]    H. Kando, T. Maeda, M. Terao, M. Miyamoto, A. Hirotsune and H. Ohnuki: . Proc. Int. Symp. on Optical Memory, 1998, We-H-01

[36]    A.H. Shivola, IEEE Trans. Geosci. & Remote Sens., 1980, 403

[37]    J.B. Judkins, C.W. Haggans and R.W. Ziolkowski: . Applied Optics, 35. No.14 (1996) 2477

[38]    Y. He, T. Kojima, T. Uno and S. Adachi. IEICE Trans. Electron., Vol. E81-C, No. 12 (1998) 1881

[39]    H.X. Yang, L.P. Shi, J.M. Li, K.G. Lim, T.C. Chong. Thermal deformation analysis of bl-ray optical disks. Proc. Int. Symp. on Optical Memory, 2004, 188-190

# Publications

1. H.X. Yang, L.P. Shi, J.M. Li, K.G.Lim, T.C.Chong. Thermal deformation analysis of high density optical disks. Jpn. J. Appl. Phys., accepted

2. J.M. Li, L.P. Shi, X.S. Miao, K.G. Lim, H.X. Yang and T.C. Chong. Enhanced Scattering of Random-Distribution Nanoparticles and Evanescent Field in Super-Resolution Near-Field Structure. Jpn. J. Appl. Phys. 44 (2005) 3620.

3. J.M. Li, L.P. Shi, X.S. Miao, K.G. Lim, H.X. Yang and T.C. Chong. Integrated thermal and optical analyses of phase-change optical disk. Jpn. J. Appl. Phys. 43 (2004) 4724.

4. H.X. Yang, L.P. Shi, J.M. Li, K.G. Lim, T.C. Chong. Thermal deformation analysis of bl-ray optical disks. Proc. Int. Symp. on Optical Memory (2004) 188.

5. L.P. Shi, T.C. Chong, J.M. Li, H.X. Yang, and J.Q. Mou. Thermal analysis of nonvolatile and nonrotation phase change memory cell. MRS, proceeding. Vol. 803 HH1.8.1

6. L.P. Shi, T.C. Chong, J.M. Li, Darry S.C. Koh, R. Zhao, H. X. Yang, P.K. Tan X.Q. Wei and W.D. Song. Thermal modeling and simulation of nonvolatile and non-rotating phase change memory cell. Non-volatile memory technology symposium (2004) 83.

7. J.M. Li, L.P. Shi, K.G. Lim, X.S. Miao, H.X. Yang, T.C. Chong. Enhanced scattering of random-distribution nanoparticles and evanescent field in a super-RENS structure. Proc. Int. Symp. on Optical Memory (2004) 214.

# Appendix

```
! 3-D THERMAL SOLVER FOR PHASE CHANGE DVD DISK
! DEVELOPED BY OPTICAL MEDIA, DATA STORAGE INSTITUTE
! COPYRIGHT TO DSI, SINGAPORE

PROGRAM MAIN
USE PORTLIB
IMPLICIT NONE
INTEGER NODENO     ! NODE NUMBER OF THE WHOLE SYSTEM
INTEGER ELEMNO     ! ELEMENT NUMBER 3-D 8-NODE ELEMENT ONLY
INTEGER FIXTNO     ! THE NUMBER OF NODE WHOSE TEMPRATURE ARE FIXED
INTEGER MATNO      ! MATERIAL NUMBER
INTEGER QELENO     ! THE HEATED ELEMENT NUMBER
INTEGER HEATMODE   ! THE WAY TO DEFINE THE HEATED ELEMENT
INTEGER LOADCASENO                     ! LOADCASE NUMBER FOR THE PRESENT JOB
INTEGER QN,FN,FN1                      ! JUDGE WHETHER THE NODE SEQUENCE IS SORTED OR NOT
DOUBLE PRECISION DT,T0, POWER              ! THE THICKNESS OF PHASE CHANGE LAYER
DOUBLE PRECISION, ALLOCATABLE :: XYZ(:,:)          ! THE ARRAY OF THE (X,Y,Z) COORDINATES
DOUBLE PRECISION, ALLOCATABLE :: THICKNESS(:)     ! THE ARRAY TO HOLD THE THICKNESS OF LAYERS
INTEGER, ALLOCATABLE :: ELELNK(:,:)          ! THE ARRAY TO HOLD THE ELEMENT LINK
INTEGER, ALLOCATABLE :: INVINDX(:)           ! THE CORESPONDENCE OF THE NODE SEQENCE
DOUBLE PRECISION, ALLOCATABLE :: STIFF(:)           ! THE 1-D GLOBAL STIFFNESS MATRIX
DOUBLE PRECISION, ALLOCATABLE :: TEMPT(:)           ! THE TEMPERATURE VECTOR OF FIRST STEP
DOUBLE PRECISION,ALLOCATABLE :: TEMP(:)             ! THE TEMPERATURE VECTOR OF SECOND
DOUBLE PRECISION HIGHTEMP
DOUBLE PRECISION, ALLOCATABLE :: DD(:)              ! INTERMEDIATE VARIABLE
DOUBLE PRECISION, ALLOCATABLE :: GLBP(:)            ! THE LOAD VEDTOR AT TIME T
DOUBLE PRECISION, ALLOCATABLE :: DISP(:)            ! THE DISPLACEMNET VECTO AT TIME T
INTEGER, ALLOCATABLE :: NNDIAG(:)           ! THE DIAGONAL ELEMENT OF THE 2-D MATRIX IN 1-D VERSION
OF GLOBAL STIFFNESS MATRIX
DOUBLE PRECISION, ALLOCATABLE :: MATPROP(:,:)       ! THE EXTRA MATERIAL MECHANICAL PROPERTIES
INTEGER BOUNDNUM                           ! THE TOTAL NUMBER OF BOUNDED NODES
INTEGER, ALLOCATABLE :: BDISP(:,:)          ! THE DISPLACEMENT BOUNDARY CONDITION
INTEGER I,J,K,N,ANAMODE,STEP               ! INTERMEDIATE VARIABLE
CHARACTER (60) FILENAME                     ! INTERMEDIATE VARIABLE

DO WHILE(1)
   ! THE FOLLOWING IS CONCERNED WITH EACH JOB.............................................
        CALL WRITUSEDTIME(T0,'TIME TO START ANALYSIS',0)
        OPEN(3,FILE='./INTERMEDIATE/INPTFILE.NAM')
        READ(3,*) FILENAME
        READ(3,*) ANAMODE,DT
        READ(3,*) HEATMODE
        READ(3,*) MATNO,NODENO,ELEMNO,FIXTNO,QELENO,LOADCASENO
        CLOSE(3)

   ! PREPARE THE MEMORY REQUIRED FOR ANALYSIS              !+++
        ALLOCATE (XYZ(3,NODENO))        ! DEALLOCATED AFTER HEAT LOAD            !+++
        ALLOCATE (ELELNK(9,ELEMNO))     ! DEALLOCATED AFTER HEAT LOAD            !+++
        ALLOCATE (INVINDX(NODENO))      ! DEALLOCATED AT THE END                 !+++

! READ IN THE INPUT DATA FOR ANALYSIS **************************************************
        CALL READNODELEMNT(XYZ,ELELNK,NODENO,ELEMNO,QN)
! TO SORT THE NODE SEQUENCE TO MAKE THE PROBLEM SCALE SMALLER                 !***
        CALL SORT(XYZ,ELELNK,INVINDX,NODENO,ELEMNO)
        CALL WRITUSEDTIME(T0,'TIME TO SORT',0)
        ALLOCATE(MATPROP(3,MATNO))
        CALL READMMAT(MATNO,MATPROP)
        OPEN(72,FILE='./INPUT/DISPLACEMENT.TXT')
        READ(72,*)BOUNDNUM
        ALLOCATE(BDISP(4,BOUNDNUM))
        CALL READDBOUND(BDISP,BOUNDNUM)
```

112

```
        ALLOCATE (NNDIAG(3*NODENO+2))
        CALL DIAGOFGLOBK(NNDIAG,NODENO,ELELNK,ELEMNO)
        ALLOCATE(STIFF(NNDIAG(3*NODENO+1)))
! SET THE INITIAL VALUE OF 1D STIFFNESS MATRIX
        DO I=1,NNDIAG(3*NODENO+1)
                STIFF(I)=0.0D0
        ENDDO
        CALL ASSEMKE(STIFF,NNDIAG,XYZ,ELELNK,ELEMNO,NODENO,MATPROP)
        CALL WRITUSEDTIME(T0,'TIME TO ASSEMBLE K',0)
        CALL BOUNDDISP(STIFF,NNDIAG,NODENO,BDISP,BOUNDNUM,INVINDX)
        ALLOCATE (DD(3*NODENO))
        !TRIANGLE DECOMPOSITION OF THE STIFFNESS MATRIX
        CALL LDLT(NNDIAG,STIFF,DD,3*NODENO)
        ALLOCATE(DISP(4*NODENO))
        DO I=1,4*NODENO
          DISP(I)=0.0D0
        ENDDO

        ALLOCATE (TEMPT(NODENO))
        ALLOCATE(TEMP(NODENO))                          !+++
        ALLOCATE(GLBP(3*NODENO))                        !+++
        CALL INITIALIZETEMP(TEMPT,HIGHTEMP,NODENO)
        OPEN(52,FILE='./INTERMEDIATE/DISP.DAT')
        OPEN(53,FILE='./INTERMEDIATE/DISP_OW.DAT')
        OPEN(78,FILE='./INTERMEDIATE/TEMPERATURE.DAT')
        OPEN(79,FILE='./INTERMEDIATE/TEMPERATURE_OW.DAT')
        OPEN(60,FILE='./INPUT/NEW_PULSESHAPE.TXT')

        K=1
        DO WHILE (K<=LOADCASENO)
                ! THE FOLLOWING IS CONCERNED WITH EACH LOAD CASE ----------------------------------
                IF(K==1)THEN
                        FN=78
                        FN1=52
                ELSE
                        FN=79
                        FN1=53
                ENDIF
                READ(60,*) STEP
                READ(60,*) STEP,POWER
                CALL WRITLOADCASE(K)
                DO I=1,STEP
                        CALL READTEMP(FN,I,TEMP,NODENO)
                        CALL ASSEMP(GLBP,XYZ,ELELNK,ELEMNO,TEMP,TEMPT,NODENO,MATPROP)
                        CALL BOUNDLOAD(GLBP,BDISP,BOUNDNUM,INVINDX)
                        CALL BACKSUB(NNDIAG,STIFF,DD,GLBP,3*NODENO)
                        CALL GETDISP(I,GLBP,DISP,NODENO)
                        PRINT*,"===========  TIME STEP: ==========",I
                        CALL WRITUSEDTIME(T0,'TIME TO SOLVE EQUS',0)
                        DO J=1,NODENO
                                TEMPT(J)=TEMP(J)
                        ENDDO
                        WRITE(FN1,'(A8,I8)')'STEP:', I
                        WRITE(FN1,*)'NODE   UX  UY  UZ  USUM '
                        DO N=1,NODENO
                                WRITE(FN1,'(1X,I8,18E15.8)')N,(DISP(4*N-4+J),J=1,4)
                        ENDDO
                ENDDO  !END OF TRANSIENT ANALYSIS
                IF(K==1) K=0
                K=K+2
                ! THE END OF PROCESSING THE PRESENT LOAD CASE --------------------------------------
        ENDDO
        CLOSE(78)
        CLOSE(52)
        CLOSE(79)
        CLOSE(53)
        CLOSE(60)
        CALL WRITUSEDTIME(T0,'TIME TO END ANALYSIS',0)
        DEALLOCATE(XYZ)           ! FREE THE MEMORY FOR EQUATION SOLUTION.
```

113

```
                DEALLOCATE (ELELNK)      ! FREE THE MEMORY FOR EQUATION SOLUTION.
                DEALLOCATE(BDISP)                               !DEALLOCATED AT APPLIED BOUNDARY
                DEALLOCATE(MATPROP)                             !DEALLOCATED AT THE END
                DEALLOCATE(DISP)
                DEALLOCATE(GLBP)
                DEALLOCATE(NNDIAG)
                DEALLOCATE(DD)
                DEALLOCATE(STIFF)
                DEALLOCATE(TEMPT)
                DEALLOCATE(TEMP)
STOP
ENDDO
END      !OF THE MAIN PROGRAM^^^^^^^^^^^^^^^^



! 1. READNODELEMNT: READ IN NODES AND ELEMENTS
SUBROUTINE READNODELEMNT(XYZ,ELELNK,NODENO,ELEMNO,QN)

! . . . . . . . . . . . . . . . . . . . . . . . . . . . . . . . . .
!  PROGRAM TO READ THE COORDINATES OF THE NODES . . . . . . . . . . .
!        AND NODE SEQUENCE OF THE ELEMENTS . . . . . . . . . .
! . . . . . . . . . . . . . . . . . . . . . . . . . . . . . . . . .
IMPLICIT NONE

INTEGER NODENO, ELEMNO,QN
DOUBLE PRECISION XYZ(3,1)
INTEGER ELELNK(9,1)
INTEGER I,J,NODE,I1,I2,I3,I4
CHARACTER*40 FIRSTLINE
OPEN(51,FILE='./INPUT/NEW_NLIST.TXT')
READ(51,*) FIRSTLINE
DO J=1,NODENO
        READ(51,*) NODE,XYZ(1,J),XYZ(2,J),XYZ(3,J)
        IF(NODE/=J) THEN
                PRINT *, 'THE NODE LIST IS NOT SORTED, BUT DOES NOT MATTER'
                XYZ(1,NODE)= XYZ(1,J)
                XYZ(2,NODE)= XYZ(2,J)
                XYZ(3,NODE)= XYZ(3,J)
        ENDIF
ENDDO
CLOSE(51)

DO J=1,NODENO
                XYZ(1,J)= XYZ(1,J)*1.0D6
                XYZ(2,J)= XYZ(2,J)*1.0D6
                XYZ(3,J)= XYZ(3,J)*1.0D6
                IF(ABS(XYZ(1,J))<1D-10)XYZ(1,J)=0.0
                IF(ABS(XYZ(2,J))<1D-10)XYZ(2,J)=0.0
                IF(ABS(XYZ(3,J))<1D-10)XYZ(3,J)=0.0

ENDDO
QN=0
OPEN(52,FILE='./INPUT/NEW_ELIST.TXT')
READ(52,*)FIRSTLINE
DO J=1,ELEMNO
        READ(52,*) NODE,I1,I2,I3,I4,ELELNK(1,J),ELELNK(2,J),ELELNK(3,J),&
              ELELNK(4,J),ELELNK(5,J),ELELNK(6,J),ELELNK(7,J),ELELNK(8,J)
        ELELNK(9,J)=I1
        IF(I1==2) QN=QN+1
        IF(NODE/=J) THEN
                PRINT *, 'THE ELEMENT LIST IS NOT SORTED, BUT DOES NOT MATTER'
                DO I=1,9
                        ELELNK(I,NODE)=ELELNK(I,J)
                ENDDO
        ENDIF
ENDDO
CLOSE(52)
```

114

```
RETURN
END

SUBROUTINE SORT(XYZ,ELELNK,NPLACE,NODENO,ELEMNO)
! THIS SUBROUTINE SORTS THE NODES IN A SEQUENCE OF Z,Y,X COORDINATES
IMPLICIT NONE
!INPUT & OUTPUT PARAMETERS
DOUBLE PRECISION XYZ(3,1) ! THE COORDINATE OF ALL THE NODES, BEFORE AND AFTER SORTING
INTEGER ELELNK(9,1)        ! THE ELEMENT LINK ARRAY, BEFORE AND AFTER SORTING
!INPUT PARAMTERS
INTEGER NODENO,ELEMNO
!OUTPUT PARAMETERS
INTEGER NPLACE(1) ! THE CORESPONDENCE BETWEEN THE OLD AND THE NEW NODE NUMBERS

!LOCAL NOUSE
DOUBLE PRECISION XP,TMP(NODENO)
DOUBLE PRECISION XYZB(3,NODENO)
INTEGER I,J,INDX(NODENO)
DO I=1,NODENO
        DO J=1,3
                XYZB(J,I)=XYZ(J,I)
        ENDDO
ENDDO
XP=1.0D5
DO I=1,NODENO
        TMP(I)=XYZ(1,I)*XP*XP+XYZ(2,I)*XP+XYZ(3,I)
ENDDO
CALL INDEXX(NODENO,TMP,INDX)
OPEN (61,FILE='./INTERMEDIATE/SORTRESULT.TXT')
DO I=1,NODENO
        WRITE(61,2001) (XYZ(J,INDX(I)),J=1,3) ,TMP(INDX(I))
ENDDO

DO I=1,NODENO
        DO J=1,3
                XYZ(J,I)=XYZB(J,INDX(I))
        ENDDO
ENDDO

DO I=1,NODENO
        NPLACE(INDX(I))=I
ENDDO

DO I=1,NODENO
        WRITE(61,'(3I5,3E12.5)') I, INDX(I),NPLACE(I),XYZ(1,I),XYZ(2,I),XYZ(3,I)
ENDDO

DO I=1,ELEMNO
        DO J=1,8
                ELELNK(J,I)=NPLACE(ELELNK(J,I))
        ENDDO
ENDDO

CLOSE (61)

2001 FORMAT (4E15.3)

RETURN
END


SUBROUTINE INDEXX(N,ARR,INDX)
! A STANDARD ALGORITHM FROM BOOKS
IMPLICIT NONE
INTEGER N,INDX(N)
DOUBLE PRECISION ARR(N)
INTEGER I,INDXT,IR,ITEMP,J,JSTACK,K,L,ISTACK(N)
DOUBLE PRECISION A
DO J=1,N
```

```
                INDX(J)=J
ENDDO
JSTACK=0
L=1
IR=N
DO WHILE (1)
        IF(IR-L<7)THEN
                DO J=L+1,IR
                        INDXT=INDX(J)
                        A=ARR(INDXT)
                        DO I=J-1,L,-1
                                IF(ARR(INDX(I))<=A)EXIT
                                INDX(I+1)=INDX(I)
                        ENDDO

                        INDX(I+1)=INDXT

                ENDDO

        IF(JSTACK==0)RETURN

                IR=ISTACK(JSTACK)
        L=ISTACK(JSTACK-1)
                JSTACK=JSTACK-2

        ELSE
                K=(L+IR)/2
ITEMP=INDX(K)
INDX(K)=INDX(L+1)
INDX(L+1)=ITEMP
IF(ARR(INDX(L))>ARR(INDX(IR)))THEN
                        ITEMP=INDX(L)
                        INDX(L)=INDX(IR)
                        INDX(IR)=ITEMP
ENDIF
IF(ARR(INDX(L+1))>ARR(INDX(IR)))THEN
                        ITEMP=INDX(L+1)
                        INDX(L+1)=INDX(IR)
                        INDX(IR)=ITEMP
ENDIF
IF(ARR(INDX(L))>ARR(INDX(L+1)))THEN
                        ITEMP=INDX(L)
                        INDX(L)=INDX(L+1)
                        INDX(L+1)=ITEMP
                ENDIF
                I=L+1
J=IR
INDXT=INDX(L+1)
A=ARR(INDXT)
                DO WHILE (1)
                        I=I+1
                        DO WHILE(ARR(INDX(I))<A)
                                I=I+1
                        ENDDO
                        J=J-1
                        DO WHILE(ARR(INDX(J))>A)
                                J=J-1
                        ENDDO
                        IF(J<I)EXIT
                        ITEMP=INDX(I)
                        INDX(I)=INDX(J)
                        INDX(J)=ITEMP
                ENDDO

        INDX(L+1)=INDX(J)
        INDX(J)=INDXT
        JSTACK=JSTACK+2
        IF(IR-I+1>=J-L)THEN
          ISTACK(JSTACK)=IR
```

116

```
      ISTACK(JSTACK-1)=I
       IR=J-1
      ELSE
       ISTACK(JSTACK)=J-1
       ISTACK(JSTACK-1)=L
       L=I
      ENDIF
          ENDIF
ENDDO
END

!OUTPUT THE CURRENT TIME WHEN CALCULATING
SUBROUTINE WRITUSEDTIME(T0,STR,PNFLG)
        USE PORTLIB
        IMPLICIT NONE
        INTEGER FN,PNFLG
        CHARACTER(*) STR
        CHARACTER(25) S
        DOUBLE PRECISION TT,T0
        TT = TIMEF()
        S=ADJUSTL(STR)
        WRITE(*,3001) S,TT-T0
        IF(PNFLG==1)WRITE(FN,3001) S,TT-T0
        T0 = TT
RETURN
3001 FORMAT(12('='),2X,A25,F10.3," SECONDS ",12('='))
END

SUBROUTINE WRITLOADCASE(K)
IMPLICIT NONE
INTEGER K
        WRITE(*,'(///)')
        WRITE(*,1002)
        WRITE(*,1001) (K+2)/2
        WRITE(*,1002)
RETURN

1001 FORMAT(24('='),5X,'LOAD CASE:',I4,5X,24('=')/)
1002 FORMAT(72('='))

END


 !READ THE MECHANICAL PROPERTIES OF ALL MATERIALS
 SUBROUTINE READMMAT(MATNO,MATPROP)
 IMPLICIT NONE
 INTEGER MATNO,J,NODE
 DOUBLE PRECISION MATPROP(3,MATNO),PROP(5,MATNO),THICKNESS(MATNO),CONDUCTIVITY(3,MATNO)
 CHARACTER*20   FILNAME
 OPEN(71,FILE='./INPUT/NEW_MAT_TE.TXT')

 READ(71,*)FILNAME
 DO J=1,MATNO
        READ(71,*) NODE,PROP(1,J),PROP(2,J),PROP(3,J),PROP(4,J),PROP(5,J),THICKNESS(J),&
         CONDUCTIVITY(1,J),CONDUCTIVITY(2,J),CONDUCTIVITY(3,J),&
         MATPROP(1,J),MATPROP(2,J),MATPROP(3,J)
        IF(NODE/=J) THEN
               PRINT *, 'THE MATERIAL LIST IS NOT SORTED, BUT DOES NOT MATTER'
               MATPROP(1,NODE)= MATPROP(1,J)
               MATPROP(2,NODE)= MATPROP(2,J)
               MATPROP(3,NODE)= MATPROP(3,J)
        ENDIF
        MATPROP(1,J)= 1.0E-6*MATPROP(1,J)
 ENDDO
 CLOSE(71)
 END

 ! READ THE DISPLACEMENT BOUNDARY CONDITION
 SUBROUTINE READDBOUND(BVALUE,BNUM)
```

117

```
 IMPLICIT NONE
 INTEGER I,BNUM,NODE
 INTEGER BVALUE(4,BNUM)

 DO I=1,BNUM
          READ(72,*)NODE,BVALUE(1,I),BVALUE(2,I),BVALUE(3,I),BVALUE(4,I)
 ENDDO
 CLOSE(72)
 END


 !ASSEMBLE GLOBAL STIFFNESS MATRIX
 SUBROUTINE ASSEMKE(STIFF,NNDIAG,XYZ,ELELNK,ELEMNO,NODENO,MATPROP)
 !ASSEMBLE THE GLOBAL STIFFNESS MATRIX AND GLOBAL THERMAL LOAD VECTOR
 IMPLICIT NONE
 INTEGER ELEMNO,J
 INTEGER NDSQ(8),NODENO,ELELNK(9,ELEMNO)
 INTEGER NNDIAG(3*NODENO+2)
 DOUBLE PRECISION STIFF(NNDIAG(3*NODENO+1)-1),XYZ(3,NODENO)
 DOUBLE PRECISION XYZE(3,8),MATPROP(3,1)
 DOUBLE PRECISION KKMATRIX(24,24)


 ! ASSEMBLE THE GLOBAL STIFFNESS MATRIX AND GLOBAL THERMAL LOAD VECTOR

 DO J=1,ELEMNO

          !PREPARE THE ELEMENT INFORMATION
                  CALL ISOLATEELEMENT(J,XYZ,ELELNK,XYZE,NDSQ)
          !CALCULATE THE ELEMENT STIFFNESS MATRIX AND ELEMENT THERMAL LOAD VECTOR
                  CALL CALCULATEKE(NODENO,J,KKMATRIX,XYZE,NDSQ,ELELNK,MATPROP)
          ! ADD TO THE GLOBAL STIFFNESS MATRIX AND GLOBAL THERMAL LOAD VECTOR
                  CALL ADDTOGLBK(NODENO,STIFF,NNDIAG,KKMATRIX,NDSQ)

 ENDDO

 RETURN

 END

 SUBROUTINE ADDTOGLBK(NODENO,STIFF,NNDIAG,KKMATRIX,NDSQ)

 !. . . . . . . . . . . . . . . . . . . . . . . . . . . . . . . . .
 !PROGRAM TO ADD THE ELEMENT STIFFNESS MATRIX TO THE GLOBAL STIFFNESS MATRIX AND ADD THE ELEMENT
 ! THERMAL LOAD VECTOR TO GLOBAL THERMAL LOAD VECTOR. . . . . . .
 !. . . . . . . . . . . . . . . . . . . . . . . . . . . . . . . .

 IMPLICIT NONE
 INTEGER NDSQ(1),NODENO                   !THE 8 NODES OF THE ELEMENT
 INTEGER NNDIAG(3*NODENO+2)
 ! CHANGED PARAMETERS
 DOUBLE PRECISION STIFF(NNDIAG(3*NODENO+1)-1) !THE 1-D GLOBAL MATRIX

 ! INPUT PARAMETERS
 ! INTEGER NDIAG(1)         !THE PLACE OF DIAGONAL ELEMENTS
 DOUBLE PRECISION KKMATRIX(24,24)  !THE UP TRIANGULAR OF ELEMENT MTX

 ! LOCAL PARAMETERS
 INTEGER I,J,II,JJ,M,N,ME,NE !LOCAL VARIABLES

 DO I=1,8
          II=NDSQ(I)
          DO J=1,8
                  JJ=NDSQ(J)
                    IF(JJ.GE.II)THEN
                            M=3*II-2
                            N=3*JJ-2
                            ME=3*I-2
```

118

```
                                NE=3*J-2
                                STIFF(NNDIAG(N)+N-M)=STIFF(NNDIAG(N)+N-M)+KKMATRIX(ME,NE)
                                STIFF(NNDIAG(N+1)+N-M+1)=STIFF(NNDIAG(N+1)+N-M+1)+KKMATRIX(ME,NE+1)
                                STIFF(NNDIAG(N+2)+N+2-M)=STIFF(NNDIAG(N+2)+N+2-M)+KKMATRIX(ME,NE+2)
                                STIFF(NNDIAG(N+1)+N-M)=STIFF(NNDIAG(N+1)+N-M)+KKMATRIX(ME+1,NE+1)
                                STIFF(NNDIAG(N+2)+N-M+1)=STIFF(NNDIAG(N+2)+N-M+1)+KKMATRIX(ME+1,NE+2)
                                STIFF(NNDIAG(N+2)+N-M)=STIFF(NNDIAG(N+2)+N-M)+KKMATRIX(ME+2,NE+2)
                                IF(JJ.GT.II)THEN
                                        STIFF(NNDIAG(N)+N-M-1)=STIFF(NNDIAG(N)+N-M-1)+KKMATRIX(ME+1,NE)
                                        STIFF(NNDIAG(N)+N-M-2)=STIFF(NNDIAG(N)+N-M-2)+KKMATRIX(ME+2,NE)
                                        STIFF(NNDIAG(N+1)+N-M-1)=STIFF(NNDIAG(N+1)+N-M-
1)+KKMATRIX(ME+2,NE+1)
                                ENDIF
                        ENDIF
                ENDDO
ENDDO
RETURN

END




!ASSEMBLE GLOBAL EQUIVALENT THERMAL LOAD VECTOR
SUBROUTINE ASSEMP(GLBP,XYZ,ELELNK,ELEMNO,TEMP,TEMPT,NODENO,MATPROP)

IMPLICIT NONE
INTEGER ELEMNO
INTEGER NDSQ(8),NODENO,ELELNK(9,ELEMNO)
DOUBLE PRECISION XYZ(3,NODENO)
DOUBLE PRECISION GLBP(3*NODENO),THMLOAD(24)
INTEGER I,J
DOUBLE PRECISION MATPROP(3,1)
DOUBLE PRECISION XYZE(3,8)
DOUBLE PRECISION TEMP(NODENO),TEMPT(NODENO)
! ASSEMBLE THE GLOBAL THERMAL LOAD VECTOR
DO I=1,3*NODENO
        GLBP(I)=0.0D0
ENDDO
DO J=1,ELEMNO


        !PREPARE THE ELEMENT INFORMATION
                CALL ISOLATEELEMENT(J,XYZ,ELELNK,XYZE,NDSQ)
        !CALCULATE THE ELEMENT STIFFNESS MATRIX AND ELEMENT THERMAL LOAD VECTOR
                CALL CALCULATEP(NODENO,J,THMLOAD,TEMP,TEMPT,XYZE,NDSQ,ELELNK,MATPROP)
        ! ADD TO THE GLOBAL STIFFNESS MATRIX AND GLOBAL THERMAL LOAD VECTOR
                CALL ADDTOGLBP(NODENO,GLBP,THMLOAD,NDSQ)
ENDDO

RETURN

END

SUBROUTINE ADDTOGLBP(NODENO,GLBP,THMLOAD,NDSQ)

! . . . . . . . . . . . . . . . . . . . . . . . . . . . . . . . . .
!PROGRAM TO ADD ADD THE ELEMENT THERMAL LOAD VECTOR TO GLOBAL THERMAL LOAD VECTOR. . . . . . .
! . . . . . . . . . . . . . . . . . . . . . . . . . . . . . . . . .

IMPLICIT NONE

INTEGER NDSQ(8),NODENO                    !THE 8 NODES OF THE ELEMENT
! INTEGER NDIAG(1)        !THE PLACE OF DIAGONAL ELEMENTS
DOUBLE PRECISION THMLOAD(24),GLBP(3*NODENO)    ! ELEMENT THERMAL LOAD AND GLOBAL THERMAL
LOAD
! LOCAL PARAMETERS
INTEGER J,JJ,M,ME !LOCAL VARIABLES

DO J=1,8
```

119

```
                    JJ=NDSQ(J)
                    M=3*JJ-2
                    ME=3*J-2
                    GLBP(M)=GLBP(M)+THMLOAD(ME)
                    GLBP(M+1)=GLBP(M+1)+THMLOAD(ME+1)
                    GLBP(M+2)=GLBP(M+2)+THMLOAD(ME+2)
ENDDO
RETURN

END


! CALCULATE ELEMENT STIFFNESS MATRIX
SUBROUTINE CALCULATEKE(NODENO,NELEM,KKMATRIX,XYZE,NDSQ,ELELNK,MATPROP)


! . . . . . . . . . . . . . . . . . . . . . . . . . . . . . . .
!  ISOPARAMETRIC FORMULATION OF 3-D ELEMENT MATRICES . . . . . . . .
! . . . . . . . . . . . . . . . . . . . . . . . . . . . . . .

IMPLICIT NONE

! INPUT PARAMETERS
INTEGER NELEM,NODENO,NDSQ(8)              !ELEMTYPE 1: HARMONIC  ELEMENT;  2: NON-HARMONIC
ELEMENT
DOUBLE PRECISION XYZE(3,8)  !THE COORDINATES OF ELEMENT NODES
DOUBLE PRECISION DCOEFF(6,6)     !DYNAMIC MATRIX
DOUBLE PRECISION E,U,A,B,C,SUM
INTEGER ELELNK(9,1)
DOUBLE PRECISION MATPROP(3,1)

! OUTPUT PARAMETERS
DOUBLE PRECISION KKMATRIX(24,24)   !THE UPTRIANGLE OF ELEMENT MTRIX

!LOCAL VIARABLES
DOUBLE PRECISION POSGP(3),WGTGP(3),BEMTX(6,24),BB(24,6), BKMATRIX(24,6)
INTEGER I,J,K,LX,LY,LZ
DOUBLE PRECISION WT,DET,R,S,T
! SHAPE FUCTION
DOUBLE PRECISION SHFN(8)

E=MATPROP(1,ELELNK(9,NELEM))
U=MATPROP(2,ELELNK(9,NELEM))

DO I=1,6
        DO J=1,6
                DCOEFF(I,J)=0.D0
        ENDDO
ENDDO

A=E*(1-U)/((1+U)*(1-2*U))
B=U/(1-U)
C=(1-2*U)/(2*(1-U))

DCOEFF(1,1)=A
DCOEFF(1,2)=A*B
DCOEFF(1,3)=DCOEFF(1,2)
DCOEFF(2,1)=DCOEFF(1,2)
DCOEFF(2,2)=DCOEFF(1,1)
DCOEFF(2,3)=DCOEFF(1,2)
DCOEFF(3,1)=DCOEFF(1,2)
DCOEFF(3,2)=DCOEFF(2,3)
DCOEFF(3,3)=DCOEFF(1,1)
DCOEFF(4,4)=A*C
DCOEFF(5,5)=DCOEFF(4,4)
DCOEFF(6,6)=DCOEFF(4,4)

! SET 3-POINT GUAUSS QUADRATURE PARAMETERS
CALL GUAUSS3POINT(POSGP,WGTGP)
```

```
DO I=1,24
        DO J=1,24
                KKMATRIX(I,J)=0.D0
        ENDDO
ENDDO


DO LX=1,3
        R=POSGP(LX)
        DO LY=1,3
                S=POSGP(LY)
                DO LZ=1,3
                        T=POSGP(LZ)
                        WT=WGTGP(LX)*WGTGP(LY)*WGTGP(LZ)
                        CALL SHPFNGRADE(R,S,T,BEMTX,SHFN,DET,XYZE,NELEM)
                        ! FOR HARMONIC
                                DO I=1,6
                                        DO J=1,24
                                                BB(J,I)=BEMTX(I,J)
                                ENDDO
                                ENDDO
                        !CALCULATE THE TRANSITIONAL MATRIX
                                DO I=1,24
                                        DO J=1,6
                                                SUM=0.D0
                                                DO K=1,6
                                                   SUM=SUM+BB(I,K)*DCOEFF(K,J)
                                                ENDDO
                                                BKMATRIX(I,J)=SUM
                                        ENDDO
                                ENDDO
                        !CALCULATE THE ELEMENT STIFFNESS MATRIX
                                DO I=1,24
                                        DO K=1,24
                                                SUM=0.D0
                                                DO J=1,6
                                                   SUM=SUM+BKMATRIX(I,J)*BEMTX(J,K)*WT*DET
                                                ENDDO
                                                KKMATRIX(I,K)=KKMATRIX(I,K)+SUM
                                        ENDDO
                                ENDDO
                        ENDDO
                ENDDO
        ENDDO


        RETURN

!2001 FORMAT('*** ERROR, SUSPICIOUS CALL TO FUNCTION GUAUSS QUADRATURE')
        END



        SUBROUTINE SHPFNGRADE(R,S,T,BEMTX,SHFN,DET,XYZC,NELEM)

! . . . . . . . . . . . . . . . . . . . . . . . . . . . . . .
! PROGRAM TO CALCULATE (8-NODE ISOPARAMETRIC HEXAHEDRON). . . . . .
! ---INTERPOLATION FUNCTIONS FOR CAPACITY STORED IN BMTX(1,8) . . .
! ---JACOBIAN MATRIX AND ITS DETERMINANT  (DET). . . . . .. . . .
! ---GRADIENT MATRIX FOR CONDUCTIVITY     STORED IN BMTX(3,8).. . . .
! . . . . . . . . . . . . . . . . . . . . . . . . . . . . . .
        IMPLICIT NONE
! INPUT PARAMETERS
        INTEGER NELEM
        DOUBLE PRECISION XYZC(3,8),R,S,T,SHFN(8)

! OUTPUT PARAMETERS
```

```
DOUBLE PRECISION BMTX(3,8), BEMTX(6,24), DET

! LOCAL VIARABLES
DOUBLE PRECISION SFDR(3,8),XJCB(3,3), XJ_1(3,3)
DOUBLE PRECISION RP,SP,TP,RM,SM,TM,DUM
INTEGER I,J,K

RP=1.0+R
SP=1.0+S
TP=1.0+T
RM=1.0-R
SM=1.0-S
TM=1.0-T

! -----------8-NODE BRICK SHAPE FUNCTIONS------------
  SHFN(1)=0.125*RM*SM*TM
  SHFN(2)=0.125*RP*SM*TM
  SHFN(3)=0.125*RP*SP*TM
  SHFN(4)=0.125*RM*SP*TM
  SHFN(5)=0.125*RM*SM*TP
  SHFN(6)=0.125*RP*SM*TP
  SHFN(7)=0.125*RP*SP*TP
  SHFN(8)=0.125*RM*SP*TP

! SHAPE FUNCTION DERIVATIVES
SFDR(1,1)=-0.125*SM*TM
SFDR(1,2)=-SFDR(1,1)
SFDR(1,3)=0.125*SP*TM
SFDR(1,4)=-SFDR(1,3)
SFDR(1,5)=-0.125*SM*TP
SFDR(1,6)=-SFDR(1,5)
SFDR(1,7)=0.125*SP*TP
SFDR(1,8)=-SFDR(1,7)

SFDR(2,1)=-0.125*RM*TM
SFDR(2,2)=-0.125*RP*TM
SFDR(2,3)=-SFDR(2,2)
SFDR(2,4)=-SFDR(2,1)
SFDR(2,5)=-0.125*RM*TP
SFDR(2,6)=-0.125*RP*TP
SFDR(2,7)=-SFDR(2,6)
SFDR(2,8)=-SFDR(2,5)

SFDR(3,1)=-0.125*RM*SM
SFDR(3,2)=-0.125*RP*SM
SFDR(3,3)=-0.125*RP*SP
SFDR(3,4)=-0.125*RM*SP
SFDR(3,5)=-SFDR(3,1)
SFDR(3,6)=-SFDR(3,2)
SFDR(3,7)=-SFDR(3,3)
SFDR(3,8)=-SFDR(3,4)

DO I=1,3
        DO J=1,3
                DUM=0.0D0
                DO K=1,8
                        DUM=DUM+SFDR(I,K)*XYZC(J,K)
                ENDDO
                XJCB(I,J)=DUM
        ENDDO
ENDDO
! COMPUTE DETERMINANT OF JACOBIAN MATRIX AT POINT (R,S,T)
DET=XJCB(1,1)*XJCB(2,2)*XJCB(3,3)&
  +XJCB(1,2)*XJCB(2,3)*XJCB(3,1)&
  +XJCB(1,3)*XJCB(2,1)*XJCB(3,2)&
  -XJCB(1,3)*XJCB(2,2)*XJCB(3,1)&
  -XJCB(1,2)*XJCB(2,1)*XJCB(3,3)&
  -XJCB(1,1)*XJCB(2,3)*XJCB(3,2)
```

```
IF(DET<1.0D-39) THEN
        WRITE (61,2000) NELEM
        CLOSE(61)
        STOP
ENDIF

! TO CALCULATE B MATRIX

DUM=1.0/DET
XJ_1(1,1)=DUM*( XJCB(2,2)*XJCB(3,3)-XJCB(2,3)*XJCB(3,2))
XJ_1(2,1)=DUM*(-XJCB(2,1)*XJCB(3,3)+XJCB(2,3)*XJCB(3,1))
XJ_1(3,1)=DUM*( XJCB(2,1)*XJCB(3,2)-XJCB(2,2)*XJCB(3,1))
XJ_1(1,2)=DUM*(-XJCB(1,2)*XJCB(3,3)+XJCB(1,3)*XJCB(3,2))
XJ_1(2,2)=DUM*( XJCB(1,1)*XJCB(3,3)-XJCB(1,3)*XJCB(3,1))
XJ_1(3,2)=DUM*(-XJCB(1,1)*XJCB(3,2)+XJCB(1,2)*XJCB(3,1))
XJ_1(1,3)=DUM*( XJCB(1,2)*XJCB(2,3)-XJCB(1,3)*XJCB(2,2))
XJ_1(2,3)=DUM*(-XJCB(1,1)*XJCB(2,3)+XJCB(1,3)*XJCB(2,1))
XJ_1(3,3)=DUM*( XJCB(1,1)*XJCB(2,2)-XJCB(1,2)*XJCB(2,1))

! EVALUATE GLOBAL DERIVATIVE OPERATOR ( B-MATRIX )
DO K=1,8
        BMTX(1,K)=0.D0
        BMTX(2,K)=0.D0
  BMTX(3,K)=0.D0
  DO I=1,3
                BMTX(1,K)=BMTX(1,K)+XJ_1(1,I)*SFDR(I,K)
                BMTX(2,K)=BMTX(2,K)+XJ_1(2,I)*SFDR(I,K)
                BMTX(3,K)=BMTX(3,K)+XJ_1(3,I)*SFDR(I,K)
        ENDDO
ENDDO
! CALCULATE THE STRAIN MATRIX B
DO I=1,6
  DO K=1,24
    BEMTX(I,K)=0.D0
  ENDDO
ENDDO

DO I=1,8
  BEMTX(1,3*(I-1)+1)=BMTX(1,I)
  BEMTX(2,3*(I-1)+2)=BMTX(2,I)
  BEMTX(3,3*(I-1)+3)=BMTX(3,I)
  BEMTX(4,3*(I-1)+1)=BMTX(2,I)
  BEMTX(4,3*(I-1)+2)=BMTX(1,I)
  BEMTX(5,3*(I-1)+1)=BMTX(3,I)
  BEMTX(5,3*(I-1)+3)=BMTX(1,I)
  BEMTX(6,3*(I-1)+2)=BMTX(3,I)
  BEMTX(6,3*(I-1)+3)=BMTX(2,I)
ENDDO
RETURN

2000 FORMAT('*** ERROR, ZERO JACOBIAN DETERMINANT IN ELEMENT:  ',I4)

END

! CALCULATE ELEMENT EQUIVALENT THERMAL LOAD VECTOR
SUBROUTINE CALCULATEP(NODENO,NELEM,THMLOAD,TEMP,TEMPT,XYZE,NDSQ,ELELNK,MATPROP)


!. . . . . . . . . . . . . . . . . . . . . . . . . . . . . . . .
!  ISOPARAMETRIC FORMULATION OF 3-D ELEMENT MATRICES . . . . . . . .
!. . . . . . . . . . . . . . . . . . . . . . . . . . . . . . . .

IMPLICIT NONE

! INPUT PARAMETERS
INTEGER NELEM,NODENO,NDSQ(8)              !ELEMTYPE  1: HARMONIC  ELEMENT;  2:  NON-HARMONIC
ELEMENT
DOUBLE PRECISION XYZE(3,8)  !THE COORDINATES OF ELEMENT NODES
!DOUBLE PRECISION CNDCAP          !COEF OF CAPACITY/CONDUCTIVITY/HEAT-RATE
```

123

```
!DOUBLE PRECISION RATIO
DOUBLE PRECISION DCOEFF(6,6)     !DYNAMIC MATRIX
DOUBLE PRECISION E,U,A,B,C,SUM
INTEGER ELELNK(9,1)
! OUTPUT PARAMETERS

!LOCAL VIARABLES
DOUBLE PRECISION POSGP(3),WGTGP(3),BEMTX(6,24),BB(24,6), BKMATRIX(24,6)
INTEGER I,J,K,LX,LY,LZ
DOUBLE PRECISION WT,DET,R,S,T,AL
! NODE TEMPERATURE, TEMPERATURE DIFFERENCE
DOUBLE PRECISION EQTEMP,EQTEMP0
DOUBLE PRECISION TEMP(NODENO),TEMPT(NODENO)
! SHAPE FUCTION
DOUBLE PRECISION SHFN(8)
DOUBLE PRECISION MATPROP(3,1)
! THERMAL STRAIN AND ELEMENT THREMAL LOAD
DOUBLE PRECISION THERMEXP,THERMSTR(6), THMLOAD(24)

E=MATPROP(1,ELELNK(9,NELEM))
U=MATPROP(2,ELELNK(9,NELEM))
AL=MATPROP(3,ELELNK(9,NELEM))

DO I=1,6
        DO J=1,6
                DCOEFF(I,J)=0.D0
        ENDDO
ENDDO

A=E*(1-U)/((1+U)*(1-2*U))
B=U/(1-U)
C=(1-2*U)/(2*(1-U))

DCOEFF(1,1)=A
DCOEFF(1,2)=A*B
DCOEFF(1,3)=DCOEFF(1,2)
DCOEFF(2,1)=DCOEFF(1,2)
DCOEFF(2,2)=DCOEFF(1,1)
DCOEFF(2,3)=DCOEFF(1,2)
DCOEFF(3,1)=DCOEFF(1,2)
DCOEFF(3,2)=DCOEFF(2,3)
DCOEFF(3,3)=DCOEFF(1,1)
DCOEFF(4,4)=A*C
DCOEFF(5,5)=DCOEFF(4,4)
DCOEFF(6,6)=DCOEFF(4,4)
EQTEMP=0.D0
EQTEMP0=0.D0

! SET 3-POINT GUAUSS QUADRATURE PARAMETERS
CALL GUAUSS3POINT(POSGP,WGTGP)


DO I=1,24
        THMLOAD(I)=0.D0
ENDDO
DO LX=1,3
        R=POSGP(LX)
  DO LY=1,3
                S=POSGP(LY)
                DO LZ=1,3
                        T=POSGP(LZ)
                        WT=WGTGP(LX)*WGTGP(LY)*WGTGP(LZ)
                        CALL SHPFNGRADE(R,S,T,BEMTX,SHFN,DET,XYZE,NELEM)
                        ! FOR HARMONIC
                                DO I=1,6
                                        DO J=1,24
                                                BB(J,I)=BEMTX(I,J)
                                        ENDDO
                                ENDDO
```

124

```
                              DO I=1,8
                                      EQTEMP=EQTEMP+SHFN(I)*TEMP(NDSQ(I))
                                      EQTEMP0=EQTEMP0+SHFN(I)*TEMPT(NDSQ(I))
                              ENDDO
                              THERMEXP=AL*(EQTEMP-EQTEMP0)
                              !GET THE  INITIAL THERMAL STRAIN
                              DO I=1,3
                                      THERMSTR(I)=THERMEXP
                                      THERMSTR(I+3)=0.D0
                              ENDDO


                              !CALCULATE THE TRANSITIONAL MATRIX
                              DO I=1,24
                                      DO J=1,6
                                              BKMATRIX(I,J)=0.0D0
                                              DO K=1,6
                                      BKMATRIX(I,J)=BKMATRIX(I,J)+BB(I,K)*DCOEFF(K,J)
                                              ENDDO
                                      ENDDO
                              ENDDO

                              !CALCULATE THE ELEMENT THERMAL EQUIVALENT  LOAD
                              DO I=1,24
                                      SUM=0.D0
                                      DO J=1,6
                                              SUM=SUM+BKMATRIX(I,J)*THERMSTR(J)*WT*DET
                                      ENDDO
                                      THMLOAD(I)=THMLOAD(I)+SUM
                              ENDDO

                      ENDDO
              ENDDO
              ENDDO
RETURN

END


SUBROUTINE BOUNDDISP(STIFF,NNDIAG,NODENO,BVALUE,BNUM,NPLACE)
!THIS IS TO ADD CONSTRAINTS TO THE GLOBAL STIFFNESS MATRIX
! TWO CASES, IF APPLIED ZERO BOUNDARY, SPECIFY 1 ON THE LEFT DIAGONAL AND 0 ON THE RIGHT
! IF APPLIED NON-ZERO BOUNDARY, MULTIPLYING A BIG NUMBER TO DIAGONAL ELEMENT AND MULTIPLY
THE RESULT TO
IMPLICIT NONE
INTEGER BNUM,NODENO
INTEGER NNDIAG(3*NODENO+1),NPLACE(NODENO),BVALUE(4,BNUM)
DOUBLE PRECISION STIFF(NNDIAG(3*NODENO+1)),KMAX
INTEGER I,J,K

KMAX=0.0D0
DO I=1,NNDIAG(3*NODENO+1)-1
          IF(STIFF(I).GT.KMAX)KMAX=STIFF(I)
ENDDO

DO I=1,BNUM
        J=BVALUE(1,I)
        J=NPLACE(J)
        DO K=1,3
                IF(BVALUE(K+1,I).EQ.1)THEN
                        STIFF(NNDIAG(3*(J-1)+K))=KMAX*1.0D10
                ENDIF
        ENDDO
ENDDO


RETURN
END
```

125

```
SUBROUTINE BOUNDLOAD(GLBLOAD,BVALUE,BNUM,NPLACE)
!THIS IS TO ADD CONSTRAINTS TO THE GLOBAL LOAD VECTOR
!BY MULTIPLYING A BIG NUMBER TO IT
IMPLICIT NONE
INTEGER BNUM
INTEGER BVALUE(4,BNUM),NPLACE(1)
DOUBLE PRECISION GLBLOAD(1)
INTEGER I,J,K

DO I=1,BNUM
        J=BVALUE(1,I)
        J=NPLACE(J)
        DO K=1,3
                IF(BVALUE(K+1,I).EQ.1)THEN
                        GLBLOAD(3*J-3+K)=0.0D0
                ENDIF
        ENDDO
ENDDO

RETURN
END



! READ THE TEMPERATURE FOR MECHANICAL ANALYSIS
SUBROUTINE READTEMP(FN,STEP,TEMP,NODENO)
IMPLICIT NONE
INTEGER FN, NODENO, I,STEP,STEP1,II
DOUBLE PRECISION TEMP(NODENO),MIDTEMP(NODENO)
CHARACTER (8) TIMESTEP
READ(FN,'(A8,I8)')TIMESTEP, STEP1
DO I=1,NODENO
  READ(FN,*)II,TEMP(I)
ENDDO
END

 SUBROUTINE DIAGOFGLOBK(NNDIAG,NODENO,ELELNK,ELEMNO)

! . . . . . . . . . . . . . . . . . . . . . . . . . . . . . . . . .
!PROGRAM TO CALCULATE THE LENGTH OF THE 1-D LIST AND. . . . . . . .
!       LOCATE DIAGNAL ELEMENTS OF THE 2D MATRIX. . . . . . . .
! . . . . . . . . . . . . . . . . . . . . . . . . . . . . . . . . .

IMPLICIT NONE

! INPUT PARAMETERS
INTEGER NODENO,ELEMNO
INTEGER ELELNK(9,ELEMNO)

! OUTPUT PARAMETERS
INTEGER NNDIAG(3*NODENO+2) !HOLD THE THE LOCATIONS OF DIAGONAL ELEMENTS

! LOCAL VARIABLES
INTEGER I,J,MINNODE,ELEHGT
INTEGER MAXHGT(NODENO)

DO I=1,NODENO
        MAXHGT(I)=0
ENDDO

! TO CALCULATE THE MAXIMUM HEIGHT OF EACH COLUME IN GLOBAL MATRIX
! BASED ON THE NODES OF EACH ELEMENT

DO I=1,ELEMNO

        !FIND THE MINIMUM NODE NUMBER IN ELEMENT I
  MINNODE=NODENO
        DO J=1,8
                IF(ELELNK(J,I)<MINNODE) THEN
```

126

```
                        MINNODE=ELELNK(J,I)
                ENDIF
        ENDDO

        !UPDATE CORRESPONDING MAX HEIGHTS RELATED WITH ELEMENT I

        DO J=1,8
                ELEHGT=(ELELNK(J,I)-MINNODE)*3
                IF( ELEHGT>MAXHGT(ELELNK(J,I)) ) THEN
                        MAXHGT( ELELNK(J,I) )=ELEHGT
                ENDIF
        ENDDO

ENDDO

! TO CALCULATE THE GLOBAL LIST LENGTH AND
! THE LOCATIONS OF DIAGONAL ELEMENTS IN THE 2-D MATRIX

NNDIAG(1)=1

DO  I=1,NODENO
        DO J=1,3
                NNDIAG(3*I-2+J)=NNDIAG(3*I-3+J)+MAXHGT(I)+J
        ENDDO
ENDDO
RETURN
END

 SUBROUTINE GUAUSS3POINT(POSGP,WGTGP)

! . . . . . . . . . . . . . . . . . . . . . . . . . . . . . . . . .
! TO CALCULATE 3*3 GAUSS QUADRATURE POINTS AND WEIGHTS. . . . . . . .
! . . . . . . . . . . . . . . . . . . . . . . . . . . . . . . . . .

IMPLICIT NONE

! OUTPUT PARAMETERS
DOUBLE PRECISION POSGP(3),WGTGP(3)

POSGP(1)=-.7745966692415D0
POSGP(2)=0.0D0
POSGP(3)=-POSGP(1)

WGTGP(1)=5.0D0/9.0
WGTGP(2)=8.0D0/9.0
WGTGP(3)=WGTGP(1)

RETURN
END


SUBROUTINE ISOLATEELEMENT(NEL,XYZ,ELELNK,XYZE,NDSQ)

! . . . . . . . . . . . . . . . . . . . . . . . . . . . . . . . . .
! TO FORM THE SUBSET ELEMENT INFORMATION TO CALCULATE . . . . . . . .
!               AND ASSEMBLE ELEMENT MATRIX . . . . . . . .
! . . . . . . . . . . . . . . . . . . . . . . . . . . . . . . . . .

IMPLICIT NONE

! INPUT PARAMETERS
DOUBLE PRECISION XYZ(3,1)
INTEGER ELELNK(9,1),NEL

! OUTPUT PARAMETERS
DOUBLE PRECISION XYZE(3,8)
INTEGER NDSQ(8)

! LOCAL VIARABLES
```

127

```
INTEGER I,J

DO I=1,8
        NDSQ(I)=ELELNK(I,NEL)
        DO J=1,3
                XYZE(J,I)=XYZ(J,NDSQ(I))
        ENDDO
ENDDO

RETURN
END


SUBROUTINE INITIALIZETEMP(TEMP,HIGHTEMP,NODENO)
! INITILIZING THE TEMPERATURE ARRAY
IMPLICIT NONE
INTEGER NODENO,I
DOUBLE PRECISION TEMP(NODENO),HIGHTEMP

DO I=1,NODENO
        TEMP(I)=300.D0
        HIGHTEMP=TEMP(I)
ENDDO

RETURN
END


! TRIANGLE DECOMPOSITION METHOD
 SUBROUTINE LDLT(DIAG,LST,D,N)
 IMPLICIT NONE
 DOUBLE PRECISION LST(1),D(1)
 INTEGER DIAG(1),N
 DOUBLE PRECISION SUM,AJI,AIK,AJK
 INTEGER I,J,MI,MJ,MAXJ(N),MH(N),K
 DO I=1,N
  MAXJ(I)=I
  MJ=I-(DIAG(I+1)-DIAG(I))+1
  MH(I)=MJ
  DO J=I,MJ,-1
   MAXJ(J)=I
  ENDDO
 ENDDO
 DO I=1,N
  MI=DIAG(I+1)-DIAG(I)
  MI=I-MI+1
  DO J=I,MAXJ(I)
   IF(I>=MH(J)) THEN
     MJ=DIAG(J+1)-DIAG(J)
     MJ=J-MJ+1
     MJ=MAX(MI,MJ)
                AJI=LST(DIAG(J)+(J-I))
     SUM=AJI
     DO K=I-1,MJ,-1
                AIK=LST(DIAG(I)+(I-K))
      IF(AIK/=0.0D0) THEN
                AJK=LST(DIAG(J)+(J-K))
       SUM=SUM-AIK*AJK*D(K)
      ENDIF
     ENDDO

     IF(I==J)THEN
      !IF(SUM<=0.0)PRINT *, 'CHOLESKY DECOMP FAILED'
      D(I)=SUM
     ELSE
                LST(DIAG(J)+(J-I))=SUM/D(I)
     ENDIF
   ENDIF
  ENDDO
ENDDO
```

128

```
   ENDDO
   RETURN
   END

SUBROUTINE BACKSUB(DIAG,LST,D,V,NODENO)

! BACK SUBSTITURION TO GET THE FINAL SOLUTION

IMPLICIT NONE

INTEGER NODENO,DIAG(NODENO+1)
DOUBLE PRECISION LST(1), V(NODENO)

INTEGER N,BOT,TOP,KK,KS,K
DOUBLE PRECISION C,D(NODENO)

DO N=1,NODENO
    BOT=DIAG(N)+1
    TOP=DIAG(N+1)-1
    IF(TOP-BOT>=0) THEN
                KS=N
                K=KS
                C=0.
                DO KK=BOT,TOP
                        K=K-1
                        C=C+LST(KK)*V(K)
                ENDDO
                V(KS)=V(KS)-C
          ENDIF
ENDDO

DO N=1,NODENO
        V(N)=V(N)/D(N)
ENDDO

DO N=NODENO,1,-1
        BOT=DIAG(N)+1
        TOP=DIAG(N+1)-1
   IF(TOP-BOT>=0) THEN
                KS=N
                K=KS
                DO KK=BOT,TOP
                        K=K-1
                        V(K)=V(K)-LST(KK)*V(KS)
    ENDDO
        ENDIF
ENDDO
RETURN
END




! THE TREATMENT OF DISPLACEMENT
SUBROUTINE GETDISP(NSTEP,GLBP,DISP,NODENO)
IMPLICIT NONE
INTEGER I,NSTEP,NODENO
DOUBLE PRECISION GLBP(1),DISP(1)
DO I=1,NODENO
        DISP(4*I-3)=GLBP(3*I-2)
        DISP(4*I-2)=GLBP(3*I-1)
        DISP(4*I-1)=GLBP(3*I)
        DISP(4*I)=SQRT(DISP(4*I-3)**2+DISP(4*I-2)**2+DISP(4*I-1)**2)
ENDDO

END
```